

A multi-color and Fourier study of RR Lyrae variables in the globular cluster NGC 5272 (M3)

C. Cacciari

Osservatorio Astronomico, Via Ranzani 1, 40127 Bologna, Italy

cacciari@bo.astro.it

T.M. Corwin¹

Department of Physics, University of North Carolina, Charlotte, NC 28223

mcorwin@uncc.edu

and

B.W. Carney¹

Department of Physics and Astronomy, University of North Carolina, Chapel Hill, NC 27599

bruce@astro.unc.edu

ABSTRACT

We have performed a detailed study of the pulsational and evolutionary characteristics of 133 RR Lyrae stars in the globular cluster NGC5272 (M3) using highly accurate BVI data taken on 5 separate epochs. M3 seems to contain no less than $\sim 32\%$ of Blazhko stars, and the occurrence and characteristics of the Blazhko effect have been analyzed in detail. We have identified a good number ($\sim 14\%$) of overluminous RR Lyrae stars that are likely in a more advanced evolutionary stage off the Zero Age Horizontal Branch (ZAHB).

Physical parameters (i.e. temperature, luminosity, mass) have been derived from (B-V) colors and accurate color-temperature calibration, and compared with Horizontal Branch evolutionary models and with the requirements of stellar pulsation theory. Additional analysis by means of Fourier decomposition of the V light curves confirms, as expected, that no metallicity spread is present in M3. Evolution off the ZAHB does not affect [Fe/H] determinations, whereas Blazhko stars at low amplitude phase do affect [Fe/H] distributions as they appear more metal-rich. Absolute magnitudes derived from Fourier coefficients might provide useful average estimates for groups of stars, if applicable, but do not give reliable *individual* values. Intrinsic colors derived from Fourier

¹Visiting Astronomer, Kitt Peak National Observatory, National Optical Astronomy Observatories, which are operated by AURA, Inc. under cooperative agreement with the National Science Foundation.

coefficients show significant discrepancies with the observed ones, hence the resulting temperatures and temperature-related parameters are unreliable.

Subject headings: globular clusters: individual (M3); stars: variables: RR Lyrae

1. Introduction

M3 (NGC5272: RA[2000] = 13:42:11, DEC[2000] = +28:22:32) is one of the most important globular clusters of the Galactic halo. It is located at ~ 11.9 kpc from the Galactic centre, 10.0 kpc from the Sun and 9.7 kpc above the Galactic plane (Harris 1996). It contains by far the largest number of variable stars (Bakos et al. 2000 assign numbers to 274 variables) with a rather high specific frequency (i.e. normalized to total mass) of RR Lyrae stars. Its metallicity, for a long time considered to be $[\text{Fe}/\text{H}] = -1.66$ (Zinn & West 1984, hereafter ZW), has been revised using high resolution spectroscopic data of giant stars and appears to be somewhat higher, i.e. -1.47 (Kraft et al. 1992) or -1.50 (Kraft & Ivans 2003, hereafter KI) in the Fe_{II} metallicity scale, and -1.34 (Carretta & Gratton 1997 in their own metallicity scale).

Since the seminal paper by Oosterhoff (1939), that subdivided the globular clusters in two groups according to the mean period of their RRab variables ($\langle P_{ab} \rangle = 0.55\text{d}$ and 0.65d , respectively), M3 has traditionally been considered the prototype Oosterhoff type I (OoI) cluster. The pulsational and evolutionary properties of its RR Lyrae variables were used by Sandage et al. (1981) as a reference template for the OoI group to compare to the RR Lyrae properties in other clusters, in particular those belonging to the Oosterhoff II (OoII) group. On this basis Sandage et al. (1981) reached the conclusion that there was a systematic period-shift (at fixed light curve amplitude) as a function of metallicity with respect to the assumed template relation (i.e. M3) in the $\log P - A_B$ plane; this effect was interpreted as due to a difference in luminosity, in the sense that longer period (more metal-poor) variables were intrinsically brighter. Although the subsequent interpretations of the period-shift effect were rather controversial and involved the rôle played by several other factors (Lee et al. 1990; Carney et al. 1992, hereafter CSJ; Sandage 1993, Clement & Shelton 1999a,b), and the very existence of the period-shift was sometime questioned (e.g. Brocato et al. 1996), the position of M3 as *the* template OoI cluster was never questioned.

However, the data for the RR Lyrae variables used in all these analyses were still essentially the UBV photographic observations by Roberts and Sandage (1955), Baker and Baker (1956) and Sandage (1959). A large and detailed morphological study of the light curve characteristics for 113 variables was performed by Szeidl (1965, 1973), using photographic material taken over a long time baseline. It is only in the late '90s that systematic studies of the RR Lyrae variables in M3 with CCD detectors were undertaken, leading to large very accurate BVI photometric databases: Kaluzny et al. (1998, hereafter Kal98) with V data for 42 stars; Carretta et al. (1998, hereafter Car98) with BVI data for 60 stars; and Corwin & Carney (2001, hereafter CC01) with BV data for 207 stars. These data offer the unprecedented opportunity to study the largest number of RR

Lyrae stars ever detected within a single globular cluster, using well defined light curves obtained in more than one color and at different epochs.

In this paper we present a detailed study of the pulsational and evolutionary characteristics of 133 RR Lyrae variables in M3, selected among those with the best quality light curves. We describe in Sect. 2 the data we have used, and we introduce the Blazhko effect and the definition of mean magnitudes and colors. In Sect. 3 we present the main relations between period, amplitude, magnitude and color, and in Sect. 4 we derive the reddening and discuss the calibration of temperatures and magnitudes. In Sect. 5 we derive the physical parameters of the stars and compare them with evolutionary models, and discuss specifically the stars that are in a more advanced stage of evolution. Finally, in Sect. 6 we present the Fourier analysis of the light curves and discuss the implications on the estimate of the stellar physical parameters. A summary and the conclusions of this analysis are given in Sect. 7.

2. The data

The data sets we have used for the present analysis are:

- The BV data described in detail by CC01. These consist of 83 pairs of BV frames taken in May 1992, 102 pairs taken in April 1993, and 5 V and 4 B frames taken in June 1997, on a total of 207 variable stars. This is the main data set we have used for our analysis in the B and V bandpasses.
- The BVI data described by Car98. These consist of 65 to 69 frames in each color, taken in March 1990 and in Feb-Apr-May 1992, on a total of 60 RR Lyrae variables. This data set is the only one that provides information on the I bandpass. The B and V data have been used mainly to support and provide complementary information to the CC01 data.
- The data described by Kal98. These consist of 176 V frames taken in March-April 1996, on a total of 42 RR Lyrae variable stars. Also these data were used to support and provide complementary information to the CC01 data.

2.1. Comparison with previous data sets

A detailed comparison of the intensity-averaged magnitudes from the CC01 data set with Car98, using common non-Blazhko variable stars, shows that CC01 V magnitudes are brighter than Car98 V photometry in the EAST and WEST fields by 0.065 and 0.020 mags, respectively. As for the B magnitudes, CC01 photometry is brighter than Car98 EAST and WEST fields by 0.107 and 0.025 mags, respectively. We remind the reader that Car98 EAST field contains the variables n. 10, 31, 32, 34, 43, 57, 68, 69, 70, 74, 75, 78, 84, 87, 100, 101, 128, 146, 149, 150, 178 and 197, and the WEST field contains the variables n. 6, 24, 25, 27, 28, 29, 30, 41, 42, 46, 47, 58, 66, 67, 76, 77, 88, 109, 110, 111, 121, 129, 130, 131, 132, 133, 134, 135, 136, 140, 142, 143, 155,

167, 168, 170, 188 and 209. Finally, Car98 provided also I photometry with the warning that it may be affected by a zero-point error in the absolute calibration. We treat this problem in some detail in Sect. 4.1, but we anticipate here that indeed Car98 I data are most likely too faint by ~ 0.083 mag.

The same type of comparison with Kal98 data, using intensity integrated $\langle V \rangle$ magnitudes for both data sets (note however that the published Kal98 $\langle V \rangle$ are magnitude integrated), shows that the CC01 V magnitudes are brighter than Kal98 V photometry in the SOUTH and NORTH fields by 0.028 and 0.018 mags, respectively.

Car98 and Kal98 data have been corrected by the above offsets, when they have been used along with CC01 data (e.g. for Blazhko stars).

On the other hand, a comparison of CC01 photometry with 15 randomly selected secondary standard stars from Sandage (1970) shows that CC01 V magnitudes are fainter by 0.009 ± 0.024 mag, and the B magnitudes are brighter by 0.004 ± 0.014 mag, as already noted by CC01.

Only the stars with well defined light curves in both B and V bands have been taken into account for the present study. This led us to consider a total of 133 stars out of the 201 RR Lyraes observed by CC01, in particular 23 RRC out of 43, 67 RRab out of 111, and 43 Blazhko stars out of 47. The stars we have not considered in the present study all have very noisy light curves, which may be due to photometric errors (contamination from companions) or to intrinsic phenomena such as double-mode pulsation or unidentified Blazhko modulation. They may be very interesting objects in themselves, and surely deserve further and more careful investigation (cf. Clementini et al. 2004). However, for the purpose of the present analysis, we shall use only those stars that show the “cleanest” light curves so as to keep the noise at the minimum level, taking advantage of the fact that M3 is probably the only cluster where one can afford to be very selective, due to the richness of its variable star population.

2.2. The Blazhko variables

The Blazhko effect, first noticed and studied by Blazhko (1907), is a modulation of the basic pulsation variability that produces variations of the light curve shape showing as larger photometric scatter and significant changes in the light curve amplitude. The timescale of this modulation is typically tens of days but can be as large as a few hundred days. Several mechanisms have been proposed to explain the origin of this phenomenon, which however is still an open question. We refer the reader to Smith (1995) for a recent and comprehensive discussion on this topic.

According to CC01 data no less than $\sim 32\%$ of the total RR Lyrae variable star population in M3 is affected by Blazhko variability. This fraction might easily be larger if some of the stars with noisy light curves, that we have not considered in the present analysis, turn out to be Blazhko variables in future studies. The frequency of this phenomenon we find in M3 is consistent with previous results in other stellar systems (cf. Smith 1995) and has been recently confirmed in another cluster, NGC3201, where Piersimoni et al. (2002) have identified about 30% such stars. However,

the detection of Blazhko variability is not straightforward and needs monitoring the variables over several epochs, therefore it can easily go undetected even in relatively well studied clusters.

The presence of Blazhko stars within a population of regular RR Lyrae variables may affect the global characteristics of this population, for example in all cases where the light curve amplitude is involved (e.g. the period-amplitude or color-amplitude relations). It certainly produces a scatter in the relations among various parameters, possibly masking other subtle effects by drawing them into the noise. Therefore, *the knowledge of the Blazhko star population is essential in order to select a pure sample of regular stars that define the average characteristics of the cluster variable star population.*

In the following sections we shall investigate these effects and try to derive the main characteristics of the regular variable population.

2.3. Mean Magnitudes and Colors

Mean magnitudes $\langle B \rangle$ and $\langle V \rangle$ of the variables have been derived by integrating the light curves in intensity and converting the result of this integration to magnitudes. We have not tried to correct these values to the equivalent static values, as proposed by Marconi et al. (2003), since the amplitude-dependent correction to apply e.g. to $\langle V \rangle$ would be at most -0.02 mag at $A_V=1.4$ and all our stars have smaller amplitudes. We list the values of $\langle B \rangle$ and $\langle V \rangle$ thus derived for the RRc, RRab and Blazhko stars in Tables 1, 2 and 3, respectively, as well as the B and V light curve amplitudes A_B and A_V , and the corresponding rise time values (RT_B and RT_V) defined as the phase intervals between the minimum and maximum B and V light, respectively. For the RRab and Blazhko stars we have calculated also the magnitude-integrated B_{min} and V_{min} at minimum light, i.e. $0.5 \leq \phi \leq 0.8$. These parameters have been derived with the help of Fourier decomposition of the light curves, using 6 harmonics for the RRc-type and 6 to 15 harmonics for the RRab-type variables. For the Blazhko stars we have considered separately the CC01 data taken in 1992 and 1993, that provide different epochs for the study of the Blazhko phenomenon.

The mean colors of the RR Lyrae stars are a more controversial issue. The choice of which mean color best reproduces the color the star would have were it not pulsating is a long standing problem, and has been discussed by several authors (cf. Silbermann & Smith 1995 and references therein for a detailed review and discussion of this topic). Very briefly, several solutions have been proposed as “best mean color”, e.g. the magnitude-averaged (B–V) (Preston 1961; Sandage 1990), or the intensity-averaged $\langle B \rangle - \langle V \rangle$ (Davis & Cox 1980), or a combination such as $2/3 \langle B - V \rangle + 1/3(\langle B \rangle - \langle V \rangle)$ (Lub 1977), or $\langle B \rangle - \langle V \rangle + C(A)$ where $C(A)$ is an empirical correction for amplitude (Sandage 1990). CSJ argued that, no matter how the average is done, the (B–V) colors are poor temperature indicators because they are distorted by surface gravity and non-LTE effects during a non negligible fraction of the pulsation cycle around maximum light, that can produce excess emission in the B band. They proposed a few formulae to

estimate the temperature, involving the (B–V) colors plus corrective factors due to metallicity or amplitude or period, and also a formula involving only period, amplitude and metallicity (cf. their Eq.s 13-16). On the theoretical side, Bono et al. (1995) have calculated synthetic mean colors for convective pulsating models over a wide range of luminosities and temperatures, and found that indeed both (B–V) and $\langle B \rangle - \langle V \rangle$ colors differ from the equivalent static color by a quantity that is a function of the light curve amplitude. The corrections they derive (their Table 4) are generally similar to the empirical corrections estimated by Sandage (1990).

Given the nearly unanimous consensus that $\langle B \rangle_{int} - \langle V \rangle_{int}$ colors plus some sort of amplitude-related correction reproduce reasonably well the equivalent static colors - that we shall call $(B - V)_S$, we adopt this solution where the corrections are those estimated by Bono et al. (1995). The values of $(B - V)_S$ are listed in Tables 1 and 2, where we report for convenience also the $(B - V)_{mag}$ colors of the RRc and RRab stars taken from CC01, that were calculated as $\langle B \rangle_{mag} - \langle V \rangle_{mag}$. For a consistency check, we have calculated the values of $(B - V)_S$ both from (B–V) and $\langle B \rangle - \langle V \rangle$ colors and applying the corresponding amplitude corrections, and we have verified that the results agree within 0.02 mag, and mostly within 0.01 mag. Also the use of Marconi et al. (2003) formulation (cf. their eq. 16) to derive the static (B–V) colors produces similar values to $(B - V)_S$ within 0.01 mag. We estimate that typical internal errors of the average $\langle B \rangle$ and $\langle V \rangle$ magnitudes and $(B - V)_S$ colors are 0.01 and 0.02 mag, respectively.

For the Blazhko stars listed in Table 3 we have reported no mean colors from CC01, because they were obtained from the combined 1992 and 1993 data sets and have lost information on the Blazhko phase. Instead, the $(B - V)_S$ colors for the two epochs separately can be derived from the corresponding $\langle B \rangle_{int}$ and $\langle V \rangle_{int}$ average magnitudes, and are listed in Tab. 3.

3. The main relations between Period, Amplitude, Rise Time, Magnitude and Color

These basic parameters of the RR Lyrae variable stars are connected by relations that reveal important physical, evolutionary and pulsational characteristics. Most of the considerations that we present below were already outlined by CC01, but we repeat them here in more detail and for the sake of convenience in the following analysis.

3.1. The Color-Magnitude diagram

The Color-Magnitude diagram of the full sample of 207 variable stars has been discussed already by CC01. We present in Fig. 1 a less populous but cleaner version based on the sub-sample of RRc and RRab stars studied in this paper, using the $\langle V \rangle$ and $(B - V)_S$ values listed in Tables 1 and 2. The main characteristics already discussed by CC01 are here reconfirmed, namely:

i) the blue and red edges of the color distribution are located at $(B - V)_S=0.18$ and 0.42 mag, respectively. Note, however, that one star (V178) is slightly bluer than this limit [$(B - V)_S=0.166$],

and is the faintest of the entire group of RRc variables.

ii) There is overlap in color between RRc and RRab variables, that occurs in the interval ~ 0.24 to 0.30 . As CC01 noted, it is possible to draw a line slanting toward redder colors at brighter magnitudes that separates most of the RRab from the RRc variables, but still two unusually bright RRab stars (V42 and V96) fall in the RRc area. Whereas V96 might be dismissed because it has a somewhat incomplete light curve, V42 does not show any special problem in the photometry, and its unusual position in the CMD seems to be due to the combination of unusually bright $\langle V \rangle$ and large amplitude color-correction.

iii) The Blazhko stars (not shown to avoid confusion) overlap the area of the RRab stars avoiding however the reddest part of the color distribution: they only reach as red as $(B - V)_S \leq 0.39$ with CC01 data.

iv) The magnitude distribution (lower right panel of Fig. 1) shows that the main body of the RRab population peaks around $\langle V \rangle = 15.64 \pm 0.04$ mag, and there is a clear separate group of 12 stars (V26, 31, 42, 48, 58, 60, 65, 104, 124, 146, 186, and 202) at brighter magnitudes (all individual $\langle V \rangle \leq 15.56$, centered at $\langle V \rangle \sim 15.52 \pm 0.02$). Most of these stars were already noted as very luminous by CC01. The main distribution of the RRc stars seems to be shifted by ~ 0.05 mag towards brighter magnitudes ($\langle V \rangle = 15.59 \pm 0.06$ mag), and also shows a tail of very luminous stars, in particular six (V29, 70, 85, 129, 140, and 170) that are all brighter than 15.5. We do not see any statistically significant evidence of *four* populations from the $\langle V \rangle$ distribution, as claimed by Jurcsik et al. (2003).

v) On the faint end, the distribution appears to end statistically at $\langle V \rangle \sim 15.72$, as was found also by CC01; this value is taken to correspond to the lower envelope of the Horizontal Branch (HB) luminosity distribution, i.e. the Zero Age Horizontal Branch (ZAHB). Only 3 RRab stars are fainter than this value. Based on the $\langle V \rangle$ histogram of the RRab stars we note that the thickness of the HB is ≤ 0.20 mag or ~ 0.30 mag, depending on whether we exclude or include the brighter stellar component (cf. Sandage & Katem 1982).

vi) The $\langle V \rangle$ distribution of the Blazhko stars (not shown) reaches about the same edges of the distribution of the normal stars, but is skewed towards the brighter magnitudes. A group of seven stars (V3, 14, 24, 44, 78, 130 and 143) are as bright as the more luminous group of regular stars identified in item iv), and in fact their average magnitude is $\langle V \rangle = 15.52 \pm 0.04$. The main population of Blazhko stars has $\langle V \rangle = 15.65 \pm 0.05$ which is basically identical to the mean value we find for the regular RRab variables. We note that the average magnitude of the Blazhko stars in the small-amplitude Blazhko phase appears to be ~ 0.02 mag fainter than in the large-amplitude phase, but this difference is hardly significant from the statistical point of view.

3.2. The Period-Amplitude and Period-Rise Time diagrams

As has long been known, the amplitudes of the RRab stars are strongly correlated with period, whereas the amplitudes of the RRc stars have a nearly flat distribution. A similar behaviour is shown by the rise time. We show in Fig. 2 the amplitudes A_B (lower panel) and the rise times

RT_B (middle panel) of the blue light curves vs. period ($\log P$), and for ease of discussion the corresponding values of $\langle V \rangle$ (upper panel).

3.2.1. The RRc variables

The main body of the RRc distribution defines a clear nearly flat sequence in the A_B vs. $\log P$ plane. Then there is a group of 3 stars at the short period end of this distribution, with particularly small amplitudes, and another group of 5 stars that seem to define a nearly parallel distribution to the main one, but shifted to larger amplitudes and/or longer periods. These stars also stand out in the RT_B vs. $\log P$ plane. In more detail:

i) The three short-period small-amplitude RRc stars are V105, V178 and V203 (shown as diamonds in Fig. 2). They have normal values of $\langle V \rangle$, including V178 that has the shortest period and the faintest magnitude but its $\langle V \rangle$ is still compatible with the general trend of $\langle V \rangle$ vs period among the RRc stars. They seem to be a normal extension of the main RRc population, according to theoretical models (Bono et al. 1997) and observational evidence also in other clusters (Clement & Shelton 1999b), showing that first overtone pulsators do have decreasing amplitudes at the short period (high temperature) end of the distribution, i.e. a bell-shaped distribution. On the other hand, stars with periods shorter than ~ 0.29 day ($\log P \sim -0.54$) and sinusoidal light curves with particularly small amplitudes have been found to exist also in several other globular clusters, as well as in the large sample of field LMC variables from the MACHO survey (Alcock et al. 1996) and in the Galactic Bulge (Olech 1997), where they show a well-defined peak in the period distribution and thus may define a separate population of variable stars. These stars could be second overtone (RRe) pulsators (see Clement & Rowe 2000 for references and a detailed discussion of this topic). Thus, our three short-period small-amplitude RRc stars could be either second overtone or regular first overtone pulsators. A way to test the pulsation mode of V105, V178 and V203 is to plot the Fourier parameters ϕ_{21} vs. A_{21} of their light curves, as we have done in Sect. 6.1. Anticipating the results presented there, we suggest that only V203 is a likely RRe star, whereas V105 and V178 seem to be regular RRc stars.

ii) The group of five RRc stars defining the sequence at larger amplitudes and/or longer periods includes V70, V85, V129, V170 and V177 (shown as open triangles). They were already noticed in the previous section item iv) for being significantly brighter than the main body of the RRc distribution ($\langle V \rangle = 15.43 \pm 0.12$). We consider these stars as belonging to a category that we shall call “longP/overluminous” stars.

3.2.2. The RRab variables

Among the RRab stars, one sees that the large scatter in amplitude is closely mirrored by a scatter in $\langle V \rangle$ and appears also in the RT_B parameter. We show in Fig. 3 a blown up version of Fig. 2 for the sake of clarity, and we see that the group of the RRab variables also appears to

be made of three subgroups:

- i) The main body of the RRab distribution, defining the well known relation between $\log P$ and A_B . This relation has traditionally been taken as a linear approximation; however, we see that the distribution for our stars is better represented by a quadratic relation $A_B = -3.123 - 26.331 \log P - 35.853 \log P^2$, r.m.s. error of the fit $\sigma \sim 0.08$. Also in the $\log P - RT_B$ plane a quadratic relation (e.g. $RT_B = 0.781 + 4.269 \log P + 6.881 \log P^2$, r.m.s. error of the fit $\sigma \sim 0.02$) seems to provide a better fit of the data. Theoretical models calculated for $\log L=1.61$ and 1.72 and values of mass and metallicity quite adequate for M3 (Piersimoni et al. 2002; Marconi et al. 2003) are also reported in Fig. 3 (lower panel): they have a similar non-linear shape to our distributions (a part from a “hump” in the middle range that is not quite so evident in the data).
- ii) A group of 6 stars (V22, 54, 71, 72, 77 and 144, shown as crosses) at shorter periods or, more likely, smaller amplitudes (and larger than normal RT_B values, i.e. a different shape of the light curve) than the main body of RRab stars, with $\langle V \rangle = 15.67 \pm 0.04$. These stars are compatible with being *unrecognized* Blazhko variables observed during the low-amplitude phase of the Blazhko modulation, as we discuss below. We shall call them for convenience “low amplitude/suspected Blazhko” stars.
- iii) A group of 9 stars (V26, 31, 42, 60, 65, 104, 124, 202 and KG14, shown as filled triangles) with longer periods at a given amplitude. All of them except one (KG14) were already noticed in the previous section item iv) for being significantly brighter than the main body of the RRab distribution. They have $\langle V \rangle = 15.53 \pm 0.04$ mag and can be considered to belong to the longP/overluminous group. Some of these stars (those with the longest period) stand out from the main distribution also in the RT_B vs. $\log P$ plane. These stars seem to be well represented by the same quadratic relation defined by the RRab stars, shifted toward longer periods (at fixed amplitude) by $\Delta \log P \sim 0.06$. This shift corresponds approximately to the mean location traditionally assigned to OoII variables (cf. Sandage et al. 1981). Although a detailed discussion of the Oosterhoff dichotomy is beyond the scope of this paper, we exploit our beautiful sample to investigate briefly a few basic issues related to the period-shift effect in the next section.

3.2.3. The period-shift effect

In Fig. 4 we compare the A_V amplitude (more abundant in literature than A_B) vs period distributions for the RRc and RRab variables in nine globular clusters with the analogous data in M3. The clusters are: three OoII types, i.e. M15, M68 and M9 (data from Silbermann & Smith 1995, Walker 1994, and Clement & Shelton 1999a, respectively); three intermediate types, i.e. IC4499, NGC6934 and NGC1851 (data from Walker & Nemeč 1996, Kaluzny et al. 2001, and Walker 1998, respectively); and three OoI types, i.e. NGC3201, M5, and NGC6362 (data from Piersimoni et al. 2002, Kaluzny et al. 2000, and Olech et al. 2001, respectively). From the original datasets we have excluded the stars with indication of Blazhko variability or too noisy light curves. The values of metallicity shown in Fig. 4 have been taken from KI for all clusters except IC4499, M9 and NGC6934, for which the values listed by Harris (1996) have been used. In each panel we

have reported also the average distributions of the M3 regular (solid lines) and evolved (dotted lines) RRc and RRab variables, for ease of comparison. We note the following:

- i) OoI and intermediate type clusters show similar distributions to M3 irrespective of metallicity, including the presence and behaviour of evolved stars that in a few cases (e.g. M5, NGC1851) appear to be quite abundant. This applies to both RRc and RRab variables.
- ii) In OoII clusters the distributions of both RRc and RRab stars are again independent of metal abundance, and most stars fall on the corresponding distributions of the evolved stars in M3.

Therefore we confirm previous results that there is a unique P-A relation independent of metallicity for RRab variables in OoI (and intermediate) type clusters (Brocato et al. 1996; Clement & Shelton 1999b). However, contrarily to previous suggestions of a possibly different metal-dependent P-A relation for first overtone pulsators (Clement & Shelton 1999b), we find that there is a unique P-A relation for the RRc as well. The same happens in OoII clusters: they too are characterized by their own typical P-A relations independent of metallicity, that correspond quite closely to the relations of the *evolved* RRc and RRab stars in OoI clusters. This strongly supports the interpretation of the Oosterhoff dichotomy as due to evolution away from the ZAHB (cf. Lee et al. 1990; Clement & Shelton 1999b).

3.2.4. The Blazhko variables

We have reported in Fig. 2 upper and lower panels also the *known* Blazhko variables (see Table 3), shown as lines connecting the 1992 and 1993 CC01 results. They do not appear in the middle panel because the Blazhko light curves are generally affected by large photometric scatter and the rise times are quite uncertain. In general we note that:

- i) they all fall within the RRab group, except one (V44) that could possibly belong to the RRc group from the shape of its light curve at minimum amplitude, but the photometry is rather scattered;
- ii) a few of them, when observed at large amplitude, fall on the distribution of the 9 longP/overluminous RRab stars that we have identified above (cf. Fig. 3 where they are shown as open squares, for completeness). These stars are V3, 14, 24, 35 and 67, and their average magnitude (at large amplitude) is $\langle V \rangle = 15.54 \pm 0.04$, just like the longP/overluminous RRab stars.

We discuss in more detail the nature of all the longP/overluminous stars in Sect. 5.2.

Once again we stress that if the RRab stars were considered all together, without any knowledge of their Blazhko nature, the scatter of the distribution would be large enough to hide completely these sub-groups and their behaviour; also the mean relation in the period-amplitude plane would be less well defined and likely different in shape and/or zero-point.

3.3. The Color-Rise Time, Color-Amplitude and Color-Period diagrams

We show in Fig. 5 the relations between the $(B-V)_S$ color and RT_B , A_B and $\log P$, for all our RRc and RRab stars. The periods of the RRc stars have been fundamentalized by adding 0.127 to the $\log P$. The bottom panel shows the reduced period $\log P' = \log P + 0.336(\langle V \rangle - V_{ave})$ that is designed to take into account the intrinsic spread in magnitude of the variables and correct the periods accordingly (Bingham et al. 1984). For V_{ave} we intend the mean magnitude of all “normal” stars and we use the value 15.64 that was derived from the RRab stars in the previous section. As one can see, the relation in the bottom panel is indeed tighter. In general, the use of the reduced period helps decrease the scatter of the period-color relation; in a few cases, however, it may bring out stars that show normal pulsation characteristics (i.e. periods and amplitudes) but unusual photometric properties, e.g. their colors are slightly too red or too blue and/or their magnitudes are slightly too bright or too faint. In Fig. 5 we see four possible such stars that slip out of the mean relation when the reduced period is used, i.e. V48, V58 and V186, and V134. For the first three, the average magnitude is $\langle V \rangle \sim 15.51 \pm 0.02$, and we note that V58 and V186 are marked in Table 2 as having photometric problems. Incidentally, these characteristics might be compatible with the presence of an undetected faint and redder companion, for example a subgiant star at $V \sim 18$ and $(B-V) \sim 0.6$, of which there is abundance in globular clusters. As for V134, it is the faintest star of our sample and is unusually blue for its period and amplitude, yet quite normal in the period-amplitude plane (cf. Fig. 3).

In the color-amplitude plane there is a clear correlation between these parameters for the RRab stars, whereas the distribution of the RRc stars is nearly flat. The three RRc stars with peculiarly small amplitude (V105, V178 and V203, shown as diamonds) are clearly distinguishable off the main distribution. In the period-color plane these three stars follow the same relation as the main RRc group, whereas the longP/overluminous RRc stars stand out from the rest, as expected, but fall nicely on the mean relation when using the reduced period that corrects for their unusually high luminosity.

In the RRab group, only two of the low amplitude/suspected Blazhko stars (V22 and V54) fall out of the main relation in the A_B and RT_B vs. $(B-V)_S$ planes, but are quite normal in the period-color plane. Two more stars, V96 and V134, have unusually blue colors in all planes, but they have been marked as having some photometric uncertainties (see Table 2). Finally, the stars labelled as longP/overluminous look mostly normal in the RT_B and A_B vs. $(B-V)_S$ planes, fall out of the mean relation when period is involved, but look again normal if we use the reduced period that takes into account the effect of (over)luminosity. We note that both RRc and RRab variables seem to define quadratic rather than linear relations in the RT_B vs. $(B-V)_S$ plane, independently of their evolutionary status.

Similar plots are shown in Fig. 6 for Blazhko stars, excluding the RT_B data that are not well defined for these stars.

4. Calibrations for the determination of physical parameters

4.1. Reddening

An accurate determination of the interstellar reddening is essential before we can derive physical parameters, such as temperature and luminosity, from observed parameters such as colors and apparent magnitudes.

We consider two approaches to estimate the reddening, using the colors of the RRab variables at minimum light $(B - V)_{min}$ that are listed in Table 2, and using the mean $(B - V)_S$ colors.

- Sturch (1966) method uses the $(B - V)_{min}$ color of an RRab star, its period and metallicity to derive its reddening $E(B - V)$. Among the most recent discussions and calibrations of this method are Blanco’s (1992), based on photometric color indices of field RRab stars with known metallicity (via ΔS), and Walker’s (1998), based on Sturch’s stellar sample and the assumption of zero reddening at the Galactic poles. They both find reddening values on average ~ 0.02 mag larger than most other determinations. Also Walker (1994) and Walker & Nemec (1996) find typically ~ 0.02 mag larger values with this method than with methods involving the color of the red giant branch in the globular clusters M68 and IC 4499. Therefore, we use the formulation proposed by Walker (1998),

$$E(B - V) = (B - V)_{min} - 0.24P - 0.056[Fe/H] - 0.356 \quad (1)$$

where the zero-point has been corrected by -0.02 mag to take this offset into account. For the metallicity, the most recent spectroscopic determinations are from Kraft et al. (1992) who derived $[Fe/H] = -1.47$ based on high-dispersion spectra of a few red giant stars; this result was then confirmed as $[Fe/H] = -1.50 \pm 0.03$ from a new analysis by KI based on Fe II abundances of 23 giants. Independently, Sandstrom et al. (2001) obtained $[Fe/H] \sim -1.22 \pm 0.12$ from 29 RR Lyrae and 5 red giant stars using low resolution spectra, but they note that “the use of low resolution spectra generally causes an overestimate of about 0.25 dex in the derived abundances”. Therefore we have adopted $[Fe/H] = -1.5$ for M3. Considering only the RRab stars listed in Table 2 with good photometry and no evidence of any peculiarity, we obtain an average reddening $E(B - V) = 0.014 \pm 0.012$ for M3.

- Piersimoni et al. (2002) have defined empirical period-color-amplitude-(metallicity) relations based on several cluster and field RRab variables for which reliable photometry and reddening estimates are available. Their relation:

$$(B - V)_0 = 0.507 - 0.052A_B + 0.223 \log P + 0.036[Fe/H] \quad (2)$$

allows us to derive the reddening by comparison with the average observed color, i.e. $(B - V)_S$. Using again the 45 RRab stars in Table 2 that show no evidence of peculiarity we find an average $E(B - V) = -0.001 \pm 0.016$.

Independent estimates, such as those obtained from dust maps (Schlegel et al. 1998), and by comparing the stellar content with the DIRBE/IRAS 100 μm dust emission (Dutra & Bica 2000),

both suggest a value of $E(B-V) \sim 0.01$ for M3.

A straight average of all these results leads to $E(B-V) = 0.01$, with an r.m.s. error of ~ 0.01 to account for both internal and external uncertainties. This is the value generally accepted in all recent studies for M3 and we adopt it in the following analysis.

Considering that for 20 program stars Car98 I-band data are available, we could in principle estimate the reddening from the (V–I) colors using the relation given by Mateo et al. (1995), who estimated that the intrinsic (V–I) color of RRab variables at minimum light, $(V - I)_{0,min}$, is nearly constant with a value of 0.58 ± 0.03 mag irrespective of metallicity. However, the I photometry by Car98 is likely affected by calibration problems, as we mentioned in Sect. 2.1, therefore this method could instead be used the other way around: from the 20 stars listed in Table 2 that have I photometry and have no photometric peculiarity we derive an average $(V - I)_{min} = 0.51 \pm 0.04$. Therefore, as a byproduct of this analysis and a consequence of the adopted value of reddening for M3, we find that the correction to apply to Car98 I photometry as a calibration offset is ~ -0.083 mag.

4.2. Calibration in T_{eff} and m_{bol}

A correct determination of temperature is of basic importance for the subsequent determination of the stellar physical parameters. For this purpose, the reddening must be known as accurately as possible, and the best color and color-temperature transformation equation must be used. We feel confident that a reliable value for the reddening is available (cf. Sect. 4.1). We have defined from our data a mean $(B-V)_S$ color that is as close as possible to the static color of the equivalent non-pulsating star (cf. Sect. 2.3). However, it has been argued that blue colors may be distorted by shock-induced effects in non static atmospheres (see Sect. 2.3), and that infrared (e.g. V–K) colors are better temperature indicators (Liu & Janes 1990; CSJ; Cacciari et al. 1992, and references therein). K photometry is available only for a small number of RR Lyrae stars in M3 (29 stars of which 9 RRC and 20 RRab, Longmore et al. 1990, hereafter L90), and we have used these data to test the dependence of temperature on the choice of color. We did not try to use the (V–I) colors that are available for a good number of stars, because we don’t think they are accurate or reliable enough for this purpose.

4.2.1. The temperature scales

For this test we have used six different temperature scales. All of them are listed in Table 4 except CSJ’, which is independent of color. We discuss them below in some detail.

- The model atmospheres by Castelli (1999, hereafter C99) are based on Kurucz models and were calculated with the standard mixing-length treatment of convection with no overshooting; we have

selected the model with metallicity $[m/H]=-1.5$ and α -element enhancement $[\alpha/\alpha_{\odot}]=+0.4$, and turbulent velocity $V_{turb}=4 \text{ kms}^{-1}$ which seems more appropriate for pulsating stars than the usual value of 2 kms^{-1} (we note that models with $V_{turb}=4 \text{ kms}^{-1}$ instead of 2 kms^{-1} produce higher temperatures by ~ 7 and 20 K at $(B-V)=0.2$ and 0.4 , respectively). We have adopted for all program stars $\log g=2.75$ interpolating linearly in the models for $\log g=2.5$ and 3.0 . We remind the reader that Kurucz’ (hence C99) models give a solar bolometric correction of -0.192 , therefore the values of BC_V have been corrected by adding $+0.122$ to the model values, as we assume $BC_V(\odot)=-0.07$ (corresponding to $M_{bol}(\odot)=4.75$) to be consistent with Montegriffo et al. (1998, hereafter M98) calibration.

- The empirical calibration by M98 (M98e) is based on Population II giants, namely about 6500 RGB and HB stars in 10 globular clusters, that were observed in both optical and near-IR bands. This relation is based on and works best for $(V-K)$ colors, but is defined also for $(B-V)$ albeit with a lower level of accuracy.
- M98 provide also a theoretical temperature scale (M98t) based on Bessell et al. (1998) solar metallicity models scaled to lower metallicities by the use of C99 models.
- Sandage et al. (1999, hereafter SBT) present a new set of model atmospheres for temperatures between 5000 and 7500 K. We have considered the $(B-V)$ colors and bolometric corrections of the models with $[A/H]=-1.5$ (by linear interpolation between the bracketing models at -1.31 and -1.66), turbulent velocity $V_{turb}=5 \text{ kms}^{-1}$, and $\log g=2.75$ (by linear interpolation between the bracketing models at 2.25 and 3.0), as shown in Fig. 7. $(V-K)$ colors are not given by SBT.
- Sekiguchi & Fukugita (2000, hereafter SF), using 270 *ISO* standard stars with accurate estimates of temperature (from IR colors) and known values of metallicity, gravity and $(B-V)$ color, have derived a $(B-V)$ color-temperature relation which they think is the least model-dependent. This relation holds for both dwarf and giant stars in the range $F0-K5$ ($0.3 \leq (B-V) \leq 1.5$) with metallicity $[Fe/H]=-1.5$ to $+0.3$, and is parameterized in their eq. (2) that takes into account the contributions of $(B-V)$, the gravity and the metallicity. No bolometric corrections are given, so we have derived them from C99 $T_{eff} - BC_V$ relation, because of the similarity of these two temperature scales.
- Finally, CSJ discussed in detail the problem of the temperature determination and proposed a set of equations, of which one (their eq. 16):

$$T_{eff} = 5040 / (0.261 \log P - 0.028 A_B + 0.013 [Fe/H] + 0.891) \quad (3)$$

depends on period, B light curve amplitude and metallicity and is independent of color, and is claimed to give “the best results in the derivations of equilibrium temperatures for RR Lyrae stars”. This parameterization is defined only for RRab variables. We have also used this method to derive another estimate of temperature for the RRab stars. The values of BC_V that we use along with CSJ temperatures have been derived by interpolation in C99 models, because of the similarity of these two temperature scales.

4.2.2. *A test based on the infrared colors*

We have considered the 29 RR Lyrae stars observed in the K-band by L90. These data are in the UKIRT photometric system, and before proceeding with the application of the above calibrations we must ensure that all K values are reported to a homogeneous system. We can do that by using 2MASS as an intermediate step and the relations between the relevant IR photometric systems given by Carpenter (2001). C99 K values are based on Bessell & Brett (1988) system (cf. Kinman & Castelli 2002), whereas M98 K values are in the ESO system which, according to M98 Table 2, is 0.056 mag brighter than Bessell & Brett in the K band. For these systems Carpenter (2001) gives the following relations:

$$K_{UKIRT} = K_{2MASS} - 0.004(J - K)_{2MASS} - 0.002 \quad (4)$$

$$K_{BB} = K_{2MASS} + 0.044 \quad (5)$$

hence we deduce that L90 values of K must be made fainter by ~ 0.047 mag when used with C99 models, and brighter by ~ 0.009 mag when used with M98 calibrations, assuming that $(J-K) \sim 0.25 \pm 0.1$ represents the color range of the instability strip.

With these corrections to L90 K photometric data, we have calculated the values of temperature T_{eff} from the (V–K) colors, using C99 and M98 calibrations. The colors were obtained as $\langle V \rangle$ (taken from Tables 1 and 2) minus $\langle K \rangle$ (from L90), and are a fairly good approximation of the average colors given the low amplitude and nearly sinusoidal shape of the (V–K) curves. We assumed a reddening $E(B-V) = 0.01$ and $E(V-K) = 2.76E(B-V)$ (Mathis 1999). We have calculated T_{eff} also from the $(B-V)_S$ colors listed in Tables 1 and 2, using all the color-temperature calibrations presented above, and using the color-independent relation by CSJ.

We show the results of this test in Fig. 7 and in Table 5 where we present the average values for the RRc, RRab and RRc+RRab separately, to retain some information on the trend with temperature that is clearly visible in the figure.

We note the following:

- i) $(B-V)_S$ colors lead to temperatures that may differ by up to ~ 450 K at $(B-V)_S \sim 0.3$, SBT giving the hottest temperatures and M98e giving the coolest. This is not surprising. C99 commented on this effect noticing that all models give higher temperatures than the empirical relations, generally by about 200 K. This discrepancy is reduced by a factor ~ 2 if (V–K) colors are used. By comparison, CSJ values are very similar to SF and they both fall in the middle range of the considered temperature scales, somewhat cooler than C99.
- ii) Within the same calibration, $T_{eff}(V-K)$ are quite similar to $T_{eff}(B-V)$ in the C99 calibration, and are instead hotter than $T_{eff}(B-V)$ by ~ 100 K in M98.
- iii) The values of BC_V are quite similar within M98 calibrations, the empirical scale giving systematically larger values than the theoretical one by $\sim 0.01-0.02$ mag.; the C99 scale gives smaller values than M98's by $\sim 0.02-0.04$ mag, and SBT gives smaller values than C99 by a further ~ 0.04 mag.

In summary, the temperature calibrations we have considered produce the least dispersed values of temperatures when (V–K) colors are used, and we seem to be able to define an average temperature scale with an *internal* uncertainty somewhat smaller than ± 100 K if we could use (V–K). However, color-temperature scales with (B–V) lead to a dispersion about twice as large. In general, there may be systematic errors of up to 200–300 K due to photometric calibrations, transformations and choice of temperature scale, and we cannot say which one of these relations is the most correct in *absolute physical* terms, unless we perform tests and comparisons with other parameters derived independently.

To this purpose, in the following sections we shall further verify the impact of temperature on the determination of physical parameters such as luminosity and mass, by confronting the results of pulsation and evolution theories and independent observational evidence.

4.3. The Mass-to-Light Ratio

From the pioneering work of van Albada & Baker (1971) on stellar pulsation, it is known that the period of a fundamental mode pulsator is related to its mass, luminosity and temperature via the relation:

$$\log P_0 = 11.50 + 0.84 \log L - 0.68 \log M - 3.48 \log T_{eff} \quad (6)$$

where M is the mass of the star and L its bolometric luminosity, in solar units. A recent re-determination of this relation based on non-linear pulsation models by Bono et al. (1997) includes also some dependence on metallicity (Caputo et al. 1998), i.e.:

$$\log P_0 = 11.242 + 0.841 \log L - 0.679 \log M - 3.410 \log T_{eff} + 0.007 \log Z \quad (7)$$

If we consider that $[\alpha/\text{Fe}] \sim 0.3$ for M3 (Kraft et al. 1993, 1995) would mimic a total metallicity content $[\text{m}/\text{H}] \sim -1.3$ (cf. Salaris et al. 1993), then $\log Z = -3.06$. Therefore the effective temperatures and periods of the variables can be used to derive a mass-luminosity parameter A for the fundamental pulsators defined as:

$$A = 0.81 \log M - \log L = 13.353 - 1.19 \log P_0 - 4.058 \log T_{eff} \quad (8)$$

This definition of the A parameter can be used also for first overtone pulsators provided their periods are fundamentalized by adding 0.127 to their $\log P_1$. We note that Caputo et al. (1998) give a separate pulsation relation for the first overtone pulsators, which yields essentially the same results.

We have applied eq. (8) to derive the A parameter for the 29 test RR Lyrae stars that were considered in the previous section, using the various estimates of temperature to evaluate their impact on the mass or luminosity determination. The values of A are listed in Table 5. Incidentally, we note that a further set of pulsation relations has become recently available (Marconi et al. 2003). We have verified that they produce systematically larger values of the A parameter by ~ 0.014 (RRc

stars) and 0.011 (RRab stars) respectively, that translate into larger masses by 0.01-0.02 M_{\odot} at fixed luminosity, or fainter magnitudes by 0.01-0.02 mag at fixed mass. These differences are well below the errors of these estimates and do not affect significantly the following analysis and considerations.

4.3.1. *The luminosity of the RR Lyrae stars assuming a fixed mass*

From the A parameters derived in the previous section we can estimate the luminosity of the RR Lyrae stars if we know their mass. Masses can be obtained in two independent ways: adopting the values of the stellar evolution theory for HB stars, that usually range from 0.65 to 0.75 M_{\odot} , or from the stellar pulsation theory applied to double-mode pulsators (RRd). The most recent analysis and discussion of 8 RRd stars in M3 by Clementini et al. (2004) shows an unusually large dispersion in mass for these stars. Whether this reflects a similarly large mass dispersion for all HB (hence RR Lyrae) stars is not clear. We assume we can consider a constant mass for these stars, and for this we take the weighted average of the mass determinations for these 8 RRd stars, i.e. $0.74 \pm 0.06 M_{\odot}$. We note, however, that masses of RRd stars are quite uncertain as they depend strongly on modelling (in particular on the adopted metallicity scale), and on the accuracy of the period determinations (cf. Bragaglia et al. 2001). On the other hand, the most recent models of HB stellar evolution (e.g. Sweigart 1997; Marconi et al. 2003) would rather favour a value around 0.67-0.69 M_{\odot} , so we consider 0.68 M_{\odot} as the evolutionary mass of RR Lyrae stars in the following.

Using these values for the stellar mass and the values of $A = 0.81 \log M - \log L$ (r.m.s. error ± 0.03) listed in Table 5 we then derive the corresponding values of absolute magnitude M_V that are also listed in Table 5, assuming $M_{bol}(\odot) = 4.75$. We see that these values vary by up to nearly 0.3 mag, from 0.42 to 0.70, are very dependent on the temperature calibrations and quite sensitive as well to the adopted mass. Also the choice of color can make a difference, in particular the M98 calibrations do not produce consistent results from (B–V) vs. (V–K), whereas the discrepancy is much smaller with the C99 calibration.

How accurately and precisely do we know the masses of the RR Lyrae stars, to start with? This quantity is still quite uncertain, and we have negligible prospects to improve our knowledge by measuring any masses directly. We are more likely to improve our distance estimates to clusters in the near future, so M_V will become increasingly well known. Therefore we turn the problem around and use the mass-to-light parameter A to estimate the mass at fixed luminosity.

4.3.2. *The mass of the RR Lyrae stars assuming a fixed luminosity*

If we assume that globular cluster and field RR Lyrae stars share the same characteristics (Catelan 1998; Carretta et al. 2000), we may use the results by Cacciari & Clementini (2003) who estimated from several independent methods the average absolute magnitude for the RR Lyrae

stars with $[\text{Fe}/\text{H}]=-1.5$ as $\langle M_V \rangle = 0.59 \pm 0.03$ mag. This is in agreement with the most recent synthetic HB models by Catelan et al. (2004) that would predict $\langle M_V \rangle \sim 0.6$ at $\log Z = -3.06$ (corresponding to $[\text{Fe}/\text{H}]=-1.5$ with α -element enrichment $+0.3$). On the other hand, the accurate study of RR Lyrae stars in the LMC by Clementini et al. (2003) and the pulsational distance modulus of 15.07 ± 0.05 mag for M3 estimated by Marconi et al. (2003) would favour a brighter value around 0.54-0.55 mag. We therefore consider that values of $\langle M_V \rangle$ in the range 0.54-0.59 mag are quite reasonable based on independent empirical and/or theoretical considerations. These values, inserted in eq. (8), lead to the values of mass listed in Table 5. Typical error of these determinations is $\pm 0.05 M_\odot$.

Again, we see that the values of mass range from about 0.6 to nearly $0.8 M_\odot$ between calibrations, but vary by less than $0.05 M_\odot$ within each color/calibration. However, the estimates in the restricted range ~ 0.68 - $0.74 M_\odot$, that we regarded as “plausible” in the previous section, are not so many. Limiting for simplicity to the RRab variables, that are more numerous hence better representative of the entire population, only the M98 scales lead to acceptable results using (V–K) colors. With (B–V) colors, acceptable results come from M98 theoretical and SF (which gives nearly identical results to CSJ).

To summarize, in order to optimally exploit our large and accurate database we need to use (B–V) colors, since (V–K) colors are available only for few stars, and the color-independent scale of CSJ is only applicable to RRab variables. On this basis, there are two temperature scales that may provide plausible estimates of both mass and luminosity, i) M98 theoretical, leading to fainter and more massive stars (in agreement with the most recent results on the mass of RRd stars, with theoretical HB models by Catelan et al. 2004, and with the average of several different estimates of absolute luminosity for RR Lyrae stars), and ii) SF, leading to slightly brighter and less massive stars (in agreement with the most recent estimate of distance to the LMC and with stellar evolution and pulsation models). However, the M98 calibrations are more accurate and reliable when used with infrared colors (cf. Sect. 4.2.1), that would rather support the brighter and less massive solution. Therefore we assume for M3 the distance modulus $(m-M)_0 = 15.07$ and adopt the SF calibration as a working hypothesis for our subsequent analysis, keeping in mind that a somewhat cooler temperature scale (e.g. by ~ 150 K) or a shorter distance modulus (e.g. by ~ 0.05 mag) might be also acceptable.

In Fig. 8 we show the fundamentalized period P_0 vs $T_{eff}(B-V)$ for our 29 test stars. The line shown in the plot indicates the best fit to the data using a slope of -3.41 according to eq. (7). The corresponding zero-point yields a value $A = -1.82 \pm 0.03$. The longP/overluminous stars V85 (RRc) and V60, V65 and V124 (RRab) stand out clearly in this plot. For comparison, we show also the T_{eff} values obtained from the CSJ temperature scale (eq. 3) for the same RRab stars (indicated as crosses). We see that the SF and CSJ scales are very similar because both sets of temperatures fit the same $\log P - \log T_{eff}$ relation, the CSJ determinations with a significantly reduced scatter. The three evolved RRab stars still fall clearly off the main relation, but by a smaller amount, and this leads to a smaller value of the period shift at fixed temperature, i.e. $\Delta \log P$ decreases from

~ 0.069 (with the SF temperatures) to ~ 0.043 (with the CSJ temperatures). This shows the great potential of the CSJ reddening-independent temperature parameterization and its application to those cases where reddening can be a problem or the data are not sufficiently accurate for a good definition of the mean color.

5. The physical parameters of our program RR Lyrae stars

We have applied SF color-temperature calibration to all our RRc, RRab and Blazhko stars using the $(B-V)_S$ colors listed in Tables 1, 2 and 3. For the Blazhko stars we have used the average value of the 1992 and 1993 CC01 photometric data. We have calculated the corresponding values of temperature, hence bolometric corrections borrowing the C99 $T_{eff} - BC_V$ scale. Bolometric magnitudes and luminosities were then obtained from the values of $\langle V \rangle_0$ and $(m-M)_0=15.07$, and the A parameter and the mass were estimated from eq. (8). The results are listed in Table 6 for the RRc and RRab stars, and in Table 7 for the Blazhko stars. For the sake of completeness, we have calculated the same physical parameters using the CSJ temperature calibration (for RRab stars only) expressed in eq. (3), and we compare the results in the following sections whenever relevant.

Typical errors for the above parameters of each individual star are $\Delta T_e = \pm 100$ K, $\Delta BC_V = \pm 0.02$ mag, $\Delta \log L = \pm 0.03$, $\Delta M_V = \pm 0.07$ mag, $\Delta A = \pm 0.03$, $\Delta M/M_\odot = \pm 0.05$ and $\Delta \log g = \pm 0.10$.

5.1. Comparison with evolution and pulsation models

With our database and the adopted temperature calibration we may test recent theoretical models of HB evolution and RR Lyrae pulsation, within the limits of the respective uncertainties. We show in Fig. 9 how periods and the physical parameters we have derived in the previous sections behave as a function of temperature, for all our program RRc and RRab variables. The Blazhko stars are not shown to avoid confusion, but they behave like the RRab variables. The results obtained from the CSJ temperature calibration are shown in Fig. 10. Two recent studies of the evolutionary and pulsational characteristics of M3 RR Lyrae variables (Marconi et al. 2003; Catelan 2004) provide detailed theoretical reference frames, for comparison. The results proposed in those papers are compatible with the considerations presented below.

5.1.1. $\log P$ vs $\log T_{eff}$

First, we compare our results with the basic requirements of the pulsation theory. The preliminary test performed on a subset of 29 stars using $(V-K)$ colors (cf. Sect. 4.3) produced a $\log P - \log T_{eff}$ relation that is shown in Fig. 8. This relation, reported in Fig. 9 lower panel for

ease of comparison, represents well also the main body of the RRc and RRab stars whose temperatures have been derived from (B–V) colors. The stars with unusually long periods, that were noticed in the period-amplitude and period-color diagrams (see Sect. 3.2 and 3.3), stand out clearly in this diagram as well, as expected. The same relation is defined by the CSJ temperatures, with a somewhat smaller dispersion, as one can see in Fig. 10. The evolved stars stand out of the main relation, but with a smaller offset corresponding to a smaller period shift at fixed temperature. The temperature range defined by the CSJ scale is very nearly the same as that defined by the SF scale if one excludes the coolest evolved star V202.

5.1.2. $\log L$ vs $\log T_{eff}$

This is perhaps the most critical diagram because is a place where we can in fact test the correctness and accuracy of our own calibrations. To perform this test, we have derived for each star the offset in $\log L$ with respect to the reference ZAHB level we have estimated at $\log L \sim 1.66$ at mid temperature range ($\log T_{eff}=3.83$), and compared it with the corresponding offset in V magnitude with respect to the observed ZAHB level that we have identified at $V=15.72$ (cf. Sect. 3.1). We show the diagram of the $\Delta \log L$ vs. ΔV offsets in Fig. 11, for all the RRc and RRab stars listed in Tables 1 and 2. We see that the offsets are well represented by a relation of slope 1, and fall, with no exceptions, within ± 0.07 mag of this relation, which is the typical error we have estimated for the luminosity. The same result, with a somewhat smaller scatter, is obtained by using the CSJ temperatures (but we note that this reduced scatter is partly due to the missing RRc stars). Therefore, we deduce that our calibration is reliable and accurate, within the uncertainties of these estimates, and we proceed with a more detailed comparison with stellar evolution models.

We compare the luminosities and temperatures we have derived with three sets of theoretical evolutionary models for the ZAHB phase, i.e. Sweigart (1997, solar scaled $[\text{Fe}/\text{H}]=-1.6$, main sequence helium abundance $Y=0.23$, no helium mixing during the RGB phase), Vandenberg et al. (2000, $[\text{Fe}/\text{H}]=-1.54$, $[\alpha/\text{Fe}]=0.3$) and Straniero et al. (1997, solar scaled $[\text{Fe}/\text{H}]=-1.63$). Within the uncertainties the models are all quite similar, and our stars are fully compatible with them. The best match is given by the Sweigart ZAHB that practically coincides with the lower envelope of our distribution ($\log L=1.666$ at $\log T_{eff}=3.83$), whereas Vandenberg et al.’s is fainter by ~ 0.02 mag, and Straniero et al.’s is brighter by about the same amount. The evolved stars that were labelled as longP/overluminous in Sect. 3 stand clearly out of the main relation.

We also compare this distribution with the theoretical limits of the instability strip calculated by Bono et al. (1995) for a helium abundance $Y=0.24$ and two values of the HB stellar mass, 0.65 and $0.75 M_{\odot}$. We see that our instability strip is systematically hotter by ~ 150 K. The temperature of the blue edge of the instability strip, taken as the temperature of the second bluest RRc star in Tab. 6, is ~ 7300 K, and the width of the instability strip is $\Delta \log T_{eff}=0.074$ (see Marconi et al. 2003, and Catelan 2004, for recent discussion on the instability strip edges). As for the detailed distribution within the strip, Bono et al. (1995) assumed $M=0.65 M_{\odot}$ as appropriate for

M3 and concluded that the zone between the fundamental blue edge (FBE) and the first overtone red edge (FORE), where both pulsation modes are possible, is populated mostly by RRab stars, and, hence, the direction of evolution on/near the ZAHB is mainly blueward. This would be in agreement with Lee et al. (1990) evolutionary models, and with the interpretation of the Oosterhoff dichotomy as mostly due to the hysteresis mechanism in the pulsation modes. However, we don't quite see this effect with our data: the FBE-FORE zone appears to be populated by a nearly equal number of RRC and RRab stars in the $M=0.65 M_{\odot}$ strip, and only at $M=0.75 M_{\odot}$ the RRab stars outnumber the RRC. In a likely intermediate solution with $M\sim 0.7 M_{\odot}$ the FBE-FORE zone should still be populated by a non-negligible number of RRC stars. These considerations hold also with the temperatures and luminosities derived from the CSJ calibration, and would be even more important had we used the cooler temperature scale by M98, hence casting some doubts on the hysteresis mechanism as the only or most important way to explain the Oosterhoff dichotomy (cf. Sect. 3.2.3).

If period changes and mode switching can be taken as indicative of direction of evolution, our result is confirmed by the study of period changes by CC01 who find a nearly equal number of RR Lyrae stars near the ZAHB with decreasing and increasing periods. Also, four double-mode pulsators have been found switching pulsation mode during the last few years: of these, three have switched from fundamental to first overtone mode, i.e. V79 (Clement et al. 1997; Clement & Shelton 1999b), V166 (Corwin et al. 1999) and V200 (Clementini et al. 2004), whereas one (V251) has switched from first overtone to fundamental mode (Clementini et al. 2004), suggesting that both redward and blueward evolution can occur among the HB stars in M3. We also point out that CC01 noted several stars as having strongly variable periods over the last ~ 30 -50 years, among them the three longP/overluminous RRC stars V70, V129 and V170. These period variations are too strong to be ascribed to a normal rate of evolution, and rather suggest irregularities in the pulsation (possibly a prelude to mode switching?): V70 and V129 have increasing periods, and V170 has a decreasing period.

5.1.3. *Mass vs log T_{eff}*

In this diagram we see that the values of mass we have derived from the A parameter and the luminosity follow quite well the theoretical trend with temperature, with only few stars deviating from the mean distribution by more than $\pm 0.1 M_{\odot}$. The scatter of this relation is further reduced by the use of the CSJ temperatures (cf. Fig. 10). From the present data listed in Tables 6 and 7 the average values of mass for the regular RRab and RRC stars with no photometric anomaly are $\langle M \rangle = 0.71 \pm 0.03$ ($\langle M \rangle = 0.70 \pm 0.05$ from CSJ temperatures) and $0.70 \pm 0.05 M_{\odot}$, respectively. The average mass of the Blazhko stars is $\langle M \rangle = 0.70 \pm 0.08$, i.e. identical to the regular stars. These estimates compare very well with the mass values of ZAHB stars in Sweigart and Straniero et al. evolutionary models (i.e. 0.68 and $0.69 M_{\odot}$, respectively), but are somewhat larger than the mass of VandenBerg et al.'s model, $0.64 M_{\odot}$. This is due to the different temperature scale used

by Vandenberg et al. (2000), which is slightly steeper than SF calibration and is hotter by ~ 100 K at the reference mid range temperature $\log T_{eff}=3.83$. Such a temperature difference leads to smaller values of the A parameter by ~ 0.025 , that combined with the slightly smaller luminosities (by ~ 0.008 in the log) lead to smaller values of the mass by $\sim 9\%$, i.e. $\sim 0.06 M_{\odot}$.

5.1.4. $\log g$ vs $\log T_{eff}$

Once the values of temperature, luminosity and mass are known, the gravity can be derived from the equation of the stellar structure (cf. eq. 21). In this diagram we see that the values of gravity we have derived follow the same trend with temperature as the theoretical predictions, with little scatter. This of course mirrors the behaviour of mass, as discussed in the previous section.

From the data listed in Table 6 the average values of gravity for the RRc and RRab stars are $\langle \log g \rangle = 2.94 \pm 0.04$ and 2.81 ± 0.04 (2.80 ± 0.04 from the CSJ temperature scale), respectively. The corresponding values at $\log T_{eff}=3.83$ are ~ 2.86 in Vandenberg et al.'s ZAHB model, and 2.88 in the two other models.

5.2. On the evolutionary status of the RR Lyrae variables and the nature of the longP/overluminous stars

In order to investigate in some detail the nature of those 19 (5 RRc, 9 RRab and 5 Blazhko) stars that were identified in Sect. 3.1 as longP/overluminous we have plotted again in Fig. 12 the values of $\log L$ vs $\log T_{eff}$, and for comparison the ZAHB models calculated by Vandenberg et al. (2000) and by Sweigart (1997) that we have presented in Sect. 5.1.2. Here we show some additional models by Sweigart (1997), in particular the ZAHB corresponding to helium mixing $DX=0.05$ during the RGB phase, and three evolutionary tracks for no helium mixing and the Reimers (1975) mass loss efficiency parameter $\eta=0.446$, 0.378 and 0.300. The helium mixing parameter DX measures the depth into which the mixing currents are assumed to penetrate the hydrogen shell: all of the helium produced exterior to that point is mixed into the envelope. As an example, $DX=0.05$ increases the envelope helium abundance at the tip of the RGB by about 0.03 dex with respect to the no-mixing case $DX=0.0$ (cf. Sweigart 1997 for more details). We notice the following:

i) The lower envelope of the RRc and RRab star distribution is very well represented by the Sweigart ZAHB with $DX=0.0$. Within the errors of these determinations, also the Vandenberg et al. ZAHB, which is ~ 0.02 mag fainter, may provide an acceptable match. Four RRab stars (V76, V77, V134 and V197) fall below the ZAHB: they all have been noted for having somewhat incomplete and/or noisy light curves.

ii) If we consider that an intrinsic thickness of ~ 0.1 mag of the stellar distribution is normal (see also Fig. 1), as it corresponds to that part of the HB evolutionary phase where the stars spend

most of their HB lifetime, there is however a good number of stars that are brighter than this value. For these we can think of three possible explanations:

1. The most obvious (and least interesting) suggestion is that the photometry for some of these overluminous stars may be contaminated by the presence of a companion. Although this phenomenon is likely to be rather unfrequent, Table 2 notes that 3 of the 4 brightest RRab stars (V48, V58, V146 and V186, all with $\log L \gtrsim 1.74$) may have companions making them appear to be too bright. Further, all four stars do not have unusually long periods for their colors or temperatures, indicating they have higher gravities and lower luminosities.

2. The overluminous stars could be stars that have undergone some degree of mixing during the RGB phase, and have therefore a slightly higher abundance of helium in the atmosphere which makes them brighter (Sweigart 1997). This is compatible with observational spectroscopic evidence, e.g. enhanced C-isotope ratios and lithium abundance (Pilachowski & Sneden 2001), and the CN-CH anticorrelation (Lee 1999; Smith et al. 1996) among M3 red giants that suggests the presence of mixing and dredge-up of processed material (including helium) in the atmosphere of these stars. We have plotted for comparison the Sweigart (1997) ZAHB model for a mixing value $DX=0.05$ and we see that all our stars fall below this ZAHB, except the three brightest RRc stars. The explanation based on the mixing hypothesis can only be tested with a high-resolution abundance analysis of these stars, that should possibly be extended to include the entire HB from red to blue for a more accurate and conclusive analysis of this issue. Incidentally, high resolution spectra can also be used to explore line broadening (provided the exposure times are short enough to avoid velocity smearing and the observations are taken at carefully selected phases). In this respect we note that Carney et al. (2003) detected line broadening, that was interpreted as a sign of rotation, among luminous RGB and red HB stars in the field, and a similar behavior was found among luminous red giants in M3 by Carney et al. (2004). Rotation may contribute to either mixing or mass loss, and therefore have an influence on HB evolution.

3. Alternatively, or in addition to the previous explanation, the overluminous stars could be in a more advanced stage of evolution off the ZAHB than the main body of the RR Lyrae variables. For comparison, we have plotted three evolutionary tracks from Sweigart (1997) models, corresponding to zero mixing and different values of the Reimers mass loss parameter, i.e. $\eta=0.446$, 0.378 and 0.300 (note that the entire ZAHB is described by values of η from 0.00 to 0.74). We have selected these three values because they either start and evolve mostly within the instability strip ($\eta=0.300$), or they start hotter than the instability strip and evolve across it at a plausible luminosity ($\eta=0.378$ and 0.446). Smaller values of η start cooler than the strip and don't enter it, and larger values of η would cross the strip at too high luminosity levels and at a very fast evolutionary rate. We can see that basically all stars fall on or near the tracks with η values between 0.300 and 0.378, at various stages of evolution off the ZAHB, and some evolved stars would be consistent with higher values of mass loss ($\eta \sim 0.446$). In this respect, we don't agree with the conclusion of Jurcsik et al. (2003) that "... in M3, on the average, RRc stars are already in a later phase of their HB evolution than the RRab variables". The difference between these two groups could simply be due to stochastically different mass loss that causes the less massive stars to populate the first-overtone (bluer) part of

the instability strip. This would apply to all RRc stars, not only to the overluminous ones, in agreement with the fact that the average mass of the RRc stars seems to be about $0.02 M_{\odot}$ smaller than the mass of the RRab stars (cf. Sect. 5.1.3), although this difference is indeed smaller than the r.m.s. errors of these determinations.

To test the plausibility of this explanation we have examined the HB lifetimes at various luminosity levels off the ZAHB using the $\eta=0.300$ track. We see that the stars spend $\sim 2/3$ of their total HB lifetime (i.e. ~ 65 My) between the ZAHB luminosity level and the brighter magnitudes within 0.1 mag of the ZAHB (i.e. in a luminosity interval $\Delta \log L \sim 0.04$), progressively accelerating their evolution as they become brighter (i.e. spending 5% of the total lifetime, and then 3.5%, 3% and 2% over the following 0.05 mag steps). Nearly 80% of the total HB lifetime is spent between the ZAHB and the 0.3 mag brighter level.

In order to estimate the number of stars in the HB evolutionary phase we can use the *fuel consumption equation* by Renzini & Fusi Pecci (1988):

$$N_j = B(t)L_T t_j \tag{9}$$

where N_j is the number of stars predicted by the stellar evolution theory in a given post-main-sequence evolutionary phase, t_j is the lifetime of that phase in yr, L_T is the total luminosity (in solar units) of the stellar system and $B(t)$ is a specific evolutionary flux that is a function of age and can be taken as $2.15 \cdot 10^{-11}$ for a system as old as M3. For $t_{HB}=10^8$ yr and $L_T = 3.4 \cdot 10^5 L_{\odot}$ for M3 (Harris 1996), N_{HB} turns out to be about 730 stars. The morphology of the HB in M3 has been studied in detail with stellar counts by Ferraro et al. (1997), and from their results we can expect that about $\leq 40\%$ of all the HB stars evolve and can be detected as RR Lyrae variables, e.g. something like 290 stars. This is of course just a rough estimate, but quite consistent with the observational evidence (cf. Clement et al. 2001). Of these stars, about 65% (i.e. 190 stars) are expected to populate the zone between the ZAHB and the 0.1 mag brighter level, and about 5% (i.e. 15 stars) the brighter 0.05 magnitude interval, reaching $\log L \sim 1.75$.

These estimates agree very well with the observational data and indicate that either one of the above explanations, or more likely a combination of both, can account for the presence of the longP/overluminous RR Lyraes that have been detected in M3.

To summarize on the evolutionary status of our target stars, we can compare again Fig. 1 and Fig. 12 and note that:

- i) the main body of the RRc, RRab (and Blazhko) stars has a luminosity distribution with a FWHM ~ 0.1 mag and a range ~ 0.2 mag, whose faint end corresponds to the ZAHB at $V=15.72$. These stars are compatible with being in the first 65% of their HB life.
- ii) There is a significant number of brighter stars distributed more loosely around $V \sim 15.52$ and few outliers up to 0.2 mag brighter. Most of these stars have longer periods than the stars of similar amplitude (temperature), and are compatible with being on a more evolved stage of their HB life. Some of these unusually bright stars could have enhanced helium in their atmospheres due to extra-mixing during the RGB phase. For some, the presence of a companion affecting the

photometric data cannot be excluded.

iii) Although the evidence is marginally significant, the RRc stars might be on average slightly less massive than the RRab stars. There is no evidence that they are more evolved.

6. The Fourier analysis of the light curves

The description of pulsating variable light curves using Fourier series started with Schaltenbrand & Tammann (1971) on Cepheids, later followed by Simon & Lee (1981), Simon & Teays (1982) and Simon (1988) on RR Lyrae stars. Then, in a series of papers (Simon & Clement 1993, hereafter SC93; Kovács & Zsoldos 1995; Jurcsik & Kovács 1995, 1996; Kovács & Jurcsik 1996, 1997; Kovács & Kanbur 1998; Kovács & Walker 2001) it was shown that appropriate combinations of terms of a Fourier representation of RR Lyrae light curves, along with the periods, correlate with intrinsic parameters of the stars such as metallicity, mass, luminosity and colors. The most recent analysis of Fourier parameters and their physical meaning in the study of RR Lyrae stars is given by Sandage (2004a).

The Fourier analysis may offer tremendous potential to the study of these stars (e.g. their absolute magnitude hence distance, intrinsic colors hence reddening and temperature, mass and metal abundance), especially since large collections of good light curves are becoming available, even for distant stars, thanks to the photometric surveys dedicated to gravitational lensing events. Therefore, it is important to explore the reliability of this type of analysis in more detail, and our M3 data are very useful tests of the several calibrations between Fourier coefficients and physical parameters. We anticipate our conclusions, namely that all the physical parameters derived from Fourier Transform coefficients are affected by some (systematic) inaccuracy that in a few instances can be rather serious and make them unreliable. In general, more work is needed to reanalyse and recalibrate this technique before it can be used with confidence. In the following sections we discuss in detail how we have tested the Fourier results and reached our conclusions.

We have decomposed the V light curves of all variables listed in Tables 1, 2 and 3 in Fourier series of cosines, using 6 components for the RRc variables and 6 to 15 components for the RRab and Blazhko stars. We list in Tables 8, 9 and 10 the resulting Fourier parameters, respectively, where A_n are the amplitudes of the n-th components, A_{n1} are the amplitude ratios A_n/A_1 , and ϕ_{n1} are the phase term differences $\phi_n - n\phi_1$. For the RRab and Blazhko stars we have also estimated the Dm parameter, defined by Jurcsik & Kovács (1996) and Kovács & Kanbur (1998) as the maximum value among several combinations of Fourier coefficients, and represents a quality test on the regularity of the shape of the light curve. All the formulae defined by Kovács and collaborators relating physical stellar properties to Fourier parameters are applicable and “reliable” only if the *compatibility condition* $Dm < 3$ is met. In the calculation of the Dm parameter all values of $\phi_{41} < 2$ listed in Tables 9 and 10 have been increased by 2π in order to bring them to the typical value range of ϕ_{41} . The Dm parameter is listed in the last column of Tables 9 and 10.

Since one of the aims of this study is to get an idea of how a Blazhko star changes its observable parameters during the Blazhko modulation cycle, we have applied the Fourier analysis separately also to the Kal98 and Car98 V light curves, when available, and listed the corresponding Fourier parameters in Table 10. By comparing with Kal98 results on common non-Blazhko stars, we note that our estimates of Dm are systematically smaller, which is probably due to the fact that we have applied a different set of equations (Kovács & Kanbur 1998, their Table 2) with respect to Kal98. However, all values listed in Table 10 have been calculated with the same procedure, and are therefore homogeneous and comparable.

An inspection of the Dm values derived for both RRab and Blazhko variables leads us to two important considerations:

i) In Table 9, of the 67 RRab stars that we have selected for our analysis, 12 have $Dm > 5$, 11 have $3 < Dm < 5$, and the remaining 44 have $Dm < 3$. Therefore, in spite of the severity of our initial selection criteria on photometric quality, only 2/3 of our sample meet the strictest requirement ($Dm < 3$) set by Kovács & Kanbur (1998) for the application of their relations to derive “reliable” stellar physical parameters. This fraction goes up to 82% if this requirement is slightly relaxed ($Dm < 5$).

ii) In Table 10, of the 38 Blazhko stars selected for our analysis, 14 stars have $Dm < 3$ in at least one Blazhko phase and $Dm < 5$ at all other phases; 2 stars have $Dm < 5$ at all detected Blazhko phases; of the remaining stars, 17 show at least one value larger than 5 at some Blazhko phase, *as well as* values smaller than 5 and even 3 at some other Blazhko phase. Altogether, we detect as much as $\sim 40\%$ (63%) cases of Blazhko stars with $Dm < 3$ (5), *with no correlation with the amplitude of the corresponding light curves*.

Recall that Szeidl (1976, 1988) found that Blazhko RR Lyrae stars, when observed at the Blazhko modulation phase corresponding to the largest light curve amplitude, behave like regular stars. In order to verify whether there is any “regular” phase during Blazhko modulation, Jurcsik et al. (2002) have re-examined 4 field Blazhko RR Lyrae variables: RR Lyr at 6 Blazhko phases, RV UMa at 8 Blazhko phases, AR Her at 4 Blazhko phases, and RS Boo at 3 Blazhko phases. They set rather strict criteria for regularity, one of them being $Dm < 2$, and conclude that only stars with small Blazhko amplitude modulation can show regular light curves at some Blazhko phases, a rather small fraction ($\leq 20\%$) of the total considered cases. Therefore, a criterion such as $Dm < 2$ could be quite effective at detecting non-regular (Blazhko) stars, but is also more severe than the requirement $Dm < 3$ set by Kovács & Kanbur (1998) for the applicability of their formulae, and so excessively penalizing (e.g. only 27 of our 67 supposedly regular RRab variables would meet this criterion). On the other hand, by adopting the criterion $Dm < 3$, we find that a relatively large fraction of known Blazhko stars show regular curves at some Blazhko phase. We conclude that *the condition $Dm < 3$ is not an effective indicator of the Blazhko behaviour*, contrarily to the conclusions reached by Jurcsik & Kovács (1996).

In the following sections we shall apply Kovács & Kanbur (1998) relations to all our target

stars, but consider the results only when $Dm < 5$. We have adopted a slightly relaxed criterion with respect to the original one in order to improve the statistics, after we have verified that this does not lead to any significant difference in the resulting physical parameters.

6.1. Pulsation modes

The first use of the Fourier parameters is aimed at identifying the pulsation mode of the stars, which may be ambiguous in a few cases. In Fig. 13, upper panel, we show A_{21} as a function of ϕ_{21} , for all normal stars in Tables 1 and 2. The fundamental and first overtone pulsation modes are clearly separated at $A_{21} \sim 0.3$. We note that V202, supposedly an RRab star with very long period and small amplitude, falls in the domain of the RRC pulsators. A few stars falling off the main RRC distribution (cf. Sect. 3.2) are marked: we find again the overluminous variables V70, V129 and V170, and V203 that can be an RRe pulsator, whereas V105 and V178 fall within the group of normal first overtone pulsators. In the lower panel we show the Blazhko stars in the large amplitude (filled circles) and small amplitude (open circles) phase: they mostly fall in the typical RRab domain, except a few small-amplitude cases on the borderline and V41 in the small amplitude phase that falls clearly in the RRC domain (but its light curve is rather bad and the Dm parameter is large). Therefore we conclude that, at least in the sample we have selected, all the Blazhko stars seem to pulsate in the fundamental mode.

6.2. Physical properties derived from Fourier parameters

Although the physical link between the Fourier parameters describing the shape of a light curve and the physical parameters of that particular pulsating star is not yet understood, nevertheless clear and well defined relations have been found empirically.

The work by SC93 deals with first-overtone RR Lyrae variables using Fourier decomposition in cosine series of V light curves to estimate the mass, luminosity and temperature of these stars. The work by Kovács and collaborators has focussed instead on the fundamental pulsators, with the exception of Kovács (1998) who provides a relation to estimate the absolute magnitude M_V of RRC stars. The relations defined for the RRab stars allow to derive parameters such as M_V , $[\text{Fe}/\text{H}]$, intrinsic color and temperature, based on the Fourier decomposition in sine series of V light curves. Therefore, before applying these relations we have corrected our phase parameters ϕ_{21} , ϕ_{31} and ϕ_{41} values (listed in Tables 9 and 10), that were derived from cosine series, by -1.57 , $+3.14$ and -4.71 respectively.

Tables 11, 12 and 13 list the physical parameters we have derived for the RRC, RRab and Blazhko stars, respectively. We shall discuss them in more detail in the following sections.

6.2.1. The Metallicity $[Fe/H]$

The connection between the period and the Fourier parameter ϕ_{31} of the V light curve of a RR Lyrae variable star was investigated already several years ago (Petersen 1984; Simon 1989, 1990), and it was initially attributed to a dependence on the star mass by Simon. From the analysis of RRC stars in five globular clusters, Clement et al. (1992) found the trend with metallicity of the ϕ_{31} -period relation, which “appears to be the Sandage period shift in another guise”. Indeed, Sandage (2004a) reaches the same conclusion from the detailed analysis of 55 field RRab stars. So, although the physical significance of the ϕ_{31} -period relation may still be elusive, its connection with metallicity is well defined. This relation can therefore be used to derive estimates of metallicity for variable stars once their periods and V light curves are known with sufficiently good accuracy.

From the analysis of 272 V light curves of RRab stars taken in nearly equal number from the Galactic field, the Galactic globular clusters and the Sculptor dwarf galaxy, and using high-dispersion spectroscopy for the metallicities, Jurcsik (1998) derived the relation (for RRab stars):

$$[Fe/H] = -5.038 - 5.394P + 1.345\phi_{31} \quad (\text{r.m.s. error of the fit } 0.14 \text{ dex}) \quad (10)$$

The zero-point of this new metallicity scale compares to the traditional ZW scale as $[Fe/H]_J = 1.431[Fe/H]_{ZW} + 0.88$ (Jurcsik 1995), and for M3 yields $[Fe/H]_J = -1.50$, therefore the application of eq. (10) should give consistent values of metallicity with our assumptions.

We list these $[Fe/H]$ determinations in Tables 12 and 13. The average values of metallicity we derive, considering only the RRab (or Blazhko) stars with $Dm < 5$, are $\langle [Fe/H]_J \rangle = -1.39 \pm 0.11$ for the 45 normal RRab stars, -1.40 ± 0.14 for the 6 longP/overluminous stars, and -1.17 ± 0.05 for the 4 low amplitude/suspected Blazhko stars.

Here a few comments can be made:

i) The zero-point of eq. (10) obviously depends on the entire calibrating sample, and the spectroscopic value of metallicity for M3 (from RGB stars) is ~ 0.1 dex more metal poor than the value predicted by eq. (10). The comparison with Sandstrom et al. (2001) spectroscopic abundances of 29 RR Lyraes, that was done by Jurcsik (2003), is hardly useful since these abundances are based on low resolution spectra and their accuracy is quite poor. Direct spectroscopic abundances of RR Lyrae stars in the LMC have been obtained by Gratton et al. (2004) and compared with $[Fe/H]$ estimates from eq. (10). Because of large errors and a possible spread in metallicity, and the presence of a significant number of outliers, the comparison of the spectroscopic and Fourier metallicity determinations does not appear very conclusive, although some general agreement is indeed evident. A recalibration of the $[Fe/H]$ -period- ϕ_{31} relation has been performed by Sollima et al. (2004) using a non-parametric fitting routine based on local polynomial surface fitting on a database of 287 RRab variables in 18 globular clusters. The cluster metallicities are taken from KI, and the r.m.s. of the fit is ~ 0.16 dex. Based on the 25 calibrating clusters used by Jurcsik (1995), we have compared these two metallicity scales and found that they are roughly linearly related as $[Fe/H]_J = 0.8[Fe/H]_S - 0.2$. We show in Fig. 14 the histograms of the metallicity distributions derived from eq. (10) (shaded area) and from Sollima et al. (2004) recalibration (solid

line) for the 45 regular RRab stars considered above. The average value from this recalibration is $\langle [Fe/H]_S \rangle = -1.43 \pm 0.07$, in good agreement with the average value from eq. (10) and indicating that M3 lies indeed ~ 0.1 dex off the calibration defined by a large number of globular clusters, irrespective of the fitting method and metallicity scale. The recalibrated metallicity distribution appears to be narrower and somewhat different in shape than the distribution from eq. (10). In the case of M3 these differences are well below the errors of the respective determinations, and we may conclude that the two distributions are on average comparable, within the respective errors. However, these differences could be much more significant in the case of a composite population with an intrinsic spread in metallicity, and then it would be important to assess which fitting method and/or metallicity scale yields the metallicity distribution that best reproduces the spectroscopic one.

ii) The r.m.s. errors we estimate from our sample of 45 best stars are well below the intrinsic accuracy of the fits given by Jurcsik (1998) and Sollima et al. (2004). This argues against the recent claim by Jurcsik (2003) of the existence of a metallicity dispersion among the variable stars of M3. Similar conclusions are reached by Sandstrom et al. (2001), who find that “the compositions of RR Lyrae stars in M3 are uniform within [their] sample and consistent with the compositions of M3’s giants”, and by KI who find a dispersion of $\sigma = 0.03$ dex for the FeII abundances averaged over 23 giant stars.

iii) A further check of the above results using the metallicity data listed in Table 13 for the Blazhko stars shows that the average of all values, irrespective of the Blazhko phase, is -1.37 ± 0.30 , and the average values corresponding to the small-amplitude and large-amplitude phases are -1.29 ± 0.37 and -1.42 ± 0.24 , respectively. Note that the r.m.s. errors are significantly larger than for regular variables. Although the differences in $\langle [Fe/H] \rangle$ may not be statistically significant, given the large errors, they nevertheless indicate that Blazhko stars at large-amplitude Blazhko phase are quite similar to regular pulsators, whereas at small-amplitude Blazhko phase the light curves are more likely distorted (in spite of $Dm \leq 5$), and tend to overestimate the metallicity. Therefore, *including in the sample unrecognised Blazhko stars can produce distorted metallicity distributions*. An inspection of Jurcsik (2003) target list reveals that 10 out of her 29 stars are Blazhko, one is a suspected Blazhko and one has $Dm > 5$ in our data. If we exclude these stars from the average, we find $\langle [Fe/H] \rangle = -1.42 \pm 0.09$ using our estimates of metallicity, and -1.37 ± 0.13 using Jurcsik’s estimates. This result does not show any evidence of a metallicity spread, and we think that the inclusion of Blazhko stars in the sample is what led Jurcsik (2003) to an incorrect conclusion.

iv) Sandage (2004a) estimated the effect of evolution off the ZAHB on the metallicity determination. His conclusion is that evolution produces a noise in $[Fe/H]$, in the sense that a $\Delta \log P = 0.10$ dex at fixed ϕ_{31} due to evolution at constant $[Fe/H]$ would generate an error $\Delta [Fe/H] = 0.67$ dex. Since, as we have seen in Sect. 3.2, the period shift at fixed amplitude between the main body of the RRab stars and those labelled “longP/overluminous” is $\Delta \log P \sim 0.06$, we should expect a systematic overabundance for these evolved stars of ~ 0.40 dex: however, we find none. In his analysis, Sandage could see and identify correctly the monotonic variation within the instability strip of period, amplitude and ϕ_{31} , as we also see in our Fig. 5. On the assumption of a unique

amplitude- ϕ_{31} relation, he deduced that the same period shift that occurs in the period-amplitude plane would occur also in the period- ϕ_{31} plane, whether due to evolution or to an abundance difference. The problem seems to lie in this assumption. As one can see in Fig. 2 of Jurcsik et al. (2003), and more clearly in our Fig. 15, at fixed $[\text{Fe}/\text{H}]$ the period shift due to evolution that stands out in the period-amplitude plane disappears in the period- ϕ_{31} plane, where all stars follow the same relation irrespective of their evolutionary status. This applies also to the RRc stars, that follow their own specific relation, different from the RRab's. This effect could not be seen in Sandage's target sample because of the lack of clearly identifiable evolved stars. Therefore, if the period-shift (at fixed amplitude) that appears in the period-amplitude plane is due to metallicity differences, the same period-shift (at fixed ϕ_{31}) will appear also in the period- ϕ_{31} plane, and the variation in period will produce a variation in metallicity as estimated by Sandage. If, however, the period-shift in the period-amplitude plane is due to evolution, there is no corresponding shift in the period- ϕ_{31} plane. So *evolution off the ZAHB will produce no noise on metallicity determinations.*

6.2.2. The Intrinsic Colors ($B-V$) and ($V-K$)

The possibility of estimating intrinsic colors from the Fourier parameters of the RRab stars has some important implications, allowing e.g. to estimate reddening and temperature of these stars. These color indices, as defined by Jurcsik (1998), are the differences of the *magnitude-averaged* absolute brightnesses. The following relations are taken from Kovács & Walker (2001):

$$(B - V)_0 = 0.189 \log P - 0.313 A_1 + 0.293 A_3 + 0.460 \quad (11)$$

$$(V - K)_0 = 1.257 P - 0.273 A_1 - 0.234 \phi_{31} + 0.062 \phi_{41} + 1.585 \quad (12)$$

These intrinsic colors, that are listed in col. 5 and 6 in Tables 6 and 7, can be used to estimate reddening and temperatures. However, before any practical application it is worth checking how they compare with their observed counterparts, e.g. $(B-V)_{mag}$ from CC01 that have been reported for convenience in column 9 of Table 2, and $(B-V)_S$ that have been used to derive the temperatures in Sect. 5. We show in Fig. 16 the histograms of these three color distributions for the RRab stars, and note that the $(B-V)_0$ distribution is somewhat compressed and slightly blue-shifted with respect to the $(B-V)_{mag}$ distribution. Whereas the blue-shift corresponds, correctly, to a reddening of about 0.01 mag, the reduced width is a distortion that becomes even more evident when compared to the $(B-V)_S$ color distribution. In particular, the red and blue edges of the $(B-V)_0$ distribution occur at about 0.38 and 0.28, respectively, instead of 0.41 and 0.24. This distortion in the shape of the $(B-V)_0$ color distribution will have some consequence on the temperature determination, as we shall see below.

Reddening

From the difference of the observed $(B-V)_{mag}$ colors and the intrinsic $(B-V)_0$ colors derived from eq. (11) we derive a mean reddening $E(B-V) = 0.007 \pm 0.013$ from the RRab stars with $Dm < 5$.

If we consider the 19 RRab stars with infrared data from L90 and $Dm < 5$, and compare the observed (V–K) colors with those derived from eq. (12), we obtain an average $E(V - K) = -0.011 \pm 0.063$, hence $E(B-V) = -0.004$. This result has a larger r.m.s. error than that from $(B - V)_0$ colors, possibly due to the smaller number of stars used for this estimate.

Both results are compatible, within the respective errors, with the reddening estimated in Sect. 4.1.

Temperatures

The expressions used above to derive the intrinsic colors of the RRab variables can be used to calculate their effective temperatures:

$$\log T_{eff}(B - V) = 3.930 - 0.322(B - V)_0 + 0.007[Fe/H] \quad (13)$$

$$\log T_{eff}(V - K) = 3.929 - 0.1112(V - K)_0 - 0.0032[Fe/H] \quad (14)$$

Eq. (13) is taken from Kovács & Walker (2001, eq. 11), where the gravity is assumed as $\log g = 2.75$. A variation $\Delta \log g = \pm 0.1$ dex would reflect on the temperature as $\Delta T_{eff} = \pm 28$ K. This color-temperature relation was calibrated on Castelli et al. (1997) models that are very similar to the C99 models discussed in Sect. 4.2, and is based on a different definition of mean color for RR Lyrae variables. Eq. (14) is taken from Jurcsik (1998). These temperatures are listed in Table 12, cols 7 and 8 respectively. For both eq. (13) and (14) the value for $[Fe/H]$ is taken from Eq. (10), for self consistency within the Fourier analysis. This value is *on average* ~ 0.1 dex higher than the value adopted for M3 from high dispersion spectra. The use of the fixed adopted value -1.5 for each star would make little difference on the average temperatures, i.e. about -10 and $+5$ K from (B–V) and (V–K), respectively, with no systematic effects across the instability strip.

For the RRC-type variables, the values of temperature listed in Table 11 have been calculated from the relation (SC93):

$$\log T_{eff} = 3.7746 - 0.1452 \log P + 0.0056 \phi_{31} \quad (15)$$

where the dependence on color is replaced by the dependence on period. These temperatures are not on the same absolute scale as those derived from eq. (13) and (14).

The comparison of these temperatures with those obtained using the SF temperature scale and the $(B-V)_S$ colors is shown in Fig. 17. We can see that for the RRC variables the Fourier temperatures are about the same as the SF temperatures at the hot end of the distribution, and become progressively hotter till about $+500$ K at the cool end. For the RRab stars the difference $\Delta T_{eff}(\text{Fourier-SF})$ varies nearly linearly from about -200 K at the hot end of the distribution to about $+50$ K at the cool end (but the coolest stars could not be used for this test because they have $Dm > 5$ and their Fourier temperatures are not reliable). This effect is due to the reduced red tail of the $(B-V)_0$ distribution. For the RRC stars the only parameter besides period in eq. (15) is ϕ_{31} , so the shape of the ϕ_{31} distribution must be the source of this effect. As a consequence of these differences between the Fourier and SF temperatures, the Fourier temperature

ranges are compressed, in particular they are reduced to about 60% (RRab) and 40% (RRc) of the corresponding SF temperature ranges from $(B-V)_S$ colors.

We show in Fig. 18 (lower panel) the periods vs Fourier temperatures, for comparison with the periods vs SF temperatures shown in Fig. 9. The period-temperature distributions in Fig. 18 do not follow the basic relation derived from the stellar pulsation theory, represented by the line of slope -3.41 (cf. eq. 7), as the stars in Fig. 9 do. Also, there is a large gap between the Fourier temperature distributions of the RRc and RRab stars, in clear disagreement with the overlap in color shown e.g. in Fig. 1.

It is quite clear that the intrinsic colors derived from eq. (11) and (12) have a different distribution than the observed colors, and this in turn leads to rather questionable values of temperature via equations (13)-(15). *This method to estimate temperatures needs to be carefully re-investigated before the results can be used with any degree of confidence.*

6.2.3. The Absolute Magnitude (M_V) or Luminosity ($\log L$)

• RRc variables

Two methods are presently available for deriving the luminosities of RRc stars from Fourier parameters. One is the theoretical relation derived by SC93, based on hydrodynamic pulsation models matched with observations of globular cluster RRc stars:

$$\log L(RRc) = 1.04 \log P - 0.058\phi_{31} + 2.41 \quad (\text{r.m.s. error of the fit } 0.025) \quad (16)$$

where L is the luminosity in solar units. Excluding the 4 evolved/overluminous RRc variables commented on in Sect. 3.2, the average luminosity of the remaining 19 RRc stars turns out to be $\log \langle L \rangle = 1.710 \pm 0.015$, that translates into $\langle M_V \rangle = 0.44 \pm 0.03$ mag assuming $M_{bol}(\text{sun}) = 4.75$ mag and $BC_V = 0.03$ (cf. Tab. 5). Kal98 found an identical result by applying this same relation to 5 RRc stars. However, the application of this method to RRc stars in 7 globular clusters led Clement (1996) to derive a luminosity vs. metallicity relation $M_V = 0.19[Fe/H] + 0.82$, that would yield $M_V = 0.54$ for $[Fe/H] = -1.5$. There seems to be a problem with the definition of the zero-point with this formulation, but this is just a matter of calibration. Possibly more important, the 1σ error associated to $\langle M_V \rangle$, ± 0.03 mag, is half the value associated to the corresponding observed $\langle V \rangle$, ± 0.06 mag (cf. Sect. 3.1).

Alternatively, we can use the empirical relation by Kovács (1998) for the intensity averaged absolute magnitude

$$M_V(RRc) = 1.061 - 0.961P - 0.044\phi_{21} - 4.447A_4 \quad (\text{r.m.s. error of the fit } 0.042) \quad (17)$$

where we adopt a brighter zero-point by 0.2 ± 0.02 mag than the original value by Kovács (1998), in order to be consistent with the assumptions made in Sect. 4.3.2. The average value we obtain is $\langle M_V \rangle = 0.57 \pm 0.04$ mag, and again the 1σ error is significantly smaller than the error on $\langle V \rangle$.

In the following discussions we adopt eq. (17) to derive the Fourier luminosity of the RRc stars, using the BC_V values listed in Table 6.

• **RRab variables**

The most recent version of the relation between the intensity averaged $M_V(RR)$ and the Fourier parameters of the V light curve decomposition is from Kovács (2002):

$$M_V(RRab) = -1.876 \log P - 1.158A_1 + 0.821A_3 + 0.43 \quad (18)$$

The value for the constant, 0.43, was derived by Kinman (2002) from the Fourier decomposition of the V light curve of RR Lyr ($[Fe/H] \sim -1.4$) and its absolute magnitude $M_V = 0.61 \pm 0.10$ based on HST-FGS parallax (Benedict et al. 2002). The zero-point of this luminosity scale (i.e. $M_V = 0.59$ at $[Fe/H] = -1.5$) is about 0.05 mag fainter than the working assumptions we made in Sect. 4.3.2. In order to be consistent with these assumptions, we apply eq. (18) with a brighter zero-point by 0.05 mag (i.e. 0.38 instead of 0.43), and we obtain $\langle M_V \rangle = 0.57 \pm 0.02$ mag for the 45 regular RRab stars with $Dm < 5$ in our sample, 0.45 ± 0.04 mag for the 6 long period/overluminous stars, and 0.59 ± 0.02 mag for the 4 low amplitude/suspected Blazhko stars. All these values are in the same luminosity scale that led to $\langle M_V \rangle = 0.57 \pm 0.04$ mag for the RRc stars above.

A few considerations can be made:

i) The dispersion of the $M_V(\text{Fourier})$ estimates is significantly smaller than the dispersion in the observed V magnitudes. We show in Fig. 19 a plot of the $M_V(\text{Fourier})$ values derived above for the RRc and RRab stars vs. the corresponding V magnitudes: the correlation between these two quantities is definitely flatter than one would expect. In particular for the RRab stars, the width of the $\langle V \rangle$ distribution (~ 0.25 mag) is much larger than the width of the $M_V(\text{Fourier})$ distribution (≤ 0.1 mag), as also shown by the r.m.s. errors associated to the $\langle V \rangle$ and $\langle M_V \rangle$ determinations, i.e. ± 0.05 and ± 0.02 mag respectively. This systematic effect is present, to a somewhat lesser extent, also in other studies of this type, although it was not noted by the authors. For example, in ω Cen (Clement & Rowe 2000) and in M5 (Kaluzny et al. 2000), if one considers only the RRab variables with $Dm < 5$ and with no evidence of being “longP/overluminous”, the width of the $M_V(\text{Fourier})$ distribution is a factor ~ 1.7 smaller than that of the V distribution. In M3 this factor seems higher, up to ~ 2.5 . This “compression” effect cannot possibly be explained by reddening variations nor line-of-sight depth effects, particularly in M3, and casts serious doubts on the reliability of $\langle M_V \rangle$ determinations with this method. A careful inspection of Fig. 2 in Jurcsik et al. (2003) can help find an explanation for this distortion effect. There, all the relevant Fourier parameters are plotted as a function of period for the RR Lyrae stars of M3. Since both A_1 and A_3 are well defined linear functions of period for the main body of the regular variables, they can be substituted in eq. (18) to retain only the dependence on period. We have estimated these relations numerically using the values of A_1 and A_3 listed in Table 9, and the above eq. (18) becomes then $M_V(RRab) \propto -0.166 \log P$. The very weak dependence on period is what reduces the width of the M_V distribution by losing the connection with temperature and with the real luminosity distribution. A similar effect ($M_V(RRab) \propto -0.17P$) occurs if one uses the alternative

formulation to derive M_V as a function of P (instead of $\log P$), A_1 and ϕ_{31} (Jurcsik 1998), as was done by Clement & Rowe (2000) and Kaluzny et al. (2000), and seems to be at work with the RRc stars too, with a somewhat larger scatter.

ii) In Fig. 18 the values $M_V(\text{Fourier})$ derived from eq.s (17) and (18), transformed to $\log L$ with the help of the BC_V values in Table 6, are plotted vs the Fourier temperatures. One can see that the luminosities of both the RRc and RRab stars approximately agree with the luminosity level of the ZAHB, albeit with an unrealistically small scatter. However, these distributions are inconsistent with the requirements of the pulsation theory represented by the boundaries of the instability strip, mainly because of the distorted temperature distributions (cf. Sect. 6.2.2).

• **Blazhko variables**

We have applied eq. (18) also to the Blazhko stars separately at the various Blazhko phases, and we list the results in Table 13. The average of these values is $\langle M_V \rangle = 0.53 \pm 0.05$ mag at the large amplitude phase, 0.59 ± 0.05 mag at the small amplitude phase, and 0.47 ± 0.02 mag for the 5 evolved/overluminous stars at the large amplitude phase. We note that these values are comparable with those derived for the RRab stars, so there seems to be no significant systematic difference in average luminosity between the regular and the Blazhko variables, as already noted in Sect. 3.1.

We conclude that these relations based on the Fourier parameters may be of some use to estimate the average M_V of a group of stars, when applicable and after proper calibration, but cannot be trusted to yield *accurate individual* M_V estimates.

6.2.4. *The Mass*

Based on a grid of hydrodynamic pulsation models for RRc variables at various masses, SC93 showed (their Fig. 2) that there is a clear relation between period and ϕ_{31} that depends essentially on mass, hence they derived a relation to estimate the mass for RRc stars:

$$\log M(RRc) = 0.52 \log P - 0.11 \phi_{31} + 0.39 \tag{19}$$

The zero-point of this relation is such that intermediate metallicity clusters of Oosterhoff type I (e.g. M3, M5, NGC 6171) have RRc variables with average mass around $0.6 M_\odot$, and metal-poor clusters of Oosterhoff type II (e.g. M68 and M15) have RRc variables with average mass around $0.8 M_\odot$, in agreement with the values of mass for double-mode pulsators that were available and generally accepted at that time. However, the most recent estimates of mass for double-mode pulsators in M3 would support larger values by $\sim 0.10 - 0.15 M_\odot$, as well as a nearly flat dependence on metallicity (Clementini et al. 2004, cf. Sect. 4.3.1).

We have listed in Table 11 the mass values derived from eq. (19), and we compare them in Fig. 18 with a few ZAHB models. In addition to the clumpy distribution due to the distorted Fourier temperatures, the mass distribution shows the opposite trend with respect to the theoretical distribution.

On a different absolute scale, Jurcsik (1998) provides a relation to derive the mass of RRab-type variables:

$$\log M(RRab) = 20.884 - 1.754 \log P + 1.477 \log L - 6.272 \log T_{eff} + 0.0367[Fe/H] \quad (20)$$

where the values of luminosity, metallicity and temperature have been taken from Table 12 (all derived from Fourier coefficients via eq. 18, 10 and 13 respectively, for self-consistency). We have listed in Table 12 the mass values derived from eq. (20). Also this mass distribution, like the RRc's, shows the opposite trend with respect to the ZAHBs reported in Fig. 18, in addition to the distortion due to the temperature distribution. We conclude that the Fourier Transform approach, in its present formulation, does not provide reliable values of mass for the RR Lyrae stars.

6.2.5. The Gravity

Once the basic physical parameters mass, luminosity and temperature are known, the gravity can be calculated, for the sake of completeness, simply using the equation of the stellar structure:

$$\log g = -10.607 + \log M - \log L + 4 \log T_{eff} \quad (21)$$

where M and L are in solar units. As a consequence of the mass distributions discussed above, we can see in Fig. 18 that the gravity distributions also fail to match the ZAHBs.

As a final comment, we stress again that the use of Fourier coefficients to estimate the physical parameters of the RR Lyrae stars, that might produce acceptable *average* results in some cases, e.g. with metallicity or luminosity after careful and proper calibration, is not presently able to provide reliable estimates of intrinsic colors hence temperatures and temperature-related parameters.

7. Summary and Conclusions

We have performed a detailed study of the pulsational and evolutionary characteristics of 133 RR Lyrae variables in M3, selected among those with the best quality light curves from the CC01 data set. The availability of additional data sets (Car98 and Kal98) at different epochs has allowed us to study in good detail the characteristics of the Blazhko stars. Mean magnitudes and colors, along with periods, light curve amplitudes and rise times, have been used to discuss the pulsational properties of these stars. A critical discussion of the temperature determination process (i.e. temperature indicators and calibrations) has been presented, and the physical parameters and evolutionary characteristics of these stars have been estimated. The unusual richness of RR Lyrae stars in M3 and the excellent quality of the available data has allowed us to identify a good number of stars in a more evolved stage of evolution off the ZAHB and study their characteristics. Finally, we have performed a Fourier analysis of the V light curves and estimated the *pros* and *cons* of this technique when applied to the study of RR Lyrae properties.

Our main conclusions are the following:

- The basic characteristics of the CMD already discussed by CC01 are here reconfirmed, namely i) the blue and red edges of the instability strip are located at $(B-V)=0.18$ and 0.42 , respectively; the RRc and RRab stars overlap in color in the interval ~ 0.24 to 0.30 . ii) The $\langle V \rangle$ distribution is bimodal, with a main peak around $\langle V \rangle=15.64$ and a secondary peak around $\langle V \rangle=15.52$. There is no significant evidence of *four* populations as claimed by Jurcsik et al. (2003). The intrinsic magnitude thickness of the HB within the instability strip is ≤ 0.20 mag if we consider only the main (fainter) component, or ~ 0.30 mag if we include also the brighter one.
- At least one third of the RR Lyrae stars in M3 are affected by Blazhko modulation; in the studied sample, they all belong to the RRab group. More can be hidden in the sample we have not taken into account in the present analysis because of large scatter in the light curves. The presence of unidentified Blazhko stars causes a scatter in the relations among various observable parameters, that may be large enough to hide the presence of sub-groups with different characteristics. The properties of Blazhko stars at the Blazhko phase corresponding to the largest light curve amplitude are generally more similar to the characteristics of regular RRab stars than at smaller amplitude phases. The average $\langle V \rangle$ magnitude does not vary significantly with Blazhko phase. The $\langle V \rangle$ magnitude distribution of the Blazhko stars is the same as that of the regular RRab stars, including the bimodal shape. The average $\langle B - V \rangle$ color distribution is also similar to the RRab's, but is truncated at a bluer color, i.e. there are no Blazhko stars redder than $\langle B - V \rangle \sim 0.39$.
- In the period-amplitude diagram both RRc and RRab stars are located on well defined sequences, that are more accurately represented by quadratic rather than linear relations (especially the sequence of the RRab stars), in agreement with theoretical models. There is clear evidence of nearly parallel sequences for both RRc and RRab stars, shifted towards longer periods and populated by systematically brighter stars than the respective main stellar groups. From our sample of 133 RR Lyraes we have identified 19 such stars (9 RRab, 5 Blazhko and 5 RRc), that are all consistent with a more advanced stage of evolution off the ZAHB. Their distributions are similar to the mean distributions of OoII RRc and RRab variables. The dependence of the $P-A_V$ relation on Oosterhoff type and/or evolutionary status rather than metallicity supports the conclusion that the Oosterhoff dichotomy is due to evolution. The numbers of RR Lyrae stars we have found in M3 near the ZAHB and evolved off the ZAHB are consistent with evolutionary lifetimes according to well established theoretical considerations. One of the three shortest period and lowest amplitude RRc stars is likely to be a second overtone pulsator.
- After a critical discussion of what is the most reliable mean color as an indicator of the equivalent static color for an RR Lyrae star, we have decided to use the formulation $(B - V)_S = \langle B \rangle_{int} - \langle V \rangle_{int}$ plus amplitude related corrections based on theoretical models (Bono et al. 1995) that are quite consistent also with empirical estimates (Sandage 1990). From these colors and using a few independent methods we have estimated a mean reddening $E(B-V)=0.01\pm 0.01$ for M3. A comparative evaluation of various temperature scales has led us to identify two temperature scales

that meet both theoretical (pulsational and evolutionary) requirements and observational evidence on mass and luminosity for the RR Lyrae stars using (B–V) colors (in absence of V–K colors). These scales are from M98 (theoretical calibration) and SF. They differ by ~ 150 K (M98 being cooler), and yield on average pair values of $\text{mass}(M_{\odot})/M_V(\text{mag})$ about 0.74/0.59 and 0.69/0.54, respectively. The temperature scale by CSJ is very similar to SF’s and is independent of color, but is defined only for RRab stars. Considering that the M98 calibrations based on the (V–K) colors are supposed to be more reliable and are both ~ 100 K hotter than the corresponding calibrations based on (B–V) colors, we have adopted the hotter temperature scale by SF for our analysis (corresponding to a distance modulus of 15.07 for M3). However, our considerations would hold also with the cooler (B–V)-based M98 scale and a distance modulus of 15.02, within the errors. By using the SF temperature scale and the (B–V)_S colors we have derived the stellar physical parameters (temperature, luminosity, mass and gravity) for our stars, and compared them with the most recent stellar evolution and pulsation models. The agreement is good, and confirms that the adopted calibration is reliable and accurate, and yields fully consistent results with the theoretical framework within the respective errors. The use of the CSJ temperature scale yields equally good or better (less dispersed) results, for the RRab variables only.

- We have applied the Fourier Transform technique to our variables. The main aim was to exploit our excellent data set and investigate the reliability of this type of analysis. First, we have derived the Dm parameter, defined by Jurcsik & Kovács (1996) as a quality indicator of the regularity of the light curve shape. Only for $Dm < 3$ the physical parameters derived from Fourier coefficients are considered “reliable”, according to Kovács & collaborators’ prescriptions. We have adopted $Dm < 5$ to increase the statistics with no significant loss of accuracy. We have found that Dm is effectively unable to distinguish between Blazhko and non-Blazhko stars unless set to an unpractically low value ($Dm \leq 2$). Even among Blazhko stars, one can find the recommended value $Dm < 3$ as frequently at small-amplitude as at large-amplitude Blazhko phases. About the Fourier analysis results (for stars with $Dm < 5$), we have found the following:

i) [Fe/H] estimates seem on average acceptable, but are ~ 0.1 dex more metal-rich than the high resolution spectroscopic abundances of red giant stars derived by KI. A recalibration of the [F/H]-period- ϕ_{31} relation using 287 RRab variables in 18 globular clusters performed by Sollima et al. (2004) using a non-parametric fitting method and KI metallicity scale yields similar average metallicity values to those derived from eq. (10), within the errors. This indicates that M3 lies ~ 0.1 dex off (on the metal-poor side) the mean relation defined by the calibrating globular clusters. However, the use of a different fitting method and/or metallicity scale, such as Sollima et al.’s, produces a different *shape* of the metallicity distribution, that might become relevant in the case of a composite population with a non-negligible metallicity dispersion. Evolution off the ZAHB does not affect [Fe/H] determinations. The inclusion of Blazhko stars in a sample of regular stars does increase the scatter in the [Fe/H] determinations, as Blazhko stars at low amplitude phase appear as more metal-rich. If this effect is taken into account, there is no evidence of metallicity spread among the RR Lyrae stars in M3.

ii) Intrinsic colors and temperatures estimated from eq.s (11)-(15) show serious discrepancies with

observed color distributions and theoretical (pulsational and evolutionary) requirements, and cannot be taken as reliable results.

iii) Absolute magnitudes are affected by a “compression” effect that reduces their scatter by a factor ~ 2 compared to the observed $\langle V \rangle$ distribution. This makes them unreliable as *accurate individual* values, but they may provide useful averages for groups of stars, if applicable and after proper calibration. The r.m.s. errors are however significantly underestimated.

iv) The values of mass show a distribution with temperature that has the opposite trend with respect to the ZAHB. Consequently, also the values of gravity are affected by serious uncertainties. Neither estimates can be taken as reliable results.

In general, it appears that the physical parameters of RR Lyrae stars derived from the Fourier decomposition of the V light curves should be taken with considerable caution. In particular, intrinsic colors hence temperatures and temperature-related parameters (e.g. mass and gravity) are seriously inaccurate. Possible exceptions are $[\text{Fe}/\text{H}]$, that seem to be acceptable within r.m.s. errors of ± 0.15 dex (provided Blazhko stars are not included in the analysis and only average values are considered), and absolute magnitudes if taken as the mean value for a group and not as individual values.

We wish to thank T.D. Kinman for providing the calibration constant for our eq. (18); A.V. Sweigart for providing his HB models in electronic form and for interesting discussions and comments; D. VandenBerg for making available his ZAHB models; A. Sandage for sending his analysis on Fourier parameters in advance of publication, and inducing us to check the effect of ϕ_{31} on metallicity determinations; and G. Clementini for several interesting discussions and comments. We acknowledge the use of J. Kaluzny original data that are available on the web. TMC wishes to thank the UNC Charlotte for a Reassignment of Duties Grant. BWC thanks the US National Science Foundation for grants AST-9619881, AST-9988156, and AST-0305431 to the University of North Carolina. CC acknowledges the support by the MIUR (Ministero dell’Istruzione, dell’Università e della Ricerca).

REFERENCES

- van Albada, T.S. & Baker, N. 1971, ApJ, 169, 311
- Alcock, C. et al. 1996, AJ, 111, 1146
- Baker, R.H. & Baker, H.V. 1956, AJ, 61, 283
- Bakos, G.A, Benko, J.M & Jursik, J. 2000, Acta Astronomica, 50, 221
- Benedict, G.F. et al. 2002, AJ, 123, 473
- Bessell, M.S. & Brett, J.M. 1988, PASP, 100, 1134

- Bessell, M.S., Castelli, F. & Plez, B. 1998, A&A, 333, 231
- Bingham, E.A., Cacciari, C., Dickens, R.F. & Fusi Pecci, F. 1984, MNRAS, 209, 765
- Blanco, V.M. 1992, AJ, 104, 734
- Blazhko, S. 1907, Astron. Nachr., 175, 325
- Bono, G., Caputo, F. & Marconi, M. 1995, AJ, 110, 2365
- Bono, G., Caputo, F., Castellani, V. & Marconi, M. 1997, A&AS, 121, 327
- Bragaglia, A., Gratton, R.G., Carretta, E., Clementini, G., Di Fabrizio, L. & Marconi, M. 2001, AJ, 122, 207
- Brocato, E., Castellani, V. & Ripepi, V. 1996, AJ, 111, 809
- Cacciari, C. & Clementini, G. 2003, in *Stellar Candles for the Extragalactic Distance Scale*, Eds. D. Alloin & W. Gieren, Lecture Notes in Physics, Springer-Verlag, Vol. 635, p. 105
- Cacciari, C., Clementini, G. & Fernley, J. 1992, ApJ, 396, 219
- Caputo, F., Marconi, M. & Santolamazza, P. 1998, MNRAS, 293, 364
- Caputo, F., Castellani, V., Marconi, M. & Ripepi, V. 2000, MNRAS, 316, 819
- Carney, B. W., Storm, J. & Jones, R.V. 1992, ApJ, 386, 663 (CSJ)
- Carney, B. W., Latham, D.W., Stefanik, R.P., Laird, J.B. & Morse, J.A. 2003, AJ, 125, 293
- Carney, B. W., Latham, D.W. & Laird, J.B. 2004, in preparation
- Carpenter, J.M. 2001, AJ, 121, 2851
- Carretta, E. & Gratton, R. G. 1997, A&AS, 121, 95
- Carretta, E., Cacciari, C., Ferraro, F. R., Fusi Pecci, F. & Tessicini, G. 1998, MNRAS, 298, 1005 (Car98)
- Carretta, E., Gratton, R.G. & Clementini, G. 2000, MNRAS, 316, 721
- Castelli, F. 1999, A&A, 346, 564 (C99)
- Castelli, F., Gratton, R.G. & Kurucz, R.L. 1997, A&A, 318, 841
- Catelan, M. 1998, ApJ, 495, L81
- Catelan, M. 2004, ApJ, 600, 409 (C04)
- Catelan, M., Pritzl, B.J. & Smith, H.A. 2004, ApJS, in press (astro-ph/0406067)

- Clement, C.M. 1996, BAAS Vol. 28, p. 1384 (#81.13)
- Clement, C.M & Rowe, J. 2000, AJ, 120, 2579
- Clement, C.M & Shelton, I. 1999a, AJ, 118, 453
- Clement, C.M & Shelton, I. 1999b, ApJ, 515, L85
- Clement, C.M., Jankulak, M. & Simon, N.R. 1992, ApJ, 395, 192
- Clement, C.M., Hilditch, R.W., Kaluzny, J. & Rucinski, S.M. 1997, ApJ, 489, L55
- Clement, C.M., Muzzin, A., Dufton, Q., Ponnampalam, T., Wang, J., Burford, J., Richardson, A., Rosebery, T., Rowe, J. & Sawyer Hogg, H. 2001, AJ, 122, 2587
- Clementini, G., Corwin, T.M., Carney, B.W. & Sumere, A.N. 2004, AJ, 127, 938
- Corwin, T.M., Carney, B.W. & Allen, D.M. 1999, AJ, 117, 1332
- Corwin, T.M. & Carney, B. W. 2001, AJ, 122, 3183 (CC01)
- Davis, C.G. & Cox, A.N. 1980, in *Current Problems in Stellar Pulsation Instabilities*, NASA/GSFC (SEE N80-25229 15-90) p. 293
- Dutra, C.M & Bica, E. 2000, A&A, 359, 347
- Ferraro, F.R., Carretta, E., Corsi, C.E., Fusi Pecci, F., Cacciari, C., Buonanno, R., Paltrinieri, B. & Hamilton, D. 1997, A&A, 320, 757
- Gratton, R.G., Bragaglia, A., Clementini, G., Carretta, E., Di Fabrizio, L., Maio, M. & Taribello, E. 2004, A&A, in press (astro-ph/0405412)
- Harris, W.E. 1996, AJ, 112, 1487 (update 2003, <http://physun.physics.mcmaster.ca/Globular.html>)
- Jurcsik, J., 1995, Acta Astron., Vol. 45, p. 653
- Jurcsik, J., 1998, A&A, 333, 571
- Jurcsik, J., 2003, A&A, 403, 587
- Jurcsik, J. & Kovács, G. 1995, in *Astrophysical Applications of Stellar Pulsation*, ASP Conf. Ser. 83, eds. R.S. Stobie & P.A. Whitelock, p. 385
- Jurcsik, J. & Kovács, G. 1996, A&A, 312, 111
- Jurcsik, J., Benkő, J.M. & Szeidl, B. 2002, A&A, 390, 133
- Jurcsik, J., Benkő, J.M., Bakos, Á., Szeidl, B. & Szabó, R. 2003, ApJ, 597, L49
- Kaluzny, J., Hilditch, R. W., Clement, C. & Rucinski, S. M. 1998, MNRAS, 296, 347 (Kal98)

- Kaluzny, J., Olech, A., Thompson, I., Pych, W., Krzeminski, W. & Schwarzenberg-Czerny, A. 2000, *A&AS*, 143, 215
- Kaluzny, J., Olech, A. & Stanek, K.Z. 2001, *AJ*, 121, 1533
- Kinman, T.D. 2002, *IBVS* n. 5354
- Kinman, T. & Castelli, F. 2002, *A&A*, 391, 1039
- Kovács, G. 1998, *Mem. S.A.It.* 69, 49
- Kovács, G. 2002, in *ω Cen: A Unique Window into Astrophysics*, ASP Conf. Ser., Ed.s F. van Leeuwen, G. Piotto and J. Hughes, in press (astro-ph/0202133)
- Kovács, G. & Jurcsik, J. 1996, *ApJ*, 466, L17
- Kovács, G. & Jurcsik, J. 1997, *A&A*, 322, 218
- Kovács, G. & Kanbur, S.M. 1998, *MNRAS*, 295, 834
- Kovács, G. & Walker, A.R. 2001, *A&A*, 374, 264
- Kovács, G. & Zsoldos, E. 1995, *A&A*, 293, L57
- Kraft, R.P., Sneden, C., Langer, G.E. & Prosser, C.F., 1992, *AJ*, 104, 645
- Kraft, R.P., Sneden, C., Langer, G.E. & Shetrone, M.D. 1993, *AJ*, 106, 1490
- Kraft, R.P., Sneden, C., Langer, G.E., Shetrone, M.D. & Bolte, M. 1995, *AJ*, 109, 2586
- Kraft, R.P. & Ivans, I.I. 2003, *PASP*, 115, 143 (KI)
- Lee, Y.-W., Demarque, P. & Zinn, R. 1990, *ApJ*, 350, 155
- Lee, S.-G. 1999, *AJ*, 118, 920
- Liu, T. & Janes, K.A. 1990, *ApJ*, 354, 273
- Longmore, A.J., Dixon, R., Skillen, I., Jameson, R.F. & Fernley, J.A. 1990, *MNRAS*, 247, 684 (L90)
- Lub, J. 1977, *A&AS*, 29, 345
- Marconi, M., Caputo, F., Di Criscienzo, M. & Castellani, M. 2003, *ApJ*, 596, 299
- Mateo, M., Udalski, A., Szymanski, M., Kaluzny, J., Kubiak, M. & Krzeminski, W. 1995, *AJ*, 109, 588
- Mathis, J.S. 1999, in *Allen's Astrophysical Quantities*, ed. A.N. Cox, p. 527

- Montegriffo, P., Ferraro, F.R., Origlia, L. & Fusi Pecci, F. 1998, MNRAS, 297, 872 (M98)
- Olech, A. 1997, Acta Astronomica, 47, 183
- Olech, A., Kaluzny, J., Thompson, I.B., Pych, W., Krzeminski, W. & Schwarzenberg-Czerny, A. 2001, MNRAS, 321, 421
- Oosterhoff, P. Th 1939, Obs., 62, 104
- Petersen, J.O. 1984, A&A, 139, 496
- Piersimoni, A.M., Bono, G. & Ripepi, V. 2002, AJ, 124, 1528
- Pilachowski, C.A. & Sneden, C. 2001, AAS 199, 137.08
- Preston, G.W. 1961, ApJ, 133, 29
- Reimers, D. 1975, Mem. Soc. R. Sci. Liège 6 Ser., Vol. 8, p. 369
- Renzini, A. & Fusi Pecci, F. 1988, ARA&A 26, 199
- Roberts, M.S. & Sandage, A. 1955, AJ, 60, 185
- Salaris, M., Chieffi, A. & Straniero, O. 1993, ApJ, 414, 580
- Sandage, A. 1959, ApJ, 129, 596
- Sandage, A. 1970, ApJ, 162, 841
- Sandage, A. 1990, ApJ, 350, 603
- Sandage, A. 1993, AJ, 106, 719
- Sandage, A. 2004a, ApJ, in press
- Sandage, A. 2004b, ApJ, in press
- Sandage, A. & Katem, B. 1982, AJ, 87, 537
- Sandage, A., Katem, B., & Sandage, M. 1981, ApJS, 46, 41
- Sandstrom, K., Pilachowski, C.A & Saha, A., 2001, AJ, 122, 3212
- Shaltenbrand, R. & Tammann, G.A. 1971, A&AS, 4, 265
- Schlegel, D.J., Finkbeiner, D.P. & Davis, M. 1998, ApJ, 500, 525
- Silbermann, N.A. & Smith, H.A. 1995, AJ, 110, 704
- Simon, N.R. 1988, ApJ, 328, 747

- Simon, N.R. 1989, ApJ, 343, L17
- Simon, N.R. 1990, ApJ, 360, 119
- Simon, N.R. & Clement, C.M. 1993, ApJ, 410, 526 (SC93)
- Simon, N.R. & Lee, A.S. 1981, ApJ, 248, 291
- Simon, N.R. & Teays, T.J. 1982, ApJ, 261, 586
- Smith, H.A. 1995, *RR Lyrae Stars*, (Cambridge: Cambridge Univ. Press)
- Smith, G.H., Shetrone, M.D., Bell, R.A., Churchill, C.W. & Briley, M.M. 1996, AJ, 112, 1511
- Sollima, A., Cacciari, C., Ferraro, F.R. & Pancino E. 2004, in preparation
- Straniero, O., Chieffi, A. & Limongi, M. 1997, ApJ, 490, 425
- Sturch, C.R. 1966, ApJ, 143, 774
- Sweigart, A.V. 1997, ApJ, 474, L23
- Szeidl, B. 1965, Mitt. Sternw. Ungar. Akad. Budapest, 58
- Szeidl, B. 1973, Mitt. Sternw. Ungar. Akad. Budapest, 63
- Szeidl, B. 1976, in *Multiple Periodic RR Lyrae Stars: Observational Review*, IAU Colloq. 29, ed. W.S. Fitch., D. Reidel Publishers, p.133
- Szeidl, B. 1988, in *Multimode Stellar Pulsations*, eds. G. Kovács, L. Szabados & B. Szeidl., Budapest: Konkoly Observatory, Kultura, p. 45
- VandenBerg, D.A., Swenson, F.J., Rogers, F.J., Iglesias, C.A. & Alexander, D.R. 2000, ApJ, 532, 430
- Walker, A.R. 1994, AJ, 108, 555
- Walker, A.R. 1998, AJ, 116, 220
- Walker, A.R. & Nemec, J.M. 1996, AJ, 112, 2026
- Zinn, R. & West, M. J. 1984, ApJS, 55, 45 (ZW)

Table 1. Photometric parameters for the RRc-type variables.

Star	Period	$\langle B \rangle$	A_B	RT_B	$\langle V \rangle$	A_V	RT_V	$(B - V)_{mag}$	$(B - V)_S$	Notes
12	0.317540	15.770	0.66	0.40	15.563	0.51	0.35	0.218	0.207	
29	0.331684	15.712	0.58	0.40	15.486	0.44	0.35	0.236	0.226	
37	0.3266387	15.856	0.62	0.35	15.624	0.49	0.35	0.245	0.232	
56	0.329600	15.834	0.61	0.40	15.607	0.47	0.35	0.243	0.227	
70	0.486093	15.636	0.47	0.50	15.350	0.36	0.50	0.279	0.286	b
75	0.314080	15.855	0.62	0.35	15.625	0.49	0.35	0.240	0.230	
85	0.355817	15.706	0.65	0.45	15.483	0.50	0.45	0.239	0.223	b
86	0.292659	15.857	0.66	0.35	15.640	0.52	0.35	0.231	0.217	
97	0.3349326	15.916	0.54	0.40	15.661	0.41	0.40	0.262	0.255	
105	0.287744	15.728	0.42	0.45	15.534	0.32	0.45	0.202	0.194	
107	0.309035	15.851	0.67	0.40	15.630	0.53	0.40	0.240	0.221	
125	0.349823	15.886	0.54	0.35	15.620	0.41	0.35	0.273	0.266	
126	0.348410	15.883	0.52	0.45	15.622	0.40	0.45	0.265	0.261	
128	0.292040	15.818	0.69	0.40	15.624	0.54	0.40	0.216	0.194	
129	0.406102	15.770	0.57	0.45	15.481	0.45	0.45	0.290	0.289	a b
131	0.297691	15.863	0.67	0.30	15.650	0.54	0.30	0.228	0.213	
132	0.339851	15.871	0.57	0.40	15.594	0.42	0.40	0.282	0.277	
140	0.333499	15.700	0.58	0.40	15.479	0.47	0.40	0.232	0.221	
152	0.326135	15.693	0.60	0.45	15.506	0.45	0.45	0.209	0.187	
170	0.435694	15.523	0.56	0.45	15.271	0.46	0.45	0.243	0.252	a b
177	0.348749	15.744	0.71	0.45	15.563	0.56	0.45	0.186	0.181	b
178	0.267387	15.876	0.45	0.50	15.710	0.35	0.45	0.170	0.166	
203	0.289794	15.733	0.20	0.50	15.546	0.16	0.50	0.188	0.187	c

^a Large scatter

^b Long period/overluminous

^c Suspected second overtone pulsator

Table 2. Photometric parameters for the RRab-type variables.

Star	Period	$\langle B \rangle$	B_{min}	A_B	RT_B	$\langle V \rangle$	V_{min}	A_V	RT_V	$(B - V)_{mag}$	$(B - V)_S$	Notes
1	0.5205959	15.881	16.360	1.49	0.12	15.603	15.952	1.21	0.12	0.323	0.304	
6	0.5143332	15.960	16.405	1.50	0.13	15.676	15.996	1.18	0.12	0.324	0.310	
9	0.5415528	15.916	16.328	1.38	0.14	15.628	15.924	1.03	0.13	0.325	0.309	
10	0.5695439	15.942	16.278	1.10	0.15	15.611	15.861	0.88	0.15	0.364	0.340	
11	0.507894	15.839	16.353	1.63	0.12	15.585	15.960	1.28	0.13	0.288	0.285	
15	0.5300874	15.899	16.329	1.41	0.12	15.602	15.915	1.13	0.12	0.334	0.319	
16	0.5114943	15.960	16.418	1.47	0.11	15.683	16.008	1.13	0.12	0.315	0.302	
19	0.631972	16.065	16.273	0.59	0.20	15.679	15.830	0.45	0.20	0.390	0.386	
21	0.5157556	15.962	16.396	1.45	0.12	15.649	15.972	1.14	0.12	0.349	0.337	
22	0.481424	15.908	16.398	1.31	0.20	15.658	16.020	1.03	0.20	0.290	0.268	c
25	0.480062	15.906	16.436	1.64	0.11	15.651	16.026	1.23	0.11	0.318	0.286	
26	0.5977405	15.848	16.217	1.25	0.14	15.543	15.809	0.98	0.14	0.338	0.320	b
27	0.579073	15.948	16.279	1.13	0.15	15.621	15.854	0.91	0.15	0.355	0.337	
31	0.5807196	15.825	16.288	1.54	0.13	15.531	15.855	1.21	0.13	0.345	0.322	b
32	0.49535	15.843	16.310	1.48	0.11	15.568	15.886	1.14	0.12	0.315	0.303	a
36	0.5455989	15.910	16.352	1.44	0.12	15.615	15.930	1.15	0.14	0.333	0.319	
40	0.551535	15.991	16.368	1.26	0.15	15.668	15.945	0.97	0.15	0.356	0.339	
42	0.5900984	15.740	16.251	1.67	0.12	15.488	15.854	1.29	0.12	0.314	0.284	b
46	0.6133832	16.044	16.278	0.72	0.18	15.676	15.852	0.55	0.18	0.388	0.367	
48	0.6278299	15.869	16.123	0.80	0.17	15.487	15.680	0.61	0.18	0.391	0.382	d
51	0.5839702	15.979	16.294	1.07	0.16	15.639	15.870	0.83	0.16	0.370	0.348	
53	0.5048815	15.917	16.397	1.52	0.11	15.640	15.985	1.11	0.11	0.338	0.304	
54	0.506247	15.986	16.348	0.91	0.20	15.689	15.943	0.66	0.20	0.322	0.299	c
55	0.5298217	15.943	16.370	1.39	0.12	15.654	15.968	1.07	0.12	0.325	0.310	
57	0.5121908	15.974	16.414	1.48	0.12	15.674	15.988	1.18	0.12	0.340	0.325	
58	0.517054	15.828	16.295	1.50	0.11	15.512	15.873	1.19	0.12	0.340	0.342	a d
60	0.7077271	15.871	16.156	0.88	0.18	15.516	15.726	0.69	0.19	0.369	0.357	b
64	0.605465	16.019	16.294	0.93	0.17	15.659	15.865	0.72	0.17	0.380	0.363	
65	0.668347	15.823	16.181	1.21	0.15	15.493	15.746	0.96	0.15	0.361	0.343	b
69	0.5666151	16.000	16.344	1.15	0.15	15.666	15.922	0.91	0.15	0.360	0.345	
71	0.549053	16.015	16.347	0.96	0.17	15.678	15.920	0.73	0.17	0.372	0.341	a c
72	0.4560780	15.929	16.475	1.67	0.13	15.684	16.079	1.29	0.14	0.298	0.277	c
73	0.670799	16.022	16.150	0.33	0.35	15.622	15.726	0.26	0.33	0.401	0.409	
74	0.492152	15.922	16.425	1.58	0.11	15.653	16.022	1.24	0.12	0.310	0.298	
76	0.5017678	15.999	16.512	1.57	0.12	15.752	16.125	1.24	0.11	0.309	0.276	a
77	0.4593496	15.946	16.504	1.64	0.12	15.717	16.139	1.30	0.12	0.279	0.260	c
81	0.529122	15.956	16.382	1.40	0.12	15.653	15.955	1.06	0.12	0.341	0.325	
82	0.5245239	15.934	16.369	1.41	0.15	15.652	15.969	1.11	0.15	0.330	0.304	
83	0.5012636	15.924	16.408	1.57	0.12	15.659	16.013	1.23	0.12	0.298	0.294	
84	0.595732	15.990	16.270	0.93	0.17	15.631	15.839	0.74	0.17	0.383	0.362	
89	0.548481	15.920	16.301	1.34	0.13	15.605	15.884	1.06	0.13	0.364	0.334	
90	0.517031	15.937	16.397	1.47	0.13	15.649	15.981	1.18	0.13	0.329	0.313	
92	0.502760	15.885	16.345	1.43	0.15	15.619	15.953	1.14	0.15	0.313	0.289	
93	0.602294	15.982	16.261	0.92	0.18	15.640	15.845	0.73	0.18	0.360	0.345	
94	0.523696	15.957	16.395	1.43	0.13	15.675	15.993	1.16	0.13	0.316	0.305	
96	0.4994160	15.794	16.372	1.46	—	15.564	15.956	1.12	0.12	—	0.254	a

Table 2—Continued

Star	Period	$\langle B \rangle$	B_{min}	A_B	RT_B	$\langle V \rangle$	V_{min}	A_V	RT_V	$(B - V)_{mag}$	$(B - V)_S$	Notes
100	0.6188126	16.043	16.295	0.79	0.20	15.677	15.870	0.63	0.20	0.378	0.366	
104	0.5699305	15.820	16.298	1.59	0.13	15.539	15.879	1.20	0.13	0.333	0.311	b
108	0.5196153	15.955	16.402	1.46	0.13	15.678	15.999	1.12	0.13	0.322	0.301	
109	0.5339163	15.974	16.397	1.47	0.13	15.682	15.988	1.17	0.13	0.349	0.317	
114	0.5977230	16.043	16.373	1.13	0.15	15.684	15.907	0.82	0.15	0.379	0.369	a
119	0.517692	15.901	16.368	1.50	0.11	15.614	15.955	1.20	0.12	0.336	0.313	
120	0.6401387	16.041	16.244	0.58	0.22	15.663	15.820	0.44	0.22	0.392	0.378	
124	0.752436	15.923	16.100	0.46	0.25	15.530	15.667	0.36	0.26	0.399	0.396	b
133	0.5507177	15.970	16.405	1.33	0.14	15.672	15.981	1.02	0.13	0.320	0.317	
134	0.618057	16.103	16.380	0.80	0.19	15.786	15.982	0.60	0.20	0.333	0.317	a
135	0.5683966	16.001	16.318	0.99	0.16	15.656	15.880	0.72	0.16	0.382	0.350	a
137	0.575161	15.928	16.253	1.14	0.15	15.597	15.820	0.91	0.15	0.368	0.341	a
142	0.568628	16.035	16.381	1.27	0.13	15.706	15.953	1.02	0.13	0.354	0.345	a
144	0.5967843	15.967	16.220	0.67	0.25	15.595	15.791	0.54	0.25	0.390	0.371	c
146	0.596745	15.904	16.214	1.08	0.18	15.549	15.776	0.82	0.17	0.378	0.363	
149	0.549959	15.993	16.418	1.25	0.15	15.684	16.005	1.00	0.15	0.328	0.324	a
167	0.643973	16.015	16.221	0.58	0.22	15.627	15.783	0.43	0.22	0.382	0.388	a
186	0.663267	15.933	16.131	0.58	0.25	15.519	15.674	0.47	0.25	0.390	0.414	a d
197	0.499904	15.983	16.590	1.71	0.13	15.726	16.176	1.34	0.13	0.363	0.290	a
202	0.773562	15.921	15.994	0.21	0.40	15.526	15.588	0.16	0.40	0.400	0.414	b
KG14	0.713409	15.994	16.265	0.75	0.22	15.624	15.851	0.61	0.22	0.382	0.369	a b

^a Large scatter or gaps in the lightcurve

^b Long period/overluminous

^c Low amplitude/suspected Blazhko

^d Companion?

Table 3. Photometric parameters for the Blazhko RR Lyrae variables. Each star is listed at least twice: the first line refers to the CC01 1992 data, the second line to the 1993 data. When available, also the data from Kal98 and Car98 are listed, as indicated in the notes.

Star	Period	$\langle B \rangle$	B_{min}	A_B	$\langle V \rangle$	V_{min}	A_V	$(B - V)_S$	Notes	
3	0.558200	15.831	16.264	1.44	15.565	15.897	1.08	0.290		
		15.818	16.286	1.64	15.535	15.883	1.29	0.314	d	
5	0.504178		16.4:	1.0:		15.9:	0.9:		c	
		15.876	16.296	1.06	15.600	15.910	0.80	0.283	c	
7	0.497429			1.5:			1.2:		c	
		15.939	16.415	1.44	15.697	16.029	1.18	0.266	c	
14	0.635903	15.863	16.233	1.14	15.538	15.810	0.89	0.335		
		15.823	16.226	1.36	15.504	15.806	1.04	0.339	d	
17	0.6359019				15.507	15.759	0.85		a	
		0.5761594	15.933	16.361	1.38	15.613	15.937	1.11	0.341	
18	0.516451	15.935	16.339	1.30	15.620	15.927	0.98	0.332		
		0.5757			15.645	15.863	0.70		a	
20	0.490476	15.987	16.421	1.44	15.684	15.991	1.14	0.327		
		15.965	16.400	1.45	15.672	15.984	1.13	0.317		
23	0.5163623				15.675	15.985	1.13		a	
		0.490476	15.875:	16.325	1.31:	15.566:	15.943	1.03:		c
23	0.5953756	15.860	16.328	1.11	15.614	15.946	0.87	0.255		
		15.900	16.250	1.14	15.580	15.839	0.85	0.330		
24	0.6633722	15.957	16.222	0.78	15.619	15.814	0.62	0.338		
		15.838	16.177	1.13	15.492	15.738	0.86	0.356	a	
28	0.469909	15.857	16.151	0.92	15.499	15.721	0.72	0.361	d	
		15.906	16.207	0.93	15.503	15.731	0.74	0.406	b	
33	0.5252355	15.937	16.320	1.09	15.672	15.961	0.85	0.273	e	
		0.4706131	15.906	16.259	0.91	15.647	15.903	0.69	0.261	b
34	0.560963	15.880	16.331	1.30	15.608	15.952	0.97	0.289		
		15.873	16.381	1.58	15.591	15.981	1.26	0.311		
35	0.5591012	15.917	16.385	1.42	15.612	15.953	1.12	0.328		
		15.909	16.362	1.28	15.613	15.961	0.99	0.313		
41	0.486631	15.967	16.328	0.97	15.640	15.909	0.77	0.331		
		0.5591012	15.958	16.312	1.19	15.658	15.925	0.88	0.313	b
43	0.540510	0.530557	15.922	16.271	1.01	15.625	15.886	0.77	0.302	
		15.828	16.414	1.75	15.567	15.992	1.36	0.295	d	
44	0.506354	0.5296			15.562	15.927	1.13		a	
		15.991	16.212	0.67	15.660	15.833	0.57	0.330		
45	0.536073	15.931	16.438	1.29	15.625	16.000	0.98	0.323		
		15.959	16.312	1.08	15.633	15.896	0.85	0.334		
45	0.5404673	16.030	16.301	0.79	15.672	15.871	0.63	0.358		
		15.950	16.310	0.84	15.681	15.973	0.67	0.270	c	
45	0.506354	15.989	16.352	1.03	15.724	16.021	0.80	0.271	c	
		15.985	16.381	1.19	15.686	15.978	0.99	0.312		
45	0.536073	15.942	16.423	1.43	15.653	15.998	1.16	0.312		
		15.920	16.366	1.45	15.627	15.943	1.11	0.317	b	
45	0.506354	15.874	16.164	0.80	15.519	15.806	0.64	0.355	c	
		15.921	16.075	0.45	15.576	15.740	0.35	0.348	c	
45	0.536073	15.976	16.342	1.18	15.674	15.941	0.92	0.314		

Table 3—Continued

Star	Period	$\langle B \rangle$	B_{min}	A_B	$\langle V \rangle$	V_{min}	A_V	$(B - V)_S$	Notes
		15.943	16.404	1.39	15.643	16.000	1.10	0.321	
47	0.540896	15.927	16.342	0.97	15.636	15.943	0.74	0.295	
		15.982	16.200	0.64	15.670	15.841	0.50	0.311	c
	0.5409128	16.006	16.263	0.90	15.581	15.735	0.63	0.427	b
49	0.5482088	15.955	16.330	1.23	15.637	15.922	0.98	0.332	
		16.023	16.254	0.67	15.677	15.856	0.53	0.345	
50	0.513170	15.932	16.271	0.99	15.633	15.896	0.76	0.304	c
		15.862	16.404	1.55	15.597	15.987	1.20	0.293	
	0.5130879				15.642		0.54		a
52	0.516236	15.651:	16.478	1.15:	15.706:	16.067	1.00:		c
		16.022	16.284	0.63	15.705	15.909	0.49	0.316	
	0.5162250				15.621		1.20		a
59	0.5888259	16.015	16.279	0.85	15.672	15.868	0.68	0.344	
		15.989	16.283	1.01	15.648	15.868	0.79	0.346	
	0.5888053				15.628	15.867	0.83		a
61	0.520926	15.907	16.380	1.31	15.615	15.974	1.00	0.310	
		15.932	16.350	1.25	15.641	15.965	1.03	0.306	
	0.5209312				15.614	16.011	1.22		a
62	0.6524179	15.988	16.209	0.65	15.610	15.777	0.49	0.377	c
		15.999	16.244	0.73	15.622	15.808	0.57	0.376	
	0.6524077				15.603	15.769	0.48		a
63	0.570382	15.977	16.290	0.95	15.647	15.889	0.73	0.333	
		15.999	16.295	0.93	15.663	15.887	0.71	0.339	
	0.5704164				15.649	15.895	0.85		a
66	0.619100	15.958	16.225	0.78	15.612	15.809	0.62	0.346	
		15.965	16.261	0.96	15.608	15.826	0.78	0.361	
	0.6191				15.629	15.823	0.64		a
	0.6201631	15.964	16.247	0.85	15.627	15.846	0.63	0.338	b
67	0.5683327	15.911	16.357	1.51	15.601	15.931	1.22	0.337	d
		15.970	16.343	1.21	15.648	15.923	0.96	0.335	
	0.5683609				15.694	15.872	0.56		a
	0.5683245	16.019	16.358	1.04	15.663	15.914	0.85	0.363	b
78	0.611965	15.891	16.208	1.08	15.542	15.756	0.76	0.357	c
		15.941	16.191	0.70	15.554	15.761	0.55	0.386	c
		15.911	16.213	1.14	15.548	15.796	0.94	0.373	b
80	0.537556	15.970	16.236	0.80	15.656	15.837	0.59	0.314	
		15.978	16.232	0.69	15.648	15.843	0.53	0.329	
91	0.529369	15.940	16.292	1.00	15.635	15.878	0.76	0.310	
		15.892	16.364	1.46	15.616	15.966	1.17	0.300	c
101	0.643886	16.067	16.284	0.64	15.697	15.852	0.44	0.369	
		16.058	16.345	0.76	15.695	15.926	0.60	0.362	
	0.6438975	16.099	16.315	0.59	15.695	15.926	0.60	0.404	b
106	0.5471228	15.947	16.407	1.20	15.645	15.974	0.91	0.315	
		15.990	16.282	0.87	15.667	15.882	0.70	0.324	
	0.5471593				15.683	15.852	0.66		a
110	0.535454	15.900	16.340	1.37	15.611	15.931	1.12	0.310	

Table 3—Continued

Star	Period	$\langle B \rangle$	B_{min}	A_B	$\langle V \rangle$	V_{min}	A_V	$(B - V)_S$	Notes
		15.956	16.283	1.01	15.625	15.858	0.78	0.336	c
	0.5354435	15.948	16.401	1.33	15.599	15.884	0.88	0.368	b c
111	0.5102469	16.012	16.344	0.94	15.720	15.992	0.69	0.295	c
		16.020	16.329	0.89	15.716	15.944	0.66	0.306	c
	0.5101784	15.953	16.355	1.03	15.628	15.85:	0.77	0.331	b c
117	0.597263	15.896	16.305	1.18	15.570	15.873	0.93	0.338	
		15.917	16.252	0.98	15.597	15.847	0.75	0.324	
121	0.535211	16.013	16.336	1.14	15.719	15.962	0.86	0.304	c
		16.043	16.368	0.88	15.743	15.992	0.70	0.302	c
	0.5352048	15.963	16.448	1.02	15.701	16.067	0.90	0.268	b
130	0.567840	15.932	16.220	0.83	15.574	15.780	0.59	0.359	c
		15.895	16.278	1.09	15.537	15.816	0.83	0.366	c
	0.5692614	15.892	16.131	0.85	15.556	15.730	0.66	0.337	b
143	0.596535	15.821	16.135	1.12	15.465	15.708	0.79	0.366	c
		15.805	16.166	1.12	15.470	15.724	0.91	0.345	c
	0.5913691	15.736	16.282	1.57	15.397	15.769	1.17	0.368	b c
150	0.523919	15.900	16.420	1.61	15.632	16.007	1.27	0.298	
		15.935	16.358	1.36	15.648	15.954	1.14	0.307	
	0.5239411	16.016	16.397	1.16	15.675	15.984	0.99	0.352	b
155	0.47114	15.850	16.274	1.14	15.603	15.964	0.99	0.257	c
		15.812	16.374	1.50	15.582	16.030	1.23	0.256	c
	0.3316733	15.747	16.025	0.70	15.518	15.731	0.62	0.228	b
176	0.540593	16.048	16.386	0.94	15.807	16.089	0.79	0.244	c
		16.129	16.307	0.59	15.847	15.951	0.43	0.282	c

^a Data from Kal98

^b Data from Car98

^c Large scatter or gaps in the light curve

^d Long period/overluminous

^e Switching to RRc?

Table 4. Colors and BC_V as a function of T_{eff} for various calibrations (cf. Sect. 4.2).

	5500	5750	6000	6250	6500	6750	7000	7250	7500
Castelli (1999) - C99									
(B-V)	0.591	0.513	0.447	0.390	0.337	0.288	0.242	0.195	0.145
(V-K)	1.745	1.565	1.397	1.237	1.082	0.935	0.795	0.663	0.543
BC_V	-0.168	-0.128	-0.094	-0.063	-0.035	-0.010	0.010	0.026	0.033
Montegriffo et al. (1998) empirical - M98e									
(B-V)	0.539	0.458	0.396	0.330	0.272	0.219	0.187	0.157	0.113
(V-K)	1.707	1.523	1.355	1.188	1.030	0.873	0.724	0.584	0.448
BC_V	-0.159	-0.110	-0.074	-0.036	-0.003	0.030	0.059	0.080	0.098
Montegriffo et al. (1998) theoretical - M98t									
(B-V)	0.549	0.467	0.407	0.343	0.290	0.238	0.202	0.178	0.147
(V-K)	1.730	1.545	1.382	1.223	1.077	0.935	0.800	0.672	0.552
BC_V	-0.165	-0.115	-0.080	-0.043	-0.014	0.017	0.045	0.067	0.084
Sandage, Bell & Tripicco (1999) - SBT									
(B-V)	0.579	0.514	0.448	0.402	0.355	0.311	0.266	0.221	0.175
BC_V	-0.211	-0.175	-0.138	-0.109	-0.079	-0.060	-0.041	-0.032	-0.022
Sekiguchi & Fukugita (2000) - SF									
(B-V)	0.588	0.511	0.442	0.380	0.323	0.271	0.224	0.180	0.140

Table 5. For the 29 RR Lyrae stars with K photometry from L90, we show the comparison of T_{eff} and BC_V values derived from various calibrations (see Sect. 4.2), and (B–V) colors (columns 1-7) and (V–K) colors when available (columns 8-14). The related parameters A , M_V and $mass$ are discussed in Sect. 4.3. CSJ calibration is independent of color (cf. eq. 5).

T_{eff}	BC_V	A	M_V (1)	M_V (2)	M/M_\odot (3)	M/M_\odot (4)	T_{eff}	BC_V	A	M_V (1)	M_V (2)	M/M_\odot (3)	M/M_\odot (4)	Notes
Castelli (1999)														
7121	0.018	-1.845	0.38	0.46	0.59	0.62	7136	0.018	-1.848	0.38	0.45	0.58	0.61	(5)
6597	-0.026	-1.847	0.42	0.50	0.61	0.65	6568	-0.028	-1.839	0.45	0.52	0.63	0.66	(6)
6765	-0.012	-1.846	0.41	0.49	0.60	0.64	6751	-0.014	-1.842	0.42	0.50	0.61	0.65	(7)
Montegriffo et al. (1998) empirical														
6763	0.031	-1.754	0.60	0.67	0.75	0.79	6906	0.048	-1.791	0.49	0.56	0.66	0.70	(5)
6304	-0.029	-1.767	0.63	0.70	0.77	0.82	6391	-0.018	-1.791	0.56	0.63	0.71	0.75	(6)
6452	-0.010	-1.763	0.62	0.69	0.76	0.81	6557	0.003	-1.791	0.53	0.61	0.69	0.74	(7)
Montegriffo et al. (1998) theoretical														
6879	0.031	-1.784	0.52	0.60	0.69	0.73	7041	0.048	-1.825	0.40	0.48	0.60	0.63	(5)
6369	-0.030	-1.785	0.58	0.66	0.73	0.78	6464	-0.018	-1.811	0.51	0.58	0.67	0.71	(6)
6533	-0.010	-1.784	0.56	0.64	0.72	0.76	6650	0.003	-1.815	0.47	0.55	0.65	0.69	(7)
Sandage, Bell & Tripicco (1999)														
7258	-0.031	-1.878	0.35	0.43	0.59	0.62								(5)
6707	-0.063	-1.876	0.39	0.46	0.59	0.62								(6)
6884	-0.053	-1.877	0.38	0.45	0.59	0.62								(7)
Sekiguchi & Fukugita (2000)														
7027	0.012	-1.821	0.45	0.52	0.66	0.70								(5)
6526	-0.033	-1.828	0.48	0.55	0.65	0.69								(6)
6687	-0.019	-1.826	0.47	0.54	0.65	0.69								(7)
Carney et al. (1992)														
6536	-0.032	-1.830	0.47	0.55	0.65	0.68								(6)

- (1)– derived from the A parameter (eq. 8) assuming $mass=0.74 M_\odot$
- (2)– derived from the A parameter (eq. 8) assuming $mass=0.68 M_\odot$
- (3)– derived from the A parameter (eq. 8) assuming $M_V=0.59$, i.e. $(m-M)_0=15.02$
- (4)– derived from the A parameter (eq. 8) assuming $M_V=0.54$, i.e. $(m-M)_0=15.07$
- (5)– RRc only (9 stars)
- (6)– RRab only (20 stars)
- (7)– RRc + RRab together

Table 6. Physical parameters for RRc and RRab stars, from the $(B - V)_S$ colors and the SF temperature scale. The values of $\log L$, M_V and M/M_\odot assume $(m - M)_0=15.07$ (cf. Sect. 4.2 and 4.3).

Star	Period	T_{eff}	BC_V	A	$\log L$	M_V	M/M_\odot	$\log g$
12	0.3175400	7152	0.021	-1.846	1.707	0.462	0.67	2.93
29	0.3316840	7044	0.013	-1.842	1.741	0.385	0.75	2.92
37	0.3266387	7011	0.011	-1.826	1.686	0.523	0.67	2.92
56	0.3296000	7039	0.013	-1.837	1.692	0.506	0.66	2.91
70	0.4860930	6727	-0.012	-1.958	1.805	0.249	0.65	2.71
75	0.3140800	7022	0.012	-1.808	1.686	0.524	0.71	2.94
85	0.3558170	7061	0.014	-1.882	1.741	0.382	0.67	2.87
86	0.2926590	7095	0.017	-1.790	1.678	0.539	0.73	2.98
97	0.3349326	6887	0.001	-1.807	1.675	0.560	0.69	2.91
105	0.2877440	7228	0.025	-1.814	1.717	0.433	0.76	2.99
107	0.3090350	7072	0.015	-1.812	1.682	0.529	0.69	2.95
125	0.3498230	6829	-0.003	-1.815	1.694	0.519	0.71	2.89
126	0.3484100	6855	-0.001	-1.819	1.692	0.521	0.70	2.89
128	0.2920400	7228	0.025	-1.821	1.681	0.523	0.67	2.97
129	0.4061020	6712	-0.013	-1.861	1.753	0.380	0.74	2.81
131	0.2976910	7118	0.018	-1.804	1.673	0.549	0.69	2.97
132	0.3398510	6773	-0.008	-1.785	1.706	0.493	0.80	2.91
140	0.3334990	7072	0.015	-1.852	1.743	0.378	0.73	2.91
152	0.3261350	7269	0.027	-1.889	1.727	0.405	0.63	2.91
170	0.4356940	6903	0.003	-1.947	1.831	0.170	0.72	2.77
177	0.3487490	7305	0.028	-1.932	1.704	0.462	0.52	2.86
178	0.2673870	7397	0.031	-1.817	1.644	0.609	0.61	3.01
203	0.2897940	7269	0.027	-1.828	1.711	0.445	0.72	2.98
1	0.5205959	6638	-0.021	-1.819	1.707	0.502	0.73	2.84
6	0.5143332	6609	-0.024	-1.805	1.679	0.575	0.70	2.84
9	0.5415528	6614	-0.023	-1.833	1.698	0.527	0.68	2.81
10	0.5695439	6469	-0.038	-1.820	1.711	0.510	0.73	2.79
11	0.5078940	6732	-0.012	-1.831	1.711	0.484	0.71	2.85
15	0.5300874	6566	-0.028	-1.809	1.711	0.501	0.76	2.83
16	0.5114943	6648	-0.020	-1.813	1.675	0.582	0.68	2.84
19	0.6319720	6266	-0.061	-1.818	1.693	0.578	0.70	2.73
21	0.5157556	6482	-0.037	-1.772	1.696	0.548	0.80	2.85
22	0.4814240	6819	-0.004	-1.826	1.679	0.557	0.66	2.87
25	0.4800620	6727	-0.012	-1.801	1.685	0.550	0.72	2.88
26	0.5977405	6562	-0.028	-1.870	1.735	0.442	0.68	2.76
27	0.5790730	6482	-0.037	-1.832	1.707	0.520	0.70	2.78
31	0.5807196	6552	-0.029	-1.853	1.740	0.430	0.73	2.78
32	0.4953500	6643	-0.020	-1.795	1.721	0.467	0.81	2.87
36	0.5455989	6566	-0.028	-1.824	1.706	0.514	0.71	2.81
40	0.5515350	6473	-0.038	-1.805	1.688	0.567	0.72	2.81
42	0.5900984	6737	-0.011	-1.910	1.750	0.387	0.63	2.76
46	0.6133832	6348	-0.052	-1.825	1.691	0.575	0.68	2.75
48	0.6278299	6283	-0.059	-1.819	1.769	0.386	0.87	2.75
51	0.5839702	6432	-0.042	-1.823	1.702	0.538	0.71	2.77
53	0.5048815	6638	-0.021	-1.803	1.693	0.539	0.73	2.85
54	0.5062470	6663	-0.018	-1.811	1.672	0.588	0.67	2.84

Table 6—Continued

Star	Period	T_{eff}	BC_V	A	$\log L$	M_V	M/M_\odot	$\log g$
55	0.5298217	6609	-0.024	-1.821	1.688	0.553	0.69	2.82
57	0.5121908	6538	-0.031	-1.784	1.683	0.573	0.75	2.85
58	0.5170540	6459	-0.039	-1.768	1.751	0.411	0.96	2.86
60	0.7077271	6392	-0.047	-1.911	1.753	0.415	0.64	2.67
64	0.6054650	6365	-0.050	-1.823	1.697	0.558	0.70	2.76
65	0.6683470	6455	-0.040	-1.899	1.759	0.392	0.67	2.70
69	0.5666151	6446	-0.041	-1.811	1.690	0.565	0.71	2.79
71	0.5490530	6464	-0.039	-1.800	1.685	0.577	0.72	2.81
72	0.4560780	6773	-0.008	-1.786	1.670	0.583	0.72	2.90
73	0.6707990	6170	-0.073	-1.821	1.721	0.521	0.75	2.71
74	0.4921520	6668	-0.018	-1.798	1.686	0.552	0.73	2.86
76	0.5017678	6778	-0.008	-1.837	1.643	0.651	0.58	2.83
77	0.4593496	6861	-0.001	-1.813	1.654	0.616	0.64	2.89
81	0.5291220	6538	-0.031	-1.801	1.692	0.552	0.73	2.83
82	0.5245239	6638	-0.021	-1.823	1.688	0.551	0.68	2.83
83	0.5012636	6687	-0.016	-1.813	1.683	0.558	0.69	2.85
84	0.5957320	6370	-0.049	-1.816	1.708	0.530	0.73	2.77
89	0.5484810	6496	-0.035	-1.808	1.713	0.504	0.76	2.81
90	0.5170310	6595	-0.025	-1.804	1.691	0.548	0.72	2.84
92	0.5027600	6712	-0.013	-1.821	1.698	0.518	0.71	2.85
93	0.6022940	6446	-0.041	-1.843	1.701	0.539	0.67	2.75
94	0.5236960	6634	-0.021	-1.821	1.679	0.574	0.67	2.83
96	0.4994160	6892	0.002	-1.864	1.714	0.463	0.65	2.85
100	0.6188126	6352	-0.051	-1.831	1.690	0.576	0.67	2.74
104	0.5699305	6605	-0.024	-1.857	1.734	0.438	0.71	2.79
108	0.5196153	6653	-0.019	-1.822	1.677	0.577	0.66	2.83
109	0.5339163	6576	-0.027	-1.816	1.678	0.581	0.68	2.82
114	0.5977230	6339	-0.053	-1.809	1.688	0.583	0.71	2.76
119	0.5176920	6595	-0.025	-1.805	1.705	0.513	0.75	2.84
120	0.6401387	6300	-0.057	-1.834	1.698	0.562	0.68	2.72
124	0.7524360	6224	-0.066	-1.896	1.755	0.429	0.67	2.64
133	0.5507177	6576	-0.027	-1.832	1.682	0.571	0.65	2.80
134	0.6180570	6576	-0.027	-1.891	1.637	0.685	0.49	2.71
135	0.5683966	6423	-0.043	-1.807	1.695	0.555	0.73	2.79
137	0.5751610	6464	-0.039	-1.824	1.717	0.496	0.74	2.79
142	0.5686280	6446	-0.041	-1.813	1.674	0.605	0.67	2.78
144	0.5967843	6330	-0.054	-1.806	1.724	0.494	0.79	2.77
146	0.5967450	6365	-0.050	-1.816	1.741	0.448	0.81	2.77
149	0.5499590	6543	-0.030	-1.822	1.679	0.583	0.67	2.80
167	0.6439730	6258	-0.062	-1.825	1.714	0.526	0.73	2.73
186	0.6632670	6150	-0.075	-1.810	1.763	0.418	0.88	2.73
197	0.4999040	6707	-0.014	-1.816	1.656	0.625	0.63	2.84
202	0.7735620	6150	-0.075	-1.889	1.760	0.425	0.69	2.63
KG14	0.7134090	6339	-0.053	-1.901	1.712	0.523	0.58	2.66

Table 7. Physical parameters for Blazhko stars, from the average CC01 1992 and 1993 values of $(B-V)_S$ and $\langle V \rangle$ and the SF temperature scale. The values of $\log L$, M_V and mass assume $(m-M)_0=15.07$ (cf. Sect. 4.2 and 4.3).

Star	Period	T_{eff}	BC_V	A	$\log L$	M_V	M/M_\odot	$\log g$
3	0.5582000	6648	-0.020	-1.858	1.728	0.449	0.69	2.80
14	0.6359030	6482	-0.037	-1.881	1.747	0.420	0.68	2.73
17	0.5761594	6485	-0.037	-1.830	1.708	0.515	0.71	2.78
18	0.5164510	6552	-0.029	-1.792	1.681	0.577	0.73	2.84
20	0.4904760	6702	-0.014	-1.805	1.710	0.489	0.76	2.87
23	0.5953756	6496	-0.035	-1.850	1.715	0.498	0.68	2.76
24	0.6633722	6385	-0.048	-1.876	1.761	0.394	0.72	2.71
28	0.4699090	6824	-0.004	-1.815	1.678	0.558	0.68	2.88
33	0.5252355	6564	-0.028	-1.804	1.711	0.500	0.77	2.84
34	0.5609630	6552	-0.029	-1.835	1.702	0.525	0.68	2.79
35	0.5305570	6665	-0.018	-1.836	1.709	0.495	0.70	2.82
38	0.5580110	6531	-0.032	-1.826	1.696	0.541	0.69	2.80
39	0.5870670	6441	-0.041	-1.828	1.696	0.551	0.69	2.77
41	0.4866310	6806	-0.005	-1.828	1.661	0.601	0.62	2.86
43	0.5405100	6600	-0.025	-1.828	1.682	0.568	0.66	2.81
44	0.5063540	6416	-0.044	-1.745	1.739	0.446	0.98	2.88
45	0.5360730	6574	-0.027	-1.817	1.688	0.557	0.69	2.82
47	0.5408960	6643	-0.020	-1.840	1.687	0.552	0.65	2.81
49	0.5482088	6475	-0.038	-1.802	1.693	0.556	0.73	2.81
50	0.5131700	6665	-0.018	-1.819	1.702	0.514	0.72	2.84
59	0.5888259	6446	-0.041	-1.831	1.693	0.559	0.67	2.77
61	0.5209260	6619	-0.023	-1.814	1.698	0.527	0.72	2.83
62	0.6524179	6307	-0.056	-1.845	1.717	0.515	0.69	2.72
63	0.5703820	6487	-0.036	-1.826	1.693	0.554	0.69	2.78
66	0.6191000	6408	-0.045	-1.846	1.714	0.509	0.69	2.74
67	0.5683327	6487	-0.036	-1.824	1.705	0.523	0.71	2.79
78	0.6119650	6328	-0.054	-1.818	1.743	0.447	0.81	2.76
80	0.5375560	6555	-0.029	-1.813	1.691	0.551	0.71	2.82
91	0.5293690	6634	-0.021	-1.827	1.699	0.524	0.70	2.82
101	0.6438860	6354	-0.051	-1.852	1.682	0.595	0.62	2.71
106	0.5471228	6564	-0.028	-1.825	1.689	0.555	0.68	2.80
110	0.5354540	6547	-0.030	-1.809	1.705	0.517	0.74	2.82
111	0.5102469	6655	-0.019	-1.813	1.661	0.617	0.65	2.84
117	0.5972630	6510	-0.034	-1.856	1.721	0.482	0.68	2.76
121	0.5352110	6643	-0.020	-1.835	1.656	0.630	0.60	2.81
130	0.5678400	6368	-0.049	-1.791	1.738	0.454	0.86	2.81
143	0.5965350	6399	-0.046	-1.825	1.772	0.367	0.86	2.78
150	0.5239190	6646	-0.020	-1.824	1.692	0.539	0.69	2.83
155	0.4711400	6879	0.001	-1.830	1.703	0.492	0.70	2.88
176	0.5405930	6845	-0.002	-1.893	1.610	0.726	0.45	2.78

Table 8. Fourier parameters (cosine series) for the RRc-type variables.

Star	A_0	A_1	A_4	A_{21}	ϕ_{21}	ϕ_{31}
12	15.609	0.258	0.021	0.181	4.734	3.218
29	15.527	0.222	0.018	0.120	4.707	3.788
37	15.669	0.249	0.012	0.139	4.704	3.158
56	15.651	0.244	0.011	0.138	4.614	3.197
70	15.387	0.169	0.011	0.098	4.238	5.049
75	15.670	0.249	0.010	0.172	4.497	2.977
85	15.527	0.250	0.014	0.094	4.994	4.072
86	15.686	0.259	0.019	0.229	4.643	2.689
97	15.702	0.216	0.007	0.088	4.752	3.659
105	15.571	0.163	0.003	0.121	4.876	2.786
107	15.677	0.272	0.017	0.165	4.572	2.682
125	15.660	0.213	0.005	0.137	4.916	3.428
126	15.662	0.210	0.001	0.075	5.115	3.552
128	15.672	0.270	0.022	0.216	4.681	2.515
129	15.522	0.212	0.008	0.164	5.733	4.079
131	15.698	0.270	0.015	0.199	4.535	2.707
132	15.635	0.215	0.004	0.103	4.370	3.550
140	15.522	0.240	0.002	0.084	4.561	3.775
152	15.549	0.235	0.008	0.080	4.922	3.694
170	15.312	0.215	0.012	0.034	3.933	5.062
177	15.612	0.279	0.018	0.180	5.064	4.031
178	15.746	0.171	0.004	0.185	4.514	2.172
203	15.577	0.081	0.002	0.051	3.659	1.641

Table 9. Fourier parameters (cosine series) for the RRab-type variables.

Star	A_1	A_2	A_3	A_4	ϕ_{21}	ϕ_{31}	ϕ_{41}	Dm
1	0.409	0.181	0.144	0.098	3.906	1.561	5.827	4.6
6	0.391	0.181	0.142	0.095	3.829	1.712	5.894	0.8
9	0.366	0.161	0.124	0.085	3.820	1.609	5.840	1.0
10	0.307	0.141	0.102	0.066	3.921	1.790	6.152	1.2
11	0.435	0.203	0.153	0.098	3.867	1.624	5.873	1.4
15	0.380	0.168	0.136	0.093	3.848	1.635	5.852	0.9
16	0.396	0.182	0.148	0.097	3.804	1.649	5.893	2.5
19	0.180	0.074	0.041	0.013	4.111	2.301	0.866	3.8
21	0.376	0.174	0.136	0.089	3.800	1.690	5.926	2.5
22	0.419	0.176	0.096	0.047	3.794	1.639	5.728	2.0
25	0.437	0.197	0.148	0.102	3.869	1.618	5.862	1.5
26	0.336	0.156	0.116	0.076	3.812	1.778	6.032	0.8
27	0.301	0.152	0.105	0.066	3.885	1.940	6.264	2.1
31	0.396	0.196	0.134	0.095	3.991	1.964	6.109	3.0
32	0.388	0.169	0.137	0.092	3.733	1.477	5.698	2.8
36	0.386	0.181	0.142	0.091	3.837	1.698	5.952	2.2
40	0.343	0.156	0.112	0.069	3.839	1.790	6.069	2.6
42	0.448	0.229	0.141	0.105	3.936	1.989	6.143	3.1
46	0.219	0.092	0.057	0.024	3.956	2.049	0.154	2.3
48	0.240	0.096	0.073	0.038	3.923	1.804	0.076	3.0
51	0.292	0.134	0.098	0.061	3.850	1.882	6.199	1.1
53	0.415	0.179	0.123	0.083	3.807	1.554	5.710	1.6
54	0.289	0.120	0.036	0.015	4.242	2.478	5.107	23
55	0.384	0.173	0.138	0.085	3.831	1.660	5.864	1.7
57	0.389	0.191	0.137	0.094	3.769	1.587	5.825	1.6
58	0.424	0.186	0.146	0.082	3.847	1.591	5.853	2.8
60	0.251	0.124	0.073	0.028	4.268	2.518	0.848	2.0
64	0.257	0.120	0.082	0.045	4.017	2.138	0.298	0.5
65	0.321	0.177	0.107	0.065	4.108	2.225	0.478	2.8
69	0.315	0.147	0.107	0.065	3.970	1.896	0.018	1.2
71	0.291	0.128	0.075	0.039	3.915	1.977	0.139	1.4
72	0.460	0.208	0.158	0.104	3.786	1.528	5.743	1.2
73	0.117	0.036	0.011	0.005	4.456	3.034	1.594	69
74	0.434	0.198	0.150	0.103	3.801	1.556	5.711	1.3
76	0.437	0.190	0.160	0.100	3.806	1.561	5.686	3.6
77	0.491	0.224	0.143	0.102	3.783	1.614	5.783	1.7
81	0.369	0.166	0.132	0.090	3.863	1.671	5.865	0.9
82	0.384	0.171	0.133	0.088	3.811	1.555	5.760	2.6
83	0.420	0.192	0.147	0.096	3.806	1.523	5.737	1.2
84	0.257	0.127	0.084	0.050	3.980	1.999	0.241	1.4
89	0.346	0.167	0.135	0.079	3.939	1.785	6.165	3.3
90	0.400	0.181	0.144	0.092	3.816	1.651	5.832	1.4
92	0.411	0.190	0.133	0.081	3.697	1.566	5.658	1.9
93	0.257	0.122	0.088	0.041	4.001	2.047	0.259	2.3
94	0.388	0.186	0.138	0.085	3.838	1.687	5.945	2.4
96	0.451	0.185	0.130	0.070	3.881	1.654	5.782	2.6

Table 9—Continued

Star	A_1	A_2	A_3	A_4	ϕ_{21}	ϕ_{31}	ϕ_{41}	Dm
100	0.232	0.105	0.066	0.037	4.122	2.291	0.586	3.1
104	0.413	0.197	0.140	0.101	3.933	1.832	6.079	3.1
108	0.385	0.174	0.130	0.088	3.875	1.713	5.928	2.0
109	0.380	0.192	0.139	0.091	3.818	1.738	5.796	2.5
114	0.289	0.143	0.096	0.054	3.799	1.954	6.025	4.2
119	0.409	0.181	0.144	0.100	3.786	1.570	5.762	0.7
120	0.180	0.069	0.035	0.015	4.062	2.177	0.830	4.8
124	0.150	0.056	0.021	0.009	4.367	2.890	2.195	11
133	0.366	0.175	0.120	0.076	3.956	1.654	5.866	2.9
134	0.236	0.104	0.054	0.032	4.044	2.034	0.300	5.1
135	0.277	0.125	0.070	0.047	3.900	2.017	5.924	6.2
137	0.301	0.141	0.118	0.069	3.726	1.738	5.918	5.7
142	0.319	0.168	0.113	0.093	3.775	1.713	6.115	3.4
144	0.224	0.088	0.036	0.012	4.144	2.213	6.206	14
146	0.286	0.134	0.094	0.060	3.944	2.027	0.163	1.5
149	0.369	0.158	0.123	0.071	4.042	1.659	5.916	4.9
167	0.187	0.059	0.030	0.018	3.931	1.552	6.212	10
186	0.192	0.067	0.035	0.019	3.836	1.777	1.972	29
197	0.408	0.249	0.212	0.054	3.463	1.690	6.187	18
202	0.076	0.015	0.005	0.002	4.379	3.834	0.318	30
KG14	0.245	0.101	0.036	0.013	4.513	2.668	6.072	16

Table 10. Fourier parameters (cosine series) for the Blazhko variables. The data are displayed in the same line order as in Table 3.

Star	A_1	A_2	A_3	A_4	ϕ_{21}	ϕ_{31}	ϕ_{41}	Dm	Notes
3	0.394	0.184	0.115	0.080	4.006	1.952	6.267	1.9	
	0.415	0.197	0.135	0.095	3.805	1.747	6.112	3.8	
14	0.329	0.160	0.086	0.063	4.078	2.213	0.373	2.5	
	0.355	0.177	0.126	0.075	4.121	2.054	0.226	1.9	
17	0.303	0.151	0.091	0.055	4.055	2.139	0.345	1.6	a
	0.373	0.192	0.140	0.073	4.031	2.023	0.155	2.9	
18	0.356	0.166	0.126	0.055	3.972	1.854	0.067	4.0	
	0.268	0.114	0.078	0.038	3.893	1.817	6.045	1.9	a
23	0.365	0.194	0.130	0.092	3.841	1.813	5.719	9.5	
	0.384	0.178	0.138	0.087	3.783	1.679	5.804	2.4	
24	0.378	0.177	0.140	0.091	3.839	1.688	5.869	1.1	a
	0.315	0.139	0.100	0.066	3.850	1.785	6.086	0.7	
28	0.239	0.096	0.060	0.032	3.917	2.037	0.404	11	
	0.274	0.122	0.078	0.043	3.976	1.968	0.095	2.2	a
33	0.293	0.149	0.104	0.061	4.026	2.044	0.195	3.2	
	0.263	0.131	0.063	0.031	4.236	2.624	1.061	2.2	
34	0.264	0.128	0.078	0.046	4.228	2.382	0.553	1.3	b
	0.363	0.121	0.033	0.017	3.780	0.708	3.874	17	
35	0.296	0.085	0.013	0.005	4.090	1.398	4.082	36	
	0.404	0.168	0.085	0.064	3.737	1.626	5.820	7.1	b
38	0.456	0.204	0.158	0.094	3.854	1.735	5.883	2.4	
	0.404	0.194	0.134	0.077	3.815	1.535	5.664	5.8	
39	0.395	0.167	0.098	0.059	3.948	1.820	6.001	1.9	
	0.325	0.122	0.061	0.024	3.775	1.676	5.599	2.2	
41	0.310	0.106	0.034	0.031	3.927	0.861	4.683	13	
	0.476	0.204	0.147	0.108	3.861	1.393	5.495	3.3	
43	0.425	0.188	0.123	0.082	3.863	1.699	6.041	1.8	a
	0.210	0.097	0.056	0.020	3.919	2.000	0.108	3.4	
45	0.422	0.154	0.078	0.052	4.056	1.710	5.912	3.5	
	0.326	0.143	0.088	0.046	3.994	1.905	6.252	2.3	
47	0.245	0.109	0.055	0.030	3.900	1.876	6.142	1.9	
	0.374	0.023	0.089	0.058	3.227	3.687	0.175	27	
49	0.355	0.128	0.079	0.036	3.800	1.729	5.955	3.2	
	0.362	0.149	0.097	0.086	3.886	2.044	6.117	3.5	
50	0.408	0.181	0.138	0.084	3.825	1.712	5.888	2.4	
	0.335	0.164	0.106	0.067	3.739	1.478	5.827	2.5	
52	0.412	0.195	0.109	0.076	3.966	1.899	0.005	3.2	
	0.344	0.124	0.051	0.023	4.075	2.180	0.427	4.0	
53	0.211	0.059	0.004	0.022	3.951	0.381	5.056	17	
	0.352	0.155	0.111	0.075	3.795	1.754	6.007	3.5	
54	0.212	0.086	0.045	0.015	4.151	2.070	0.117	2.7	
	0.354	0.106	0.060	0.075	3.690	2.383	6.233	11	
55	0.456	0.191	0.124	0.084	3.751	1.278	5.507	3.4	
	0.242	0.086	0.035	0.008	3.754	1.237	3.404	3.4	a
56	0.443	0.195	0.140	0.086	3.927	1.629	5.738	1.4	
	0.232	0.069	0.024	0.020	4.089	2.456	1.693	12	

Table 10—Continued

Star	A_1	A_2	A_3	A_4	ϕ_{21}	ϕ_{31}	ϕ_{41}	Dm	Notes
	0.441	0.181	0.142	0.093	3.868	1.574	5.647	2.0	a
59	0.254	0.111	0.074	0.043	4.091	2.249	0.423	1.2	
	0.284	0.137	0.090	0.051	4.002	2.148	0.172	1.9	
	0.301	0.139	0.094	0.053	4.006	1.991	0.028	1.3	a
61	0.410	0.186	0.099	0.043	3.903	1.734	5.771	2.1	
	0.399	0.173	0.108	0.070	3.788	1.585	5.907	1.6	
	0.453	0.199	0.130	0.091	3.838	1.597	5.829	1.5	a
62	0.186	0.088	0.039	0.020	4.381	2.560	1.427	13	
	0.221	0.094	0.054	0.018	4.033	2.112	0.644	4.1	
	0.183	0.084	0.045	0.022	4.166	2.494	0.985	1.0	a
63	0.286	0.116	0.076	0.037	4.021	1.889	0.228	3.1	
	0.268	0.116	0.081	0.040	4.046	2.014	0.089	2.2	
	0.320	0.135	0.095	0.059	3.922	1.783	6.101	1.5	a
66	0.248	0.108	0.062	0.034	3.937	2.076	0.255	1.6	
	0.273	0.127	0.083	0.064	3.950	1.877	0.198	3.3	
	0.239	0.109	0.074	0.033	4.055	2.087	0.367	1.8	a
	0.256	0.098	0.067	0.032	4.045	2.024	0.180	5.4	b
67	0.389	0.194	0.137	0.095	3.855	1.797	5.998	1.7	
	0.332	0.146	0.116	0.069	3.944	1.855	6.202	1.6	
	0.227	0.085	0.057	0.030	3.872	2.043	0.238	5.1	a
	0.307	0.139	0.103	0.064	3.966	1.896	6.030	1.9	b
78	0.280	0.136	0.086	0.050	3.731	1.822	5.651	6.1	
	0.222	0.081	0.045	0.013	4.487	2.662	1.840	33	
	0.315	0.158	0.098	0.076	3.836	1.771	6.055	3.5	b
80	0.243	0.106	0.064	0.036	3.785	1.999	0.214	3.3	
	0.233	0.080	0.030	0.008	3.991	1.985	0.910	26	
91	0.308	0.126	0.075	0.044	3.926	1.990	6.109	3.9	
	0.424	0.187	0.131	0.100	3.821	1.690	5.884	3.8	
101	0.178	0.076	0.032	0.007	4.238	2.704	1.008	31	
	0.266	0.095	0.045	0.018	4.190	2.245	0.256	5.1	
	0.180	0.061	0.046	0.018	4.374	2.809	0.867	38	b
106	0.378	0.149	0.076	0.046	3.964	1.770	5.997	2.1	
	0.265	0.126	0.072	0.038	4.149	2.408	0.400	3.1	
	0.235	0.121	0.063	0.013	4.182	2.234	0.107	5.2	a
110	0.384	0.184	0.129	0.087	3.924	1.646	5.896	1.7	
	0.293	0.122	0.083	0.059	3.942	1.882	5.883	4.2	
	0.329	0.128	0.125	0.100	3.618	1.176	5.700	5.1	b
117	0.364	0.159	0.104	0.063	3.848	1.539	5.910	5.5	
	0.302	0.128	0.082	0.050	3.841	1.516	6.202	6.3	
121	0.309	0.141	0.112	0.052	3.736	1.575	6.017	3.2	
	0.298	0.085	0.067	0.031	3.658	1.254	5.788	4.9	
	0.405	0.156	0.090	0.046	4.027	1.645	5.846	2.3	b
130	0.248	0.100	0.039	0.016	4.197	2.272	6.270	7.0	
	0.320	0.139	0.071	0.039	3.994	1.438	5.513	3.7	
	0.240	0.117	0.070	0.048	3.653	1.740	5.892	5.8	b
143	0.310	0.139	0.092	0.039	3.644	1.389	5.101	4.5	

Table 10—Continued

Star	A_1	A_2	A_3	A_4	ϕ_{21}	ϕ_{31}	ϕ_{41}	Dm	<i>Notes</i>
	0.311	0.184	0.071	0.052	4.105	2.454	5.734	15	
	0.432	0.174	0.125	0.102	3.816	1.449	6.053	5.9	^b
150	0.443	0.197	0.134	0.095	3.738	1.701	5.824	5.0	
	0.383	0.195	0.130	0.098	3.708	1.651	5.713	2.7	
	0.348	0.182	0.105	0.079	4.192	2.123	0.255	3.9	^b
155	0.405	0.148	0.090	0.025	3.906	1.400	6.147	38	
	0.505	0.210	0.110	0.076	3.725	1.775	5.826	5.1	
	0.265	0.041	0.008	0.034	3.946	5.202	3.073	89	^b
176	0.325	0.115	0.071	0.061	3.876	1.868	0.321	11	
	0.162	0.059	0.041	0.033	3.165	1.149	5.860	9.3	

^a Data from Kal98

^b Data from Car98

Table 11. Physical parameters derived from Fourier coefficients for the RRc-type variables (cf. Sect. 6.2).

Star	M_V	$\log L^1$	$\log L^2$	M/M_\odot	$\log T_e$	$\log g$	A
12	0.523	1.682	1.705	0.598	3.865	2.95	1.847
29	0.524	1.685	1.692	0.530	3.865	2.89	1.889
37	0.556	1.673	1.721	0.617	3.863	2.96	1.829
56	0.561	1.670	1.723	0.613	3.862	2.96	1.827
70	0.428	1.734	1.791	0.470	3.848	2.72	1.976
75	0.581	1.663	1.714	0.632	3.864	2.99	1.810
85	0.506	1.692	1.707	0.511	3.863	2.86	1.907
86	0.560	1.669	1.699	0.656	3.867	3.01	1.805
97	0.568	1.672	1.704	0.550	3.864	2.92	1.864
105	0.626	1.640	1.686	0.634	3.869	3.03	1.786
107	0.556	1.671	1.724	0.676	3.864	3.01	1.797
125	0.555	1.679	1.737	0.597	3.860	2.93	1.845
126	0.566	1.674	1.728	0.577	3.861	2.92	1.851
128	0.546	1.672	1.708	0.685	3.866	3.02	1.793
129	0.452	1.724	1.766	0.547	3.854	2.82	1.918
131	0.578	1.662	1.706	0.659	3.866	3.01	1.796
132	0.589	1.668	1.717	0.570	3.863	2.93	1.848
140	0.600	1.654	1.695	0.533	3.865	2.93	1.856
152	0.565	1.663	1.690	0.538	3.866	2.92	1.862
170	0.485	1.705	1.741	0.442	3.855	2.76	1.967
177	0.492	1.692	1.700	0.511	3.864	2.86	1.907
178	0.657	1.625	1.688	0.713	3.870	3.10	1.733
203	0.682	1.617	1.755	0.851	3.862	3.15	1.668

Note. — $\log L^1$ derived from M_V [eq. (17)] and BC_V from Table 6; $\log L^2$ derived from eq. (16)

Table 12. Physical and intrinsic photometric parameters derived from Fourier coefficients for the RRab-type variables (cf. Sect. 6.2).

Star	M_V	$\log L$	[Fe/H]	$(B - V)_0$	$(V - K)_0$	$\log T_e$ ($B - V$)	$\log T_e$ ($V - K$)	M/M_\odot	$\log g$	A
1	0.556	1.696	-1.523	0.321	1.097	3.816	3.812	0.84	2.87	1.759
6	0.586	1.679	-1.286	0.325	1.063	3.816	3.815	0.79	2.87	1.763
9	0.558	1.699	-1.572	0.331	1.125	3.812	3.809	0.82	2.84	1.769
10	0.567	1.695	-1.479	0.348	1.153	3.808	3.806	0.78	2.81	1.780
11	0.554	1.693	-1.370	0.313	1.062	3.820	3.815	0.83	2.88	1.757
15	0.569	1.691	-1.475	0.329	1.101	3.814	3.811	0.81	2.85	1.766
16	0.589	1.679	-1.356	0.324	1.073	3.816	3.814	0.80	2.87	1.757
19	0.579	1.689	-1.129	0.378	1.208	3.800	3.798	0.73	2.76	1.798
21	0.596	1.676	-1.324	0.328	1.076	3.815	3.814	0.79	2.87	1.759
22	0.569	1.681	-1.207	0.297	1.021	3.826	3.819	0.84	2.91	1.742
25	0.593	1.672	-1.228	0.306	1.027	3.823	3.819	0.83	2.91	1.739
26	0.505	1.724	-1.648	0.347	1.176	3.807	3.804	0.81	2.79	1.800
27	0.563	1.694	-1.329	0.352	1.138	3.807	3.807	0.75	2.80	1.792
31	0.474	1.726	-1.306	0.331	1.099	3.814	3.811	0.79	2.81	1.809
32	0.616	1.671	-1.500	0.321	1.083	3.816	3.814	0.82	2.89	1.740
36	0.543	1.702	-1.474	0.331	1.110	3.813	3.810	0.81	2.84	1.777
40	0.560	1.694	-1.382	0.337	1.115	3.812	3.810	0.79	2.83	1.778
42	0.407	1.753	-1.322	0.318	1.093	3.818	3.812	0.83	2.81	1.818
46	0.571	1.694	-1.367	0.368	1.189	3.802	3.801	0.74	2.77	1.801
48	0.541	1.717	-1.775	0.368	1.254	3.799	3.795	0.81	2.76	1.793
51	0.561	1.697	-1.433	0.353	1.157	3.806	3.805	0.76	2.80	1.791
53	0.557	1.693	-1.448	0.310	1.070	3.820	3.815	0.84	2.89	1.752
54	0.630	1.629	-0.212	0.324	0.852	3.824	3.835	0.56	2.85	1.832
55	0.566	1.691	-1.440	0.328	1.095	3.814	3.812	0.80	2.85	1.768
57	0.587	1.682	-1.443	0.323	1.086	3.816	3.813	0.81	2.87	1.754
58	0.546	1.698	-1.464	0.316	1.083	3.818	3.813	0.84	2.87	1.759
60	0.431	1.752	-1.245	0.374	1.232	3.801	3.796	0.76	2.71	1.848
64	0.559	1.695	-1.205	0.362	1.157	3.805	3.804	0.73	2.78	1.803
65	0.424	1.755	-1.427	0.358	1.209	3.805	3.799	0.80	2.74	1.833
69	0.566	1.692	-1.321	0.346	1.131	3.809	3.808	0.77	2.82	1.783
71	0.593	1.676	-1.117	0.342	1.104	3.812	3.810	0.76	2.84	1.772
72	0.617	1.661	-1.220	0.298	1.004	3.825	3.821	0.84	2.94	1.722
73	0.579	1.645	-0.352	0.394	0.758	3.801	3.846	0.31	2.62	2.061
74	0.578	1.682	-1.377	0.310	1.048	3.821	3.817	0.83	2.90	1.747
76	0.567	1.688	-1.422	0.313	1.057	3.819	3.816	0.82	2.89	1.755
77	0.563	1.680	-1.122	0.284	0.982	3.831	3.823	0.86	2.94	1.731
81	0.580	1.685	-1.421	0.331	1.095	3.813	3.812	0.79	2.85	1.767
82	0.570	1.692	-1.553	0.326	1.106	3.814	3.811	0.82	2.86	1.760
83	0.577	1.686	-1.470	0.315	1.073	3.818	3.814	0.84	2.89	1.748
84	0.573	1.692	-1.339	0.362	1.174	3.804	3.803	0.75	2.79	1.791
89	0.579	1.686	-1.372	0.342	1.118	3.810	3.809	0.78	2.83	1.774
90	0.572	1.686	-1.383	0.323	1.074	3.816	3.814	0.80	2.87	1.763
92	0.573	1.685	-1.420	0.314	1.062	3.819	3.816	0.82	2.88	1.754
93	0.568	1.694	-1.310	0.364	1.172	3.804	3.803	0.75	2.78	1.797
94	0.571	1.687	-1.371	0.326	1.084	3.815	3.813	0.80	2.86	1.764

Table 12—Continued

Star	M_V	$\log L$	[Fe/H]	$(B - V)_0$	$(V - K)_0$	$\log T_e$ ($B - V$)	$\log T_e$ ($V - K$)	M/M_\odot	$\log g$	A
96	0.530	1.699	-1.284	0.300	1.034	3.824	3.818	0.85	2.90	1.757
100	0.557	1.694	-1.071	0.367	1.163	3.804	3.803	0.72	2.77	1.808
104	0.475	1.728	-1.425	0.326	1.110	3.815	3.810	0.82	2.82	1.796
108	0.574	1.684	-1.314	0.324	1.073	3.816	3.814	0.80	2.87	1.764
109	0.565	1.689	-1.357	0.330	1.078	3.814	3.814	0.77	2.85	1.778
114	0.543	1.703	-1.411	0.355	1.147	3.806	3.806	0.74	2.78	1.809
119	0.561	1.693	-1.495	0.320	1.087	3.816	3.813	0.83	2.87	1.760
120	0.564	1.701	-1.340	0.377	1.245	3.799	3.795	0.77	2.76	1.793
124	0.455	1.743	-0.986	0.396	1.312	3.796	3.786	0.78	2.69	1.830
133	0.541	1.705	-1.561	0.332	1.127	3.812	3.809	0.82	2.83	1.776
134	0.543	1.707	-1.413	0.362	1.203	3.803	3.800	0.77	2.77	1.797
135	0.577	1.682	-1.168	0.347	1.092	3.810	3.811	0.71	2.81	1.802
137	0.579	1.693	-1.580	0.355	1.159	3.805	3.805	0.76	2.80	1.788
142	0.563	1.699	-1.578	0.347	1.164	3.807	3.805	0.80	2.82	1.777
144	0.571	1.684	-1.057	0.358	1.114	3.807	3.809	0.69	2.78	1.814
146	0.547	1.701	-1.307	0.356	1.156	3.806	3.805	0.76	2.79	1.799
149	0.541	1.705	-1.550	0.331	1.127	3.812	3.809	0.82	2.84	1.775
167	0.547	1.728	-2.201	0.374	1.339	3.794	3.787	0.87	2.75	1.778
186	0.521	1.742	-2.002	0.376	1.436	3.795	3.776	1.03	2.77	1.730
197	0.646	1.653	-1.238	0.338	1.063	3.813	3.815	0.76	2.88	1.748
202	0.505	1.685	0.169	0.417	1.022	3.797	3.815	0.44	2.62	1.969
KG14	0.401	1.754	-1.074	0.366	1.140	3.805	3.806	0.67	2.69	1.896

Table 13. Physical and intrinsic photometric parameters derived from Fourier coefficients for the RR-Blazhko variables (cf. Sect. 6.2).

Star	M_V	$\log L$	[Fe/H]	$(B - V)_0$	$(V - K)_0$	$\log T_e$ ($B - V$)	$\log T_e$ ($V - K$)	M/M_\odot	$\log g$	A
3	0.493	1.716	-1.200	0.323	1.084	3.818	3.812	0.81	2.83	1.790
3	0.485	1.725	-1.476	0.322	1.117	3.816	3.810	0.85	2.84	1.783
14	0.438	1.744	-1.268	0.345	1.163	3.810	3.804	0.80	2.77	1.824
14	0.441	1.748	-1.482	0.349	1.184	3.807	3.802	0.81	2.76	1.821
14	0.473	1.734	-1.368	0.355	1.185	3.806	3.802	0.79	2.76	1.818
17	0.512	1.710	-1.202	0.339	1.106	3.812	3.810	0.78	2.81	1.798
17	0.520	1.713	-1.429	0.340	1.145	3.810	3.806	0.81	2.81	1.786
17	0.583	1.689	-1.479	0.354	1.159	3.806	3.805	0.76	2.80	1.785
18	0.602	1.668	-1.162	0.330	1.038	3.816	3.817	0.74	2.86	1.776
18	0.587	1.679	-1.342	0.326	1.070	3.816	3.814	0.79	2.87	1.764
18	0.596	1.676	-1.330	0.328	1.073	3.815	3.814	0.78	2.87	1.762
23	0.520	1.718	-1.625	0.348	1.180	3.806	3.803	0.80	2.79	1.795
23	0.575	1.691	-1.286	0.360	1.179	3.805	3.802	0.76	2.79	1.785
23	0.549	1.702	-1.379	0.355	1.167	3.806	3.804	0.77	2.79	1.794
24	0.460	1.746	-1.644	0.365	1.235	3.801	3.797	0.80	2.74	1.826
24	0.462	1.728	-0.864	0.362	1.162	3.807	3.803	0.74	2.74	1.835
24	0.473	1.731	-1.189	0.367	1.186	3.804	3.801	0.74	2.74	1.835
28	0.602	1.694	-2.397	0.294	1.124	3.818	3.812	0.93	2.91	1.721
28	0.663	1.646	-1.469	0.309	0.994	3.820	3.823	0.72	2.90	1.761
28	0.597	1.669	-1.162	0.296	1.019	3.826	3.820	0.84	2.93	1.728
33	0.506	1.710	-1.314	0.311	1.053	3.821	3.816	0.83	2.87	1.777
33	0.547	1.701	-1.583	0.320	1.100	3.816	3.812	0.84	2.86	1.764
34	0.474	1.728	-1.393	0.318	1.102	3.818	3.811	0.84	2.83	1.790
34	0.525	1.712	-1.586	0.329	1.130	3.813	3.809	0.81	2.82	1.786
35	0.565	1.718	-2.518	0.321	1.229	3.809	3.800	0.95	2.85	1.737
35	0.466	1.738	-1.803	0.302	1.110	3.820	3.811	0.92	2.86	1.768
35	0.505	1.714	-1.391	0.311	1.086	3.820	3.813	0.86	2.86	1.767
38	0.658	1.652	-1.135	0.363	1.131	3.805	3.807	0.71	2.82	1.773
38	0.431	1.748	-1.525	0.303	1.111	3.822	3.810	0.90	2.84	1.784
39	0.509	1.717	-1.419	0.340	1.149	3.811	3.806	0.80	2.80	1.794
39	0.575	1.693	-1.458	0.356	1.171	3.805	3.804	0.76	2.80	1.788
41	0.607	1.594	1.519	0.310	0.605	3.841	3.857	0.45	2.88	1.874
41	0.621	1.660	-1.114	0.313	1.038	3.821	3.817	0.80	2.90	1.739
43	0.542	1.690	-0.981	0.325	1.040	3.819	3.817	0.75	2.85	1.790
43	0.522	1.708	-1.428	0.322	1.091	3.816	3.812	0.82	2.85	1.778
45	0.587	1.691	-1.718	0.335	1.156	3.810	3.806	0.84	2.85	1.753
45	0.500	1.711	-1.152	0.312	1.065	3.821	3.814	0.83	2.86	1.775
47	0.524	1.695	-0.800	0.317	1.050	3.822	3.815	0.79	2.86	1.776
47	0.640	1.711	-3.220	0.345	1.405	3.796	3.783	1.08	2.85	1.684
49	0.553	1.697	-1.413	0.333	1.113	3.813	3.810	0.80	2.84	1.776
49	0.661	1.646	-0.988	0.357	1.102	3.808	3.810	0.70	2.83	1.773
50	0.563	1.664	-0.378	0.312	0.935	3.827	3.826	0.69	2.87	1.794
50	0.497	1.727	-1.864	0.299	1.121	3.821	3.810	0.95	2.88	1.746
50	0.672	1.662	-1.919	0.340	1.183	3.807	3.804	0.83	2.87	1.726
52	0.521	1.706	-1.408	0.308	1.061	3.821	3.816	0.84	2.87	1.767

Table 13—Continued

Star	M_V	$\log L$	[Fe/H]	$(B - V)_0$	$(V - K)_0$	$\log T_e$ ($B - V$)	$\log T_e$ ($V - K$)	M/M_\odot	$\log g$	A
52	0.670	1.629	-0.296	0.340	1.064	3.818	3.812	0.75	2.89	1.729
52	0.525	1.706	-1.482	0.309	1.069	3.820	3.815	0.84	2.87	1.766
59	0.578	1.680	-0.966	0.359	1.119	3.808	3.808	0.71	2.80	1.800
59	0.557	1.691	-1.102	0.354	1.118	3.808	3.808	0.72	2.80	1.804
59	0.540	1.703	-1.313	0.350	1.142	3.808	3.806	0.76	2.80	1.798
61	0.518	1.705	-1.292	0.307	1.053	3.822	3.816	0.83	2.87	1.771
61	0.538	1.703	-1.493	0.313	1.099	3.819	3.812	0.86	2.87	1.755
61	0.493	1.719	-1.477	0.303	1.077	3.822	3.814	0.88	2.88	1.764
62	0.545	1.699	-0.891	0.378	1.207	3.802	3.798	0.74	2.75	1.806
62	0.516	1.723	-1.493	0.372	1.253	3.800	3.795	0.80	2.75	1.803
62	0.553	1.696	-0.979	0.381	1.195	3.800	3.799	0.71	2.74	1.817
63	0.569	1.693	-1.351	0.347	1.159	3.809	3.805	0.80	2.82	1.773
63	0.594	1.678	-1.183	0.354	1.126	3.808	3.808	0.73	2.81	1.786
63	0.545	1.704	-1.493	0.342	1.149	3.809	3.806	0.80	2.82	1.783
66	0.534	1.709	-1.362	0.361	1.188	3.804	3.801	0.76	2.77	1.804
66	0.523	1.720	-1.630	0.360	1.225	3.803	3.798	0.81	2.77	1.794
66	0.555	1.701	-1.347	0.368	1.195	3.802	3.801	0.75	2.77	1.801
66	0.529	1.713	-1.432	0.360	1.194	3.804	3.801	0.77	2.77	1.803
67	0.502	1.718	-1.463	0.332	1.118	3.813	3.809	0.81	2.82	1.794
67	0.551	1.699	-1.385	0.344	1.132	3.810	3.808	0.78	2.82	1.786
67	0.624	1.666	-1.132	0.359	1.137	3.806	3.806	0.73	2.81	1.778
67	0.569	1.690	-1.330	0.348	1.119	3.809	3.809	0.75	2.81	1.793
78	0.526	1.716	-1.665	0.357	1.175	3.803	3.804	0.75	2.77	1.817
78	0.560	1.683	-0.535	0.363	1.148	3.809	3.803	0.74	2.79	1.787
78	0.496	1.731	-1.734	0.350	1.202	3.805	3.801	0.82	2.78	1.802
80	0.657	1.649	-1.026	0.352	1.103	3.809	3.810	0.73	2.84	1.761
80	0.641	1.659	-1.044	0.345	1.152	3.812	3.804	0.81	2.86	1.733
91	0.603	1.666	-0.994	0.333	1.053	3.816	3.815	0.73	2.85	1.775
91	0.515	1.710	-1.397	0.313	1.077	3.819	3.814	0.84	2.86	1.772
101	0.559	1.684	-0.651	0.378	1.138	3.804	3.805	0.66	2.75	1.828
101	0.468	1.733	-1.268	0.354	1.175	3.807	3.802	0.77	2.75	1.826
101	0.568	1.676	-0.510	0.381	1.104	3.804	3.808	0.62	2.74	1.842
106	0.496	1.719	-1.385	0.314	1.100	3.819	3.811	0.85	2.85	1.777
106	0.624	1.649	-0.527	0.349	1.024	3.814	3.817	0.66	2.83	1.793
106	0.651	1.644	-0.761	0.355	1.055	3.810	3.814	0.66	2.83	1.788
110	0.550	1.699	-1.489	0.326	1.107	3.814	3.811	0.82	2.85	1.768
110	0.618	1.665	-1.172	0.341	1.076	3.812	3.813	0.72	2.84	1.778
110	0.611	1.693	-2.121	0.342	1.220	3.805	3.800	0.89	2.85	1.735
117	0.464	1.749	-1.966	0.334	1.216	3.809	3.800	0.90	2.80	1.786
117	0.518	1.730	-1.997	0.347	1.256	3.804	3.796	0.90	2.80	1.769
121	0.623	1.674	-1.583	0.345	1.151	3.808	3.806	0.80	2.85	1.752
121	0.599	1.695	-2.015	0.335	1.215	3.808	3.800	0.90	2.85	1.732
121	0.494	1.721	-1.489	0.308	1.098	3.820	3.812	0.87	2.86	1.769
130	0.586	1.671	-0.822	0.347	1.061	3.812	3.814	0.68	2.81	1.805
130	0.529	1.720	-1.944	0.334	1.190	3.809	3.803	0.86	2.82	1.774

Table 13—Continued

Star	M_V	$\log L$	[Fe/H]	$(B - V)_0$	$(V - K)_0$	$\log T_e$ ($B - V$)	$\log T_e$ ($V - K$)	M/M_\odot	$\log g$	A
130	0.621	1.676	-1.537	0.359	1.165	3.804	3.805	0.75	2.81	1.779
143	0.517	1.730	-2.164	0.348	1.215	3.803	3.801	0.82	2.78	1.799
143	0.499	1.700	-0.732	0.341	1.004	3.815	3.820	0.64	2.78	1.857
143	0.403	1.775	-2.084	0.319	1.226	3.813	3.799	0.99	2.81	1.780
150	0.504	1.712	-1.353	0.308	1.059	3.821	3.816	0.84	2.87	1.773
150	0.570	1.688	-1.420	0.325	1.080	3.815	3.814	0.79	2.86	1.769
150	0.590	1.667	-0.785	0.329	1.030	3.819	3.817	0.74	2.86	1.772
155	0.598	1.679	-1.473	0.298	1.093	3.824	3.812	0.94	2.94	1.700
155	0.499	1.701	-0.969	0.272	0.958	3.835	3.826	0.87	2.94	1.749
155	0.693	1.488	3.641	0.318	0.051	3.853	3.912	0.18	2.81	2.089
176	0.563	1.691	-1.218	0.329	1.121	3.816	3.808	0.83	2.86	1.755
176	0.727	1.652	-2.185	0.371	1.288	3.795	3.793	0.84	2.84	1.713

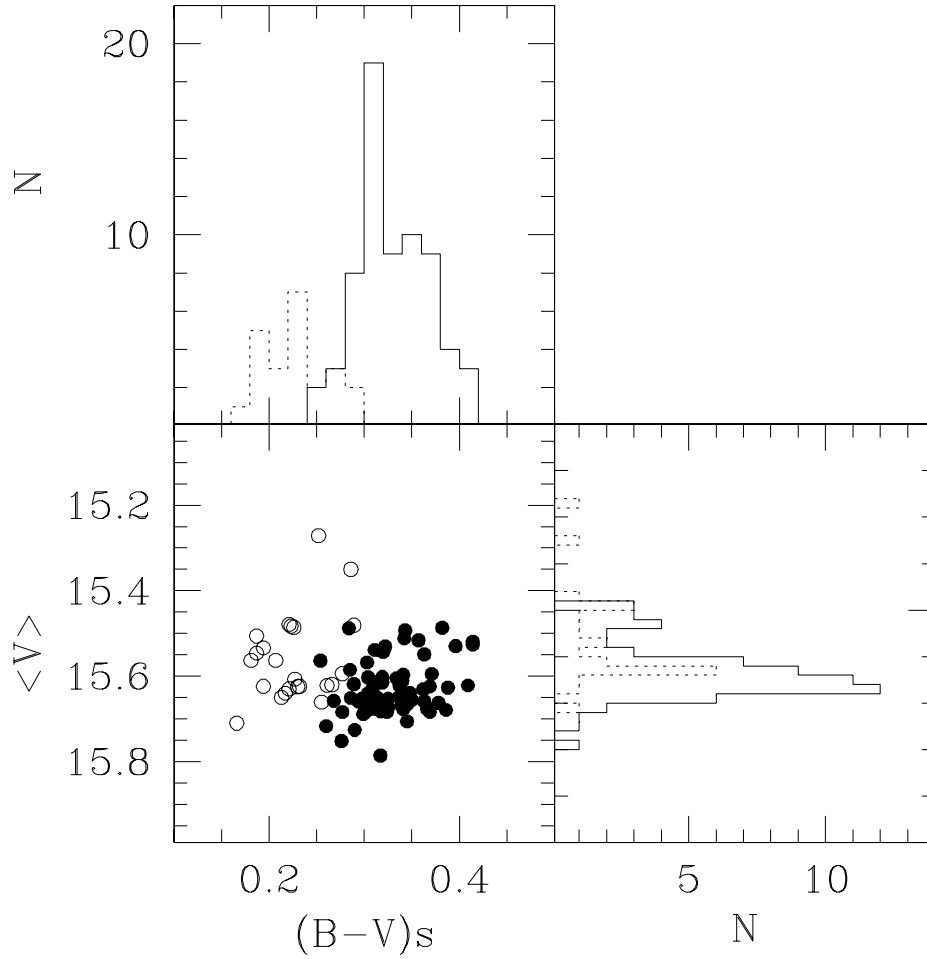


Fig. 1.— Color-Magnitude diagram for the c-type (open circles) and ab-type (filled circles) RR Lyrae variables listed in Table 1 and 2, respectively (lower left panel). The histograms of the color distributions (upper panel) and the $\langle V \rangle$ magnitude distributions (lower right panel) for the RRc (dotted line) and the RRab (solid line) are also shown.

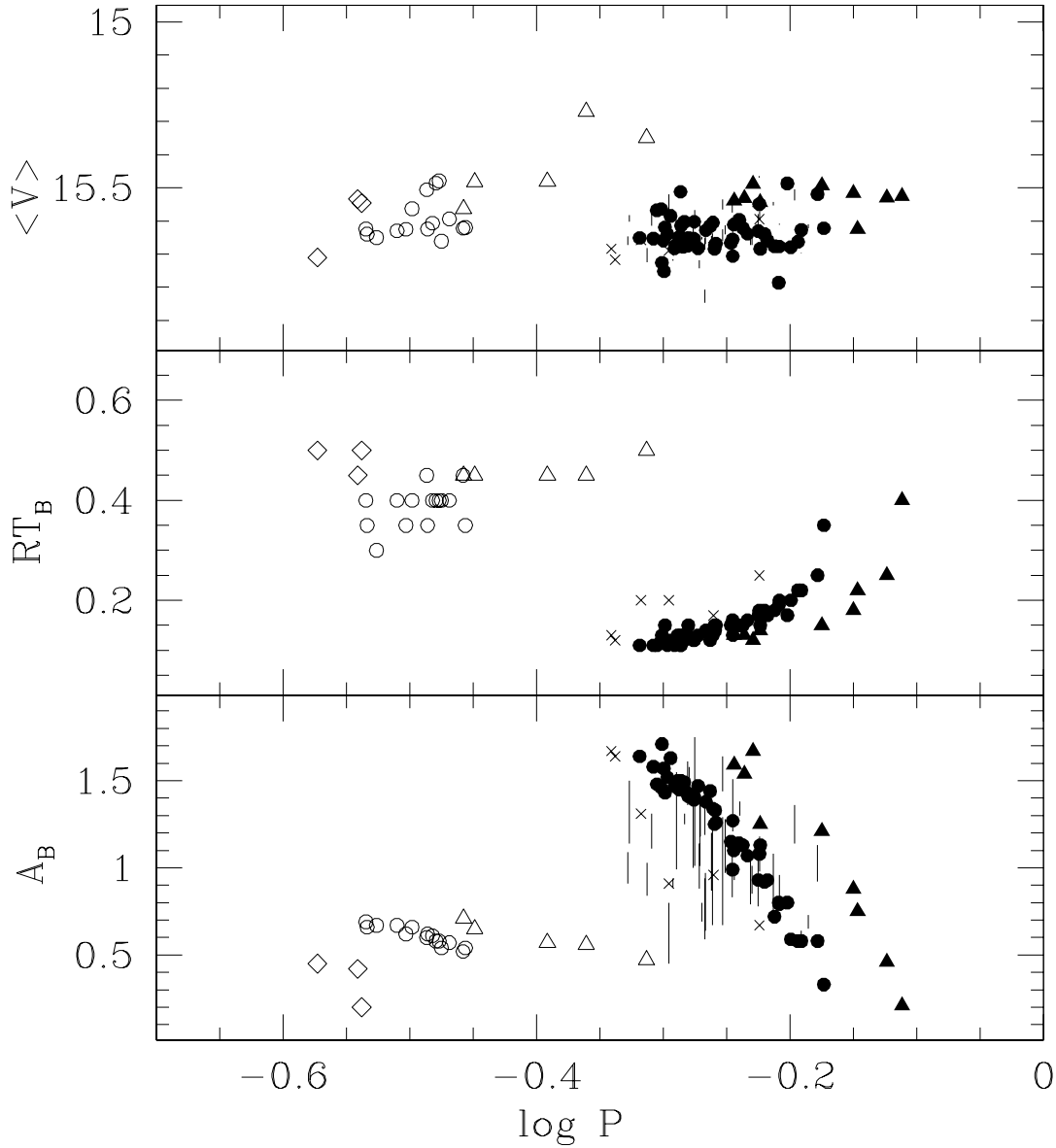


Fig. 2.— Lower panel: blue light curve amplitude A_B vs. $\log P$ for the *c*-type (open symbols) and *ab*-type (filled symbols) RR Lyrae variables listed in Table 1 and 2, respectively. The stars that are likely evolved off the ZAHB, and show up at longer period for a fixed amplitude, are indicated as triangles. The crosses indicate the suspected Blazhko stars, and the known Blazhko stars are shown as lines connecting the 1992 and 1993 data sets, from Table 3. The short-period small-amplitude RRC variables V105, V178 and V203 are shown as diamonds. Middle panel: same as lower panel, for the rise time values of the B light curves. No Blazhko stars are shown, because the rise times are quite uncertain for these stars. Upper panel: the corresponding $\langle V \rangle$ values.

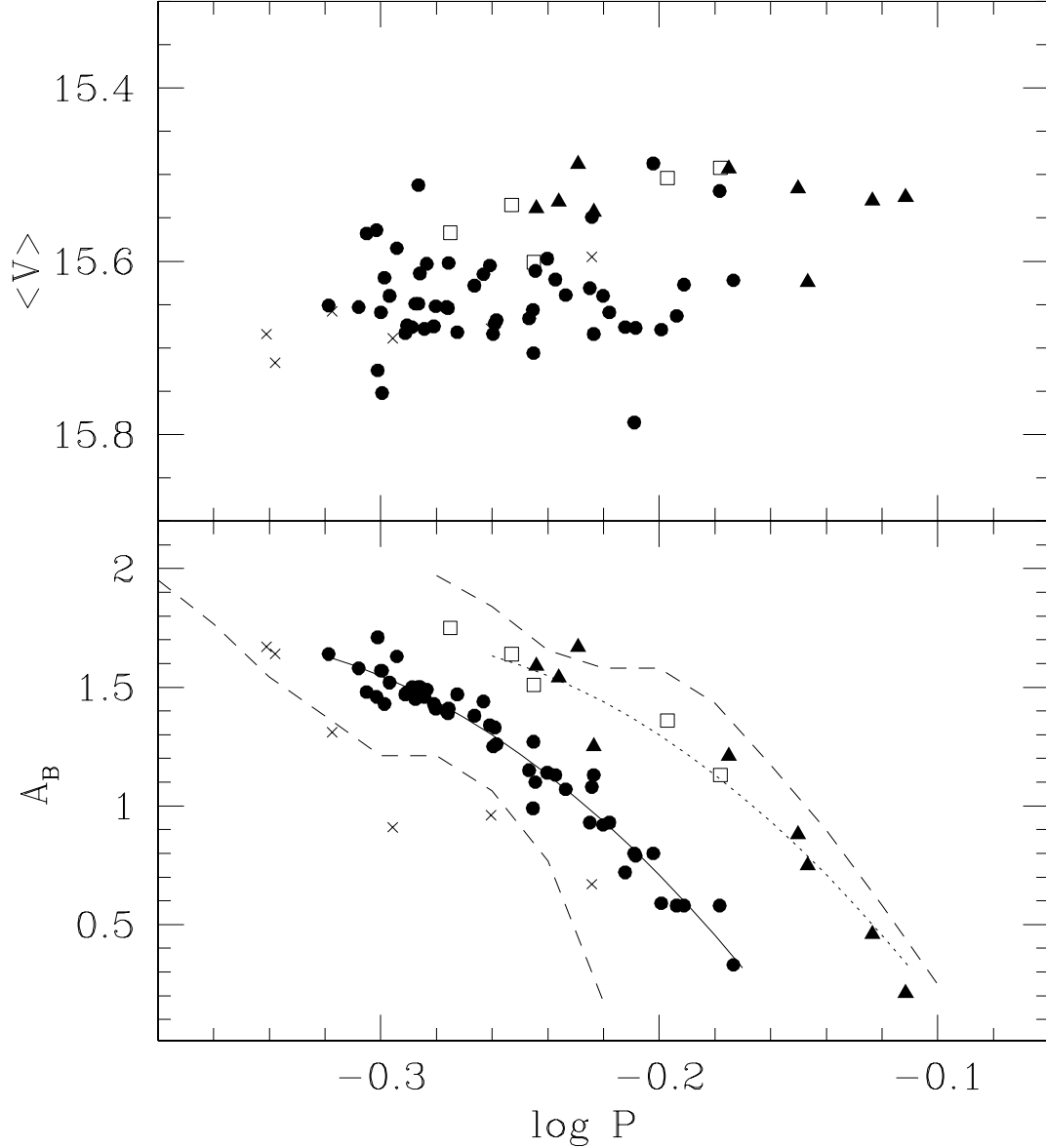


Fig. 3.— A blow-up of Fig. 1 for the RRab (and some Blazhko) stars only. Upper panel: same as upper panel in Fig. 2. Lower panel: the solid curve represents the mean distribution of the *bona fide* regular stars (filled circles). The dotted curve is obtained by shifting the solid curve to longer periods by $\Delta \log P = +0.06$, and represents quite well the long-period, candidate evolved RRab stars (filled triangles). We show for completeness also the candidate evolved Blazhko stars at the phase of maximum amplitude (open squares). Stars with smaller than normal amplitudes (suspected Blazhko) are shown as crosses. Note that the best representation of these distributions is not a linear but a quadratic relation. We show for comparison the theoretical relations calculated by Piersimoni et al. (2002) for $\log L = 1.61$ (left dashed line) and 1.72 (right dashed line).

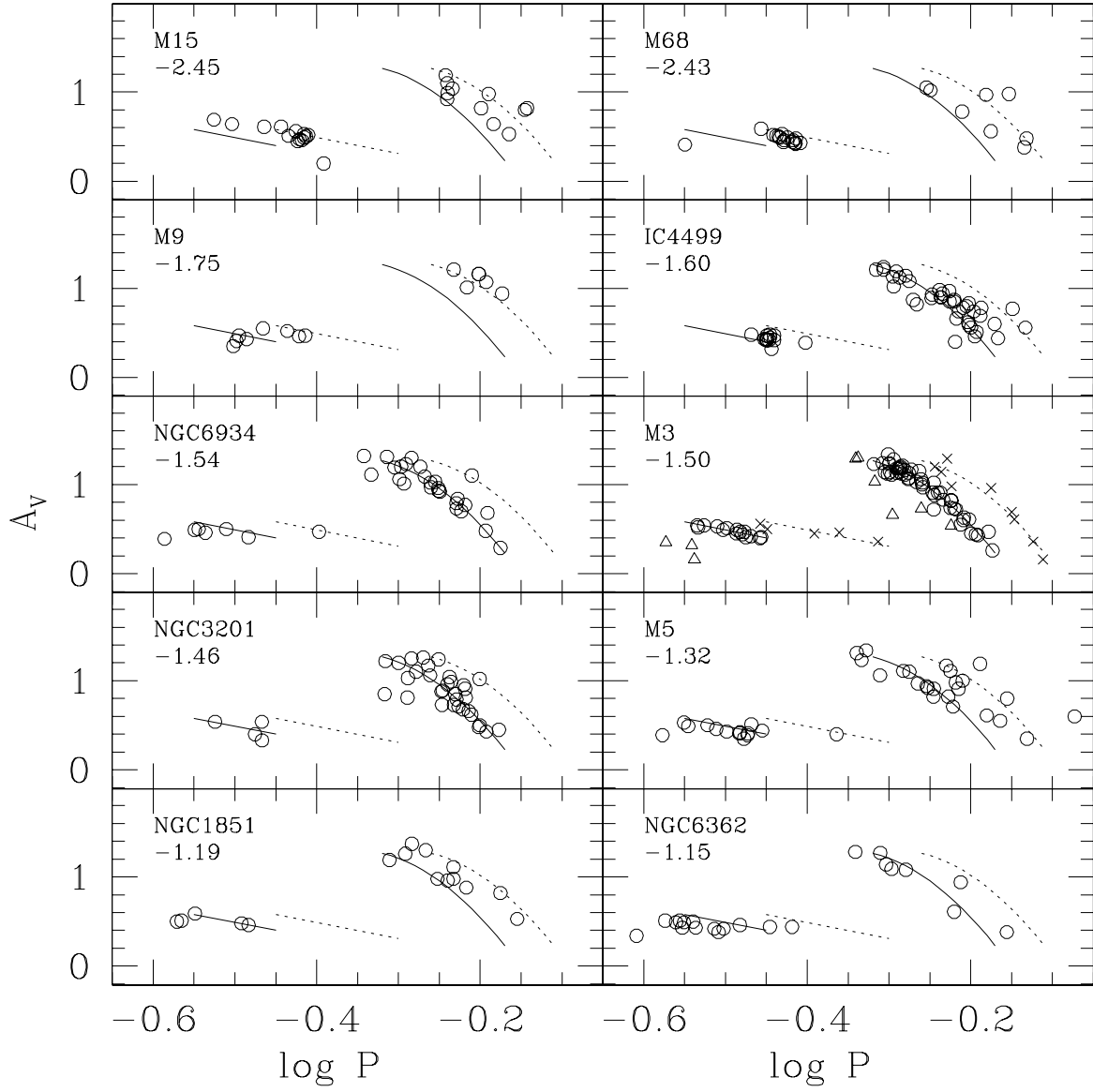


Fig. 4.— Period-amplitude distributions for RRc and RRab variables in three OoII clusters (M15, M68 and M9), three intermediate type clusters (IC4499, NGC6934 and NGC1851), and three OoI clusters (NGC3201, M5 and NGC6362), compared to M3. The mean distributions of the M3 regular (solid lines) and evolved (dotted lines) stars are shown in each panel. In the M3 panel, evolved stars are shown as crosses, and low-amplitude stars are shown as triangles. See Sect. 3.2.3 for details.

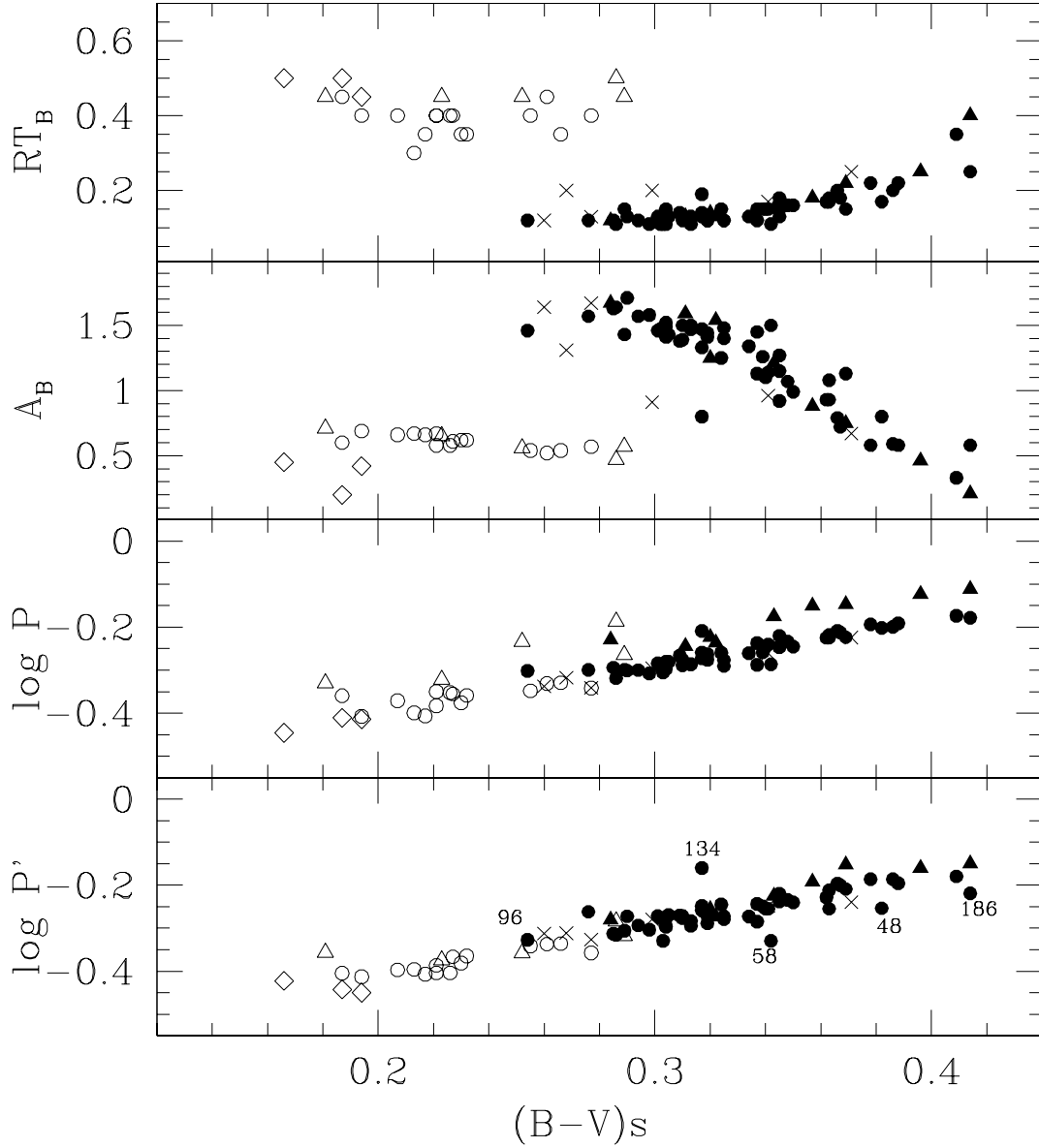


Fig. 5.— Color-rise time, color-amplitude and color-period plots for the RRc (open circles), RRab (filled circles), long-period/overluminous RRc (open triangles) and RRab (filled triangles), small-amplitude/suspected Blazhko RRab (crosses) and short-period small-amplitude RRc stars (diamonds). The periods of the RRc variables have been converted to fundamental mode periods by adding 0.127 to the $\log P$. The bottom panel shows the same as the middle panel but for the reduced period, defined as $\log P' = \log P + 0.336 (< V > -15.64)$.

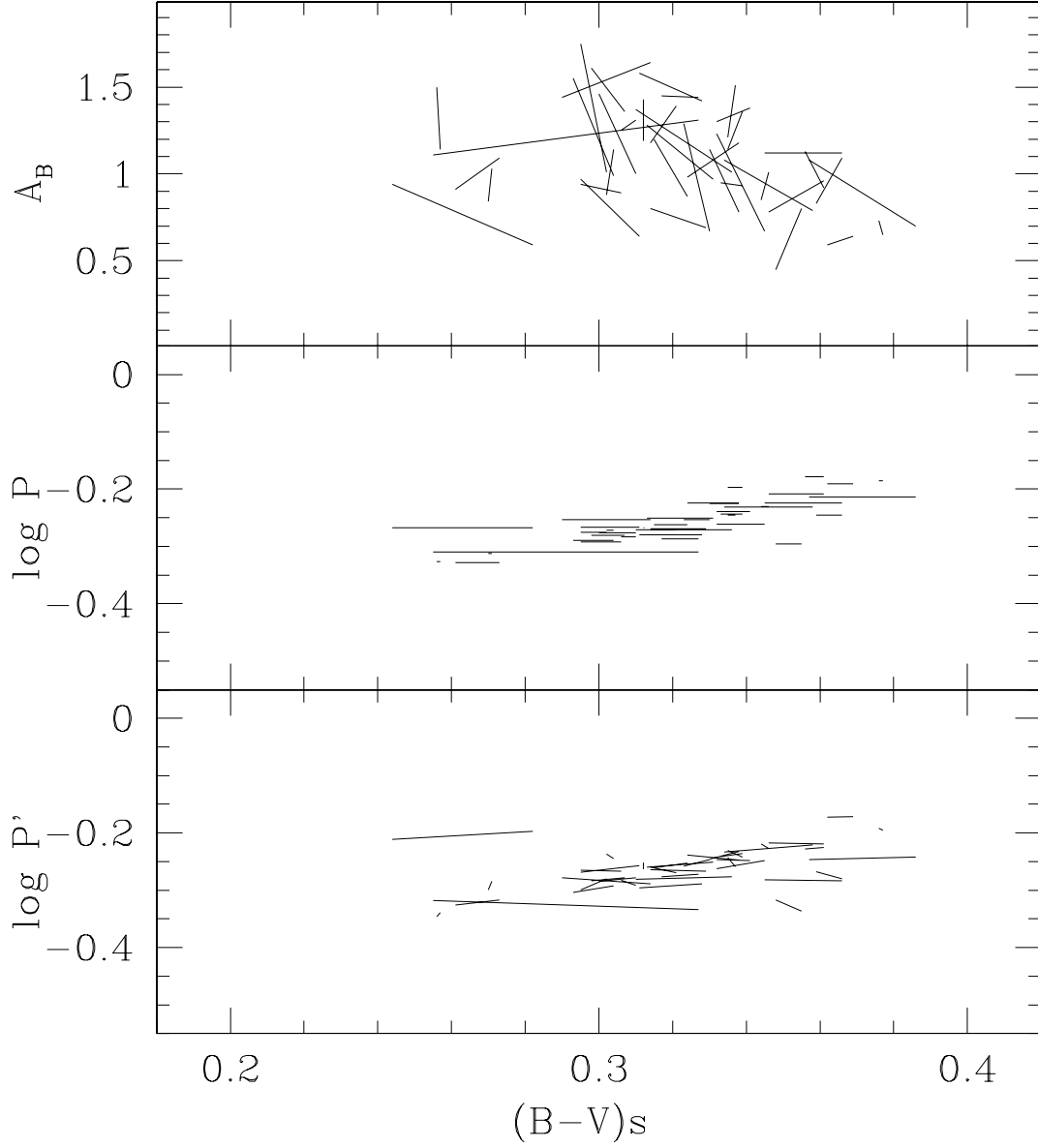


Fig. 6.— Color-amplitude and color-period plots for the Blazhko stars. The bottom panel shows the same as the middle panel but for the reduced period, defined as $\log P' = \log P + 0.336(\langle V \rangle - 15.64)$. As before, the 1992 and 1993 data are considered separately and joined by a line.

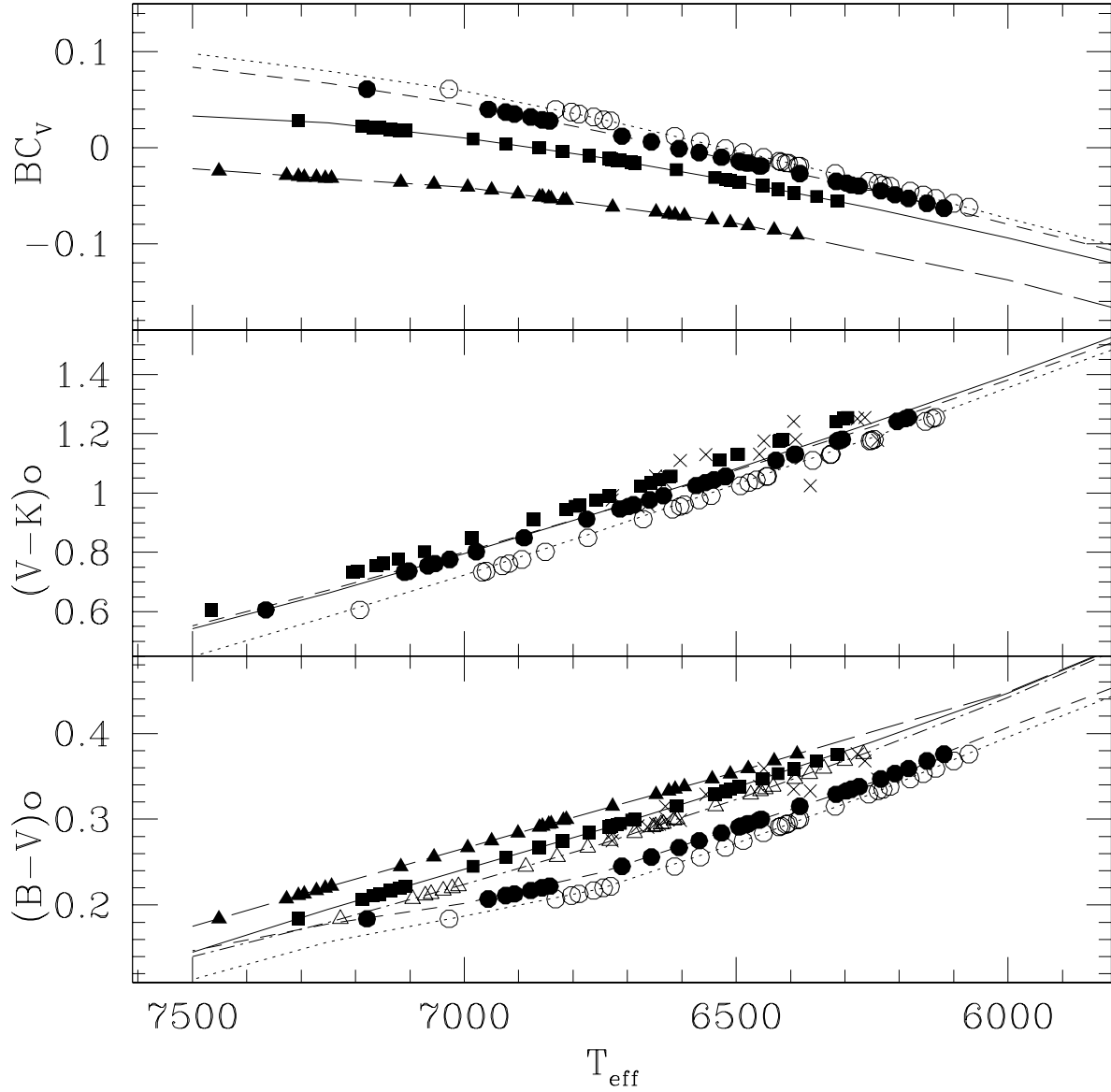


Fig. 7.— Comparison of temperatures as a function of $(B-V)_0$ (lower panel) and $(V-K)_0$ (middle panel) colors using the calibrations discussed in Sect. 4.2.1. Symbols indicate the various calibrations: M98 empirical (open circles), M98 theoretical ((filled circles), SF (open triangles), C99 (filled squares), SBT (filled triangles), and CSJ (crosses). The upper panel shows the $BC_V - T_{\text{eff}}$ relations for the calibrations that provide them independently.

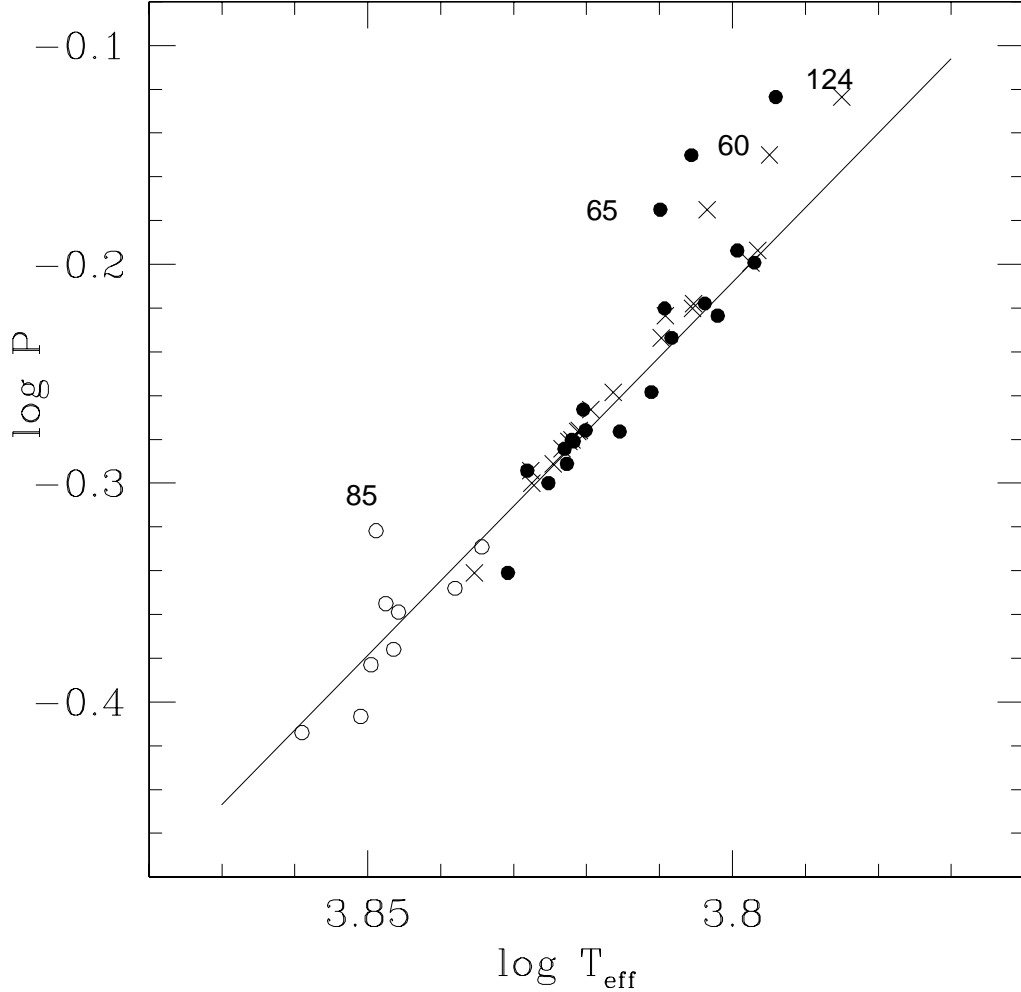


Fig. 8.— Period vs temperature for the 29 test stars discussed in Sect. 4. RRc are shown as open circles, RRab stars as filled circles. The periods of the RRc stars have been fundamentalized by adding 0.127 to their $\log P$. The temperatures have been obtained from the $(B-V)_S$ colors and the SF temperature scale. The line indicates the best fit to the data using a slope of -3.41 (cf. eq. 7), the zero-point corresponds to $A=-1.82$. The four labelled stars are evolved off the ZAHB. The crosses indicate the same RRab stars, where the temperatures have been derived from the CSJ scale (eq. 3), for comparison. The mean relation represents well also these data, and the scatter is significantly reduced. The three evolved RRab stars are still offset from the mean relation, but the shift in period ($\Delta \log P$) at fixed temperature decreases from ~ 0.069 (with the SF scale) to ~ 0.043 (with the CSJ scale).

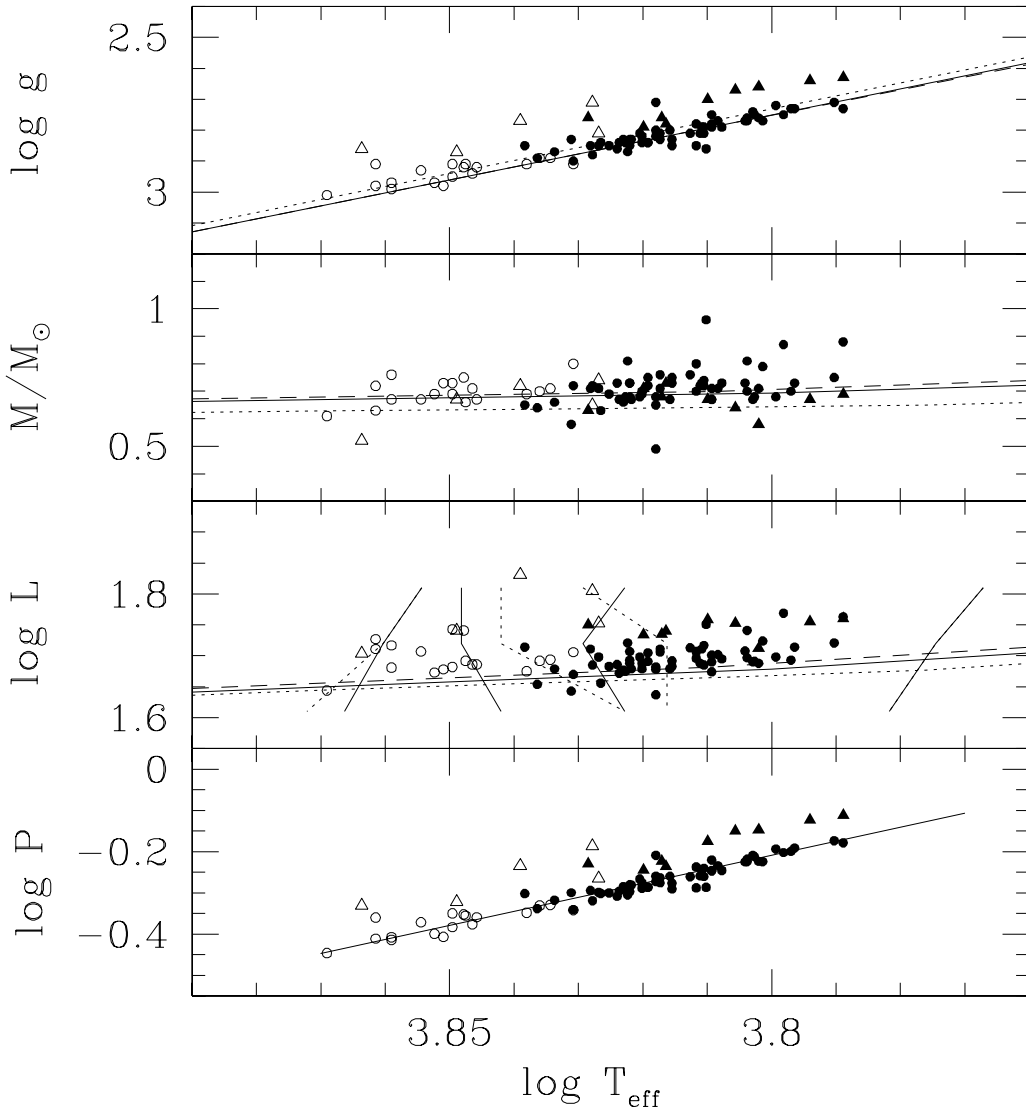


Fig. 9.— Period, luminosity, gravity and mass are shown as a function of temperature for all our regular RRc and RRab stars (cf. Sect. 4), indicated as open and filled circles, respectively. Evolved stars are shown as open and filled triangles. The line in the bottom panel is the same as in Fig. 8. The lines in the three upper panels indicate theoretical ZAHB models, for comparison: solid line (Sweigart 1997, $[\text{Fe}/\text{H}]=-1.53$, no helium mix), dotted line (VandenBerg et al. 2000, $[\text{Fe}/\text{H}]=-1.54$), and dashed line (Straniero et al. 1997, $[\text{Fe}/\text{H}]=-1.63$). The nearly vertical lines in the $\log L - \log T_{\text{eff}}$ plane show the theoretical limits of the instability strip (from Bono et al. 1995) for mass $0.65 M_{\odot}$ (solid lines) and $0.75 M_{\odot}$ (dotted lines), i.e. from left to right: first overtone blue edge, fundamental blue edge, first overtone red edge, and fundamental red edge (where the solid and dotted lines coincide).

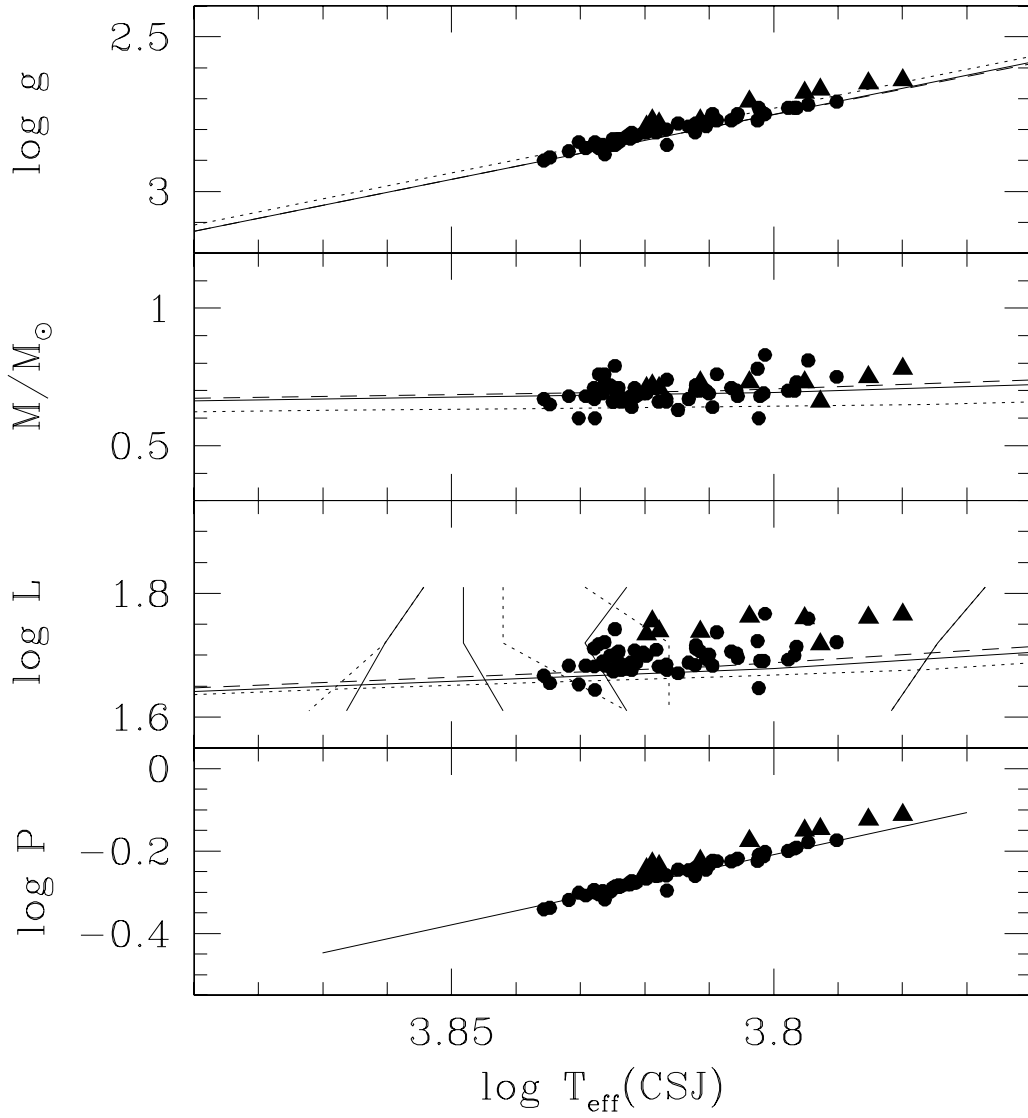


Fig. 10.— Same as Fig. 9 with the temperatures derived from the CSJ temperature calibration (RRab stars only).

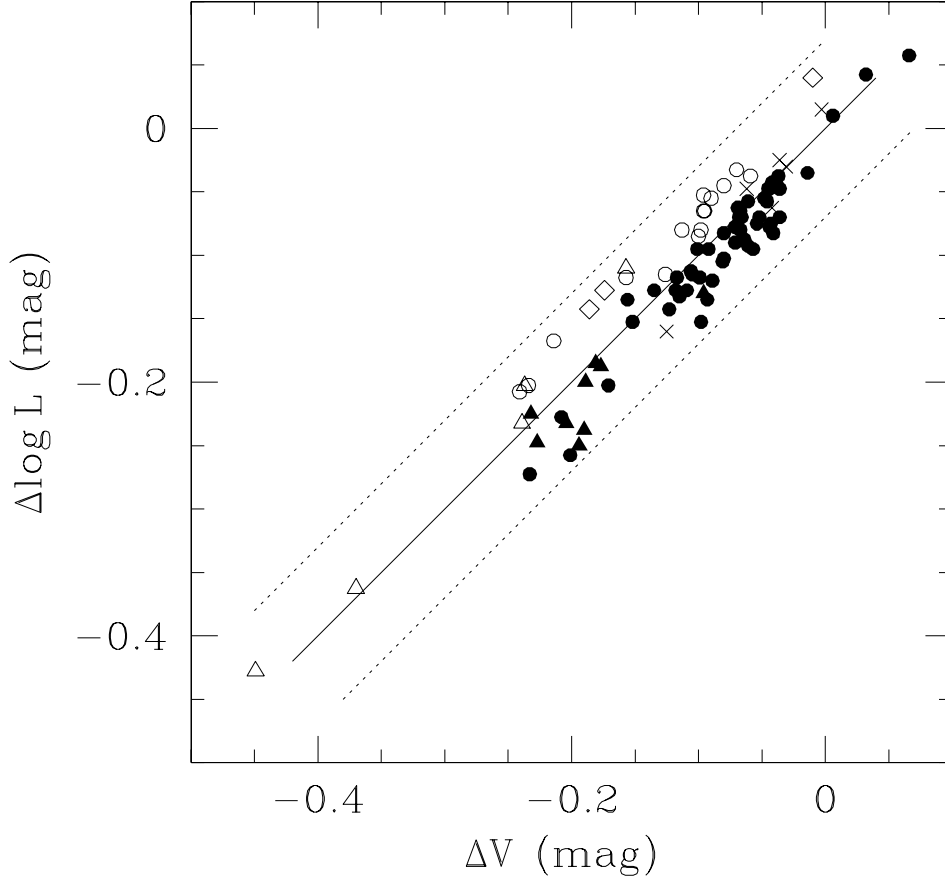


Fig. 11.— $\Delta \log L$ vs. ΔV for all the RRc and RRab stars listed in Tables 1 and 2. $\Delta \log L$ and ΔV are the calculated and observed offsets with respect to the reference ZAHB level that we observe at $V=15.72$ and calculate at $\log L \sim 1.66$ at mid range color/temperature (i.e. $B-V=0.27/\log T_{eff}=3.83$). As in previous figures, open and filled symbols represent RRc and RRab stars respectively, triangles indicate overluminous (evolved) stars, diamonds indicate short period small amplitude RRc stars, and crosses indicate low-amplitude suspected Blazhko stars. The solid line represents the relation of slope 1, and the two dotted lines are shifted by ± 0.07 mag.

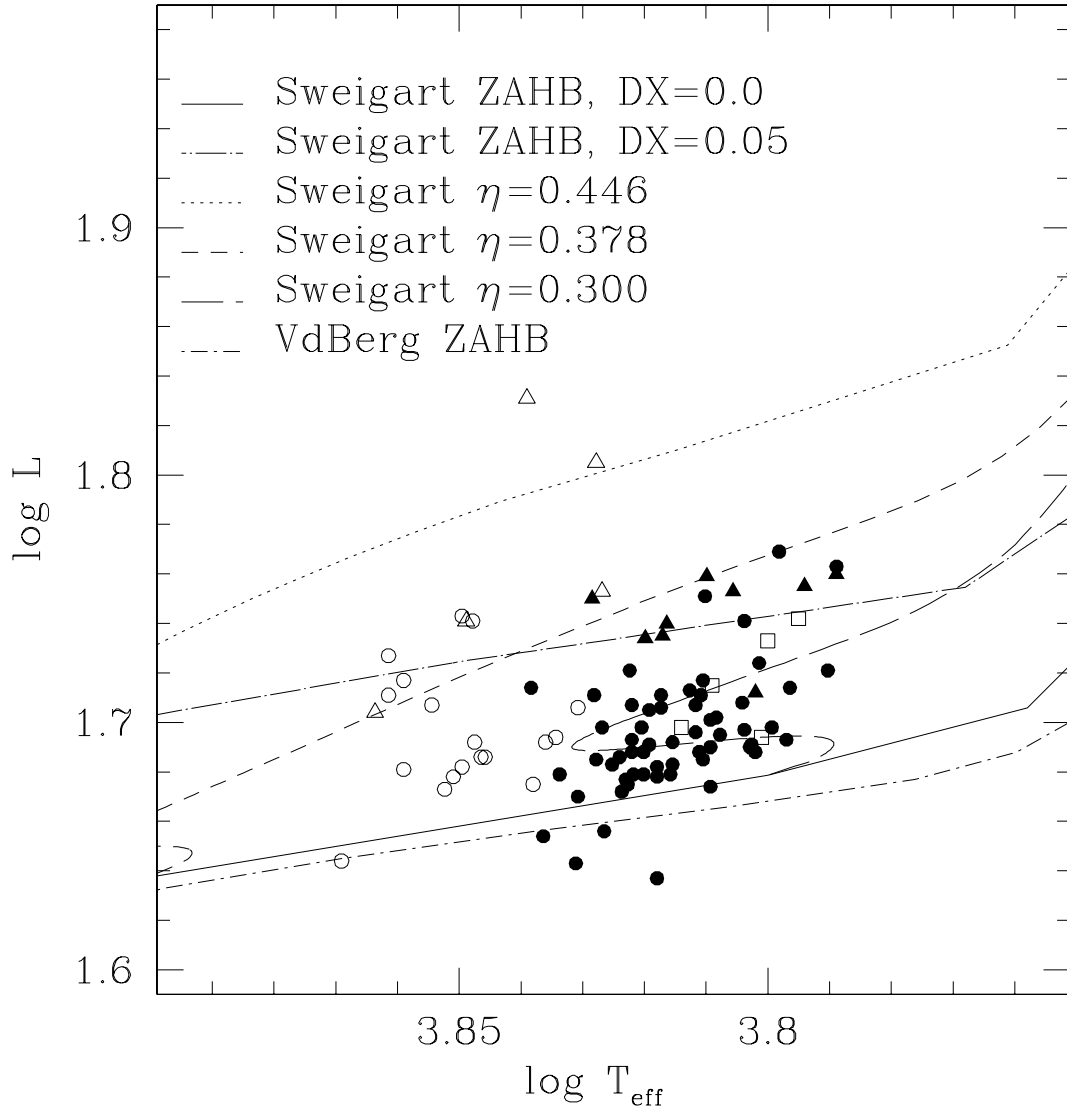


Fig. 12.— HR diagram of the RRc and RRab stars, and comparison with various sets of evolutionary models. First overtone and fundamental pulsators are shown as empty and filled circles, respectively. Overluminous/evolved stars are shown as empty and filled triangles. For completeness, the 5 evolved Blazhko stars at the phase of their maximum light curve amplitude are also shown (empty squares).

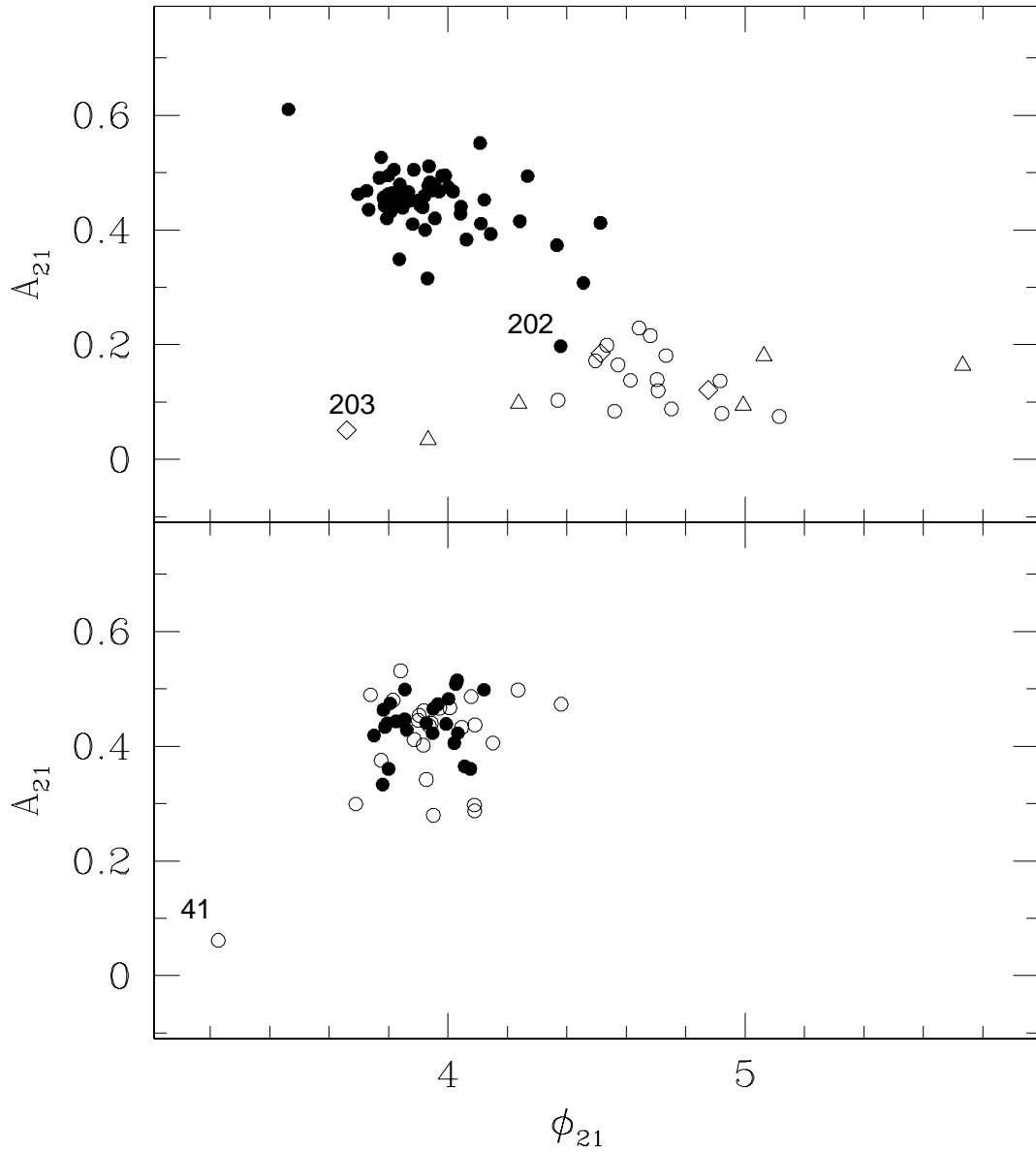


Fig. 13.— Upper panel: Fourier parameters A_{21} as a function of ϕ_{21} for our sample of RRab (filled circles) and RRc (open circles) stars. The dividing line between fundamental and first overtone pulsators occurs at $A_{21} \sim 0.3$, and V202 (the longest period RRab variable of our sample) falls in the RRc area. Of the three RRc stars V105, V178 and V203 (shown as diamonds), that are suggested as candidate second overtone pulsators, only V203 deviates significantly from the main RRc distribution. The three RRc stars shown as open triangles are V70, V129 and V170, with unusually long periods and bright magnitudes: they fall in the area of the first overtone pulsators, but off the main RRc distribution. Lower panel: same as above, for Blazhko stars in the large amplitude (filled circles) and small amplitude (open circles) Blazhko phase (lower panel).

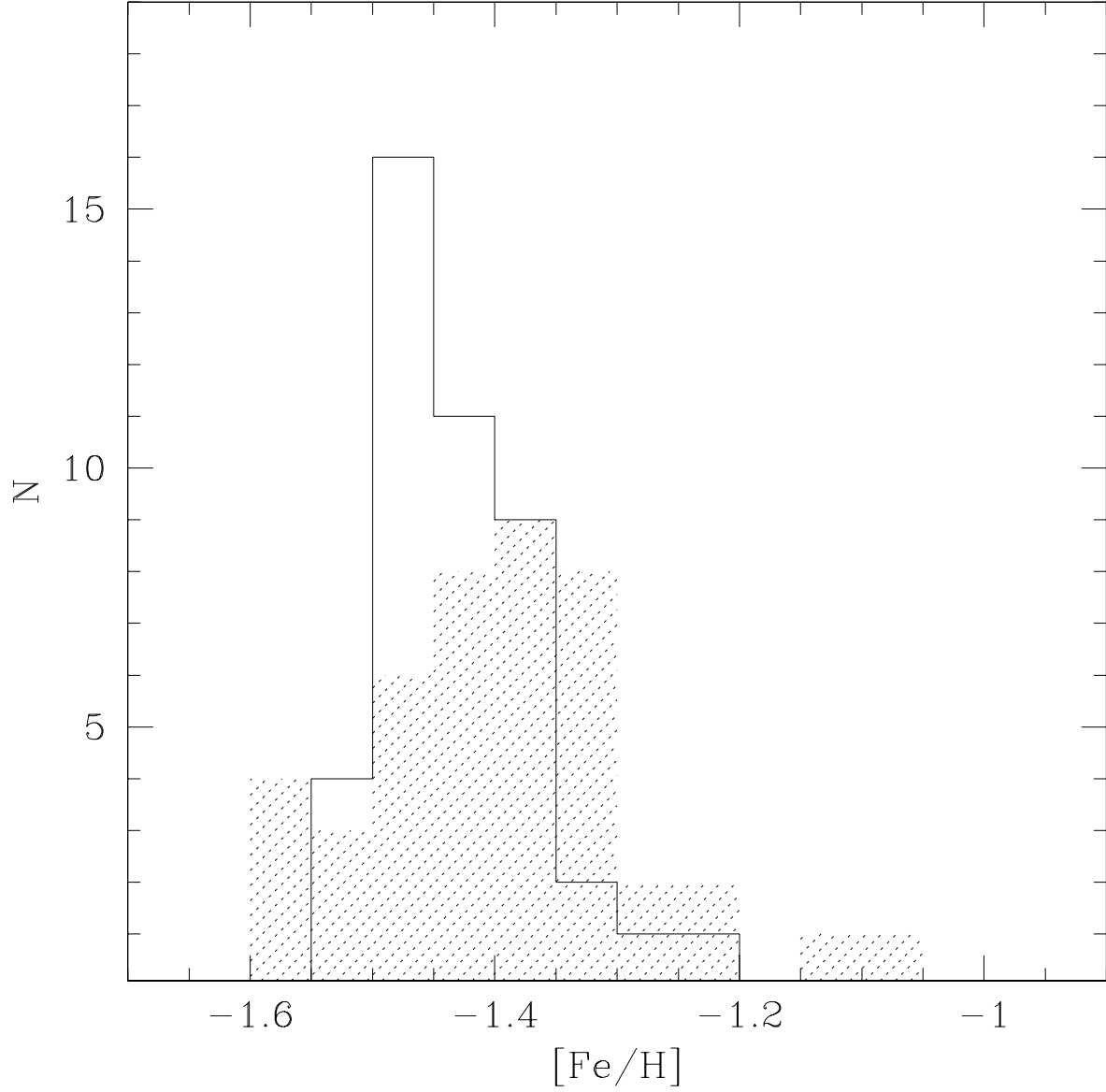


Fig. 14.— Metallicity distributions of the 45 regular RRab stars with $Dm < 5$, derived from eq. (10) (shaded area) and from Sollima et al. (2004) recalibration of the $[\text{Fe}/\text{H}]$ -period- ϕ_{31} relation (solid line). The two distributions yield similar average $[\text{Fe}/\text{H}]$ values (-1.39 ± 0.11 and -1.43 ± 0.07 , respectively), but have different (nearly specular) shapes (cf Sect. 6.2.1).

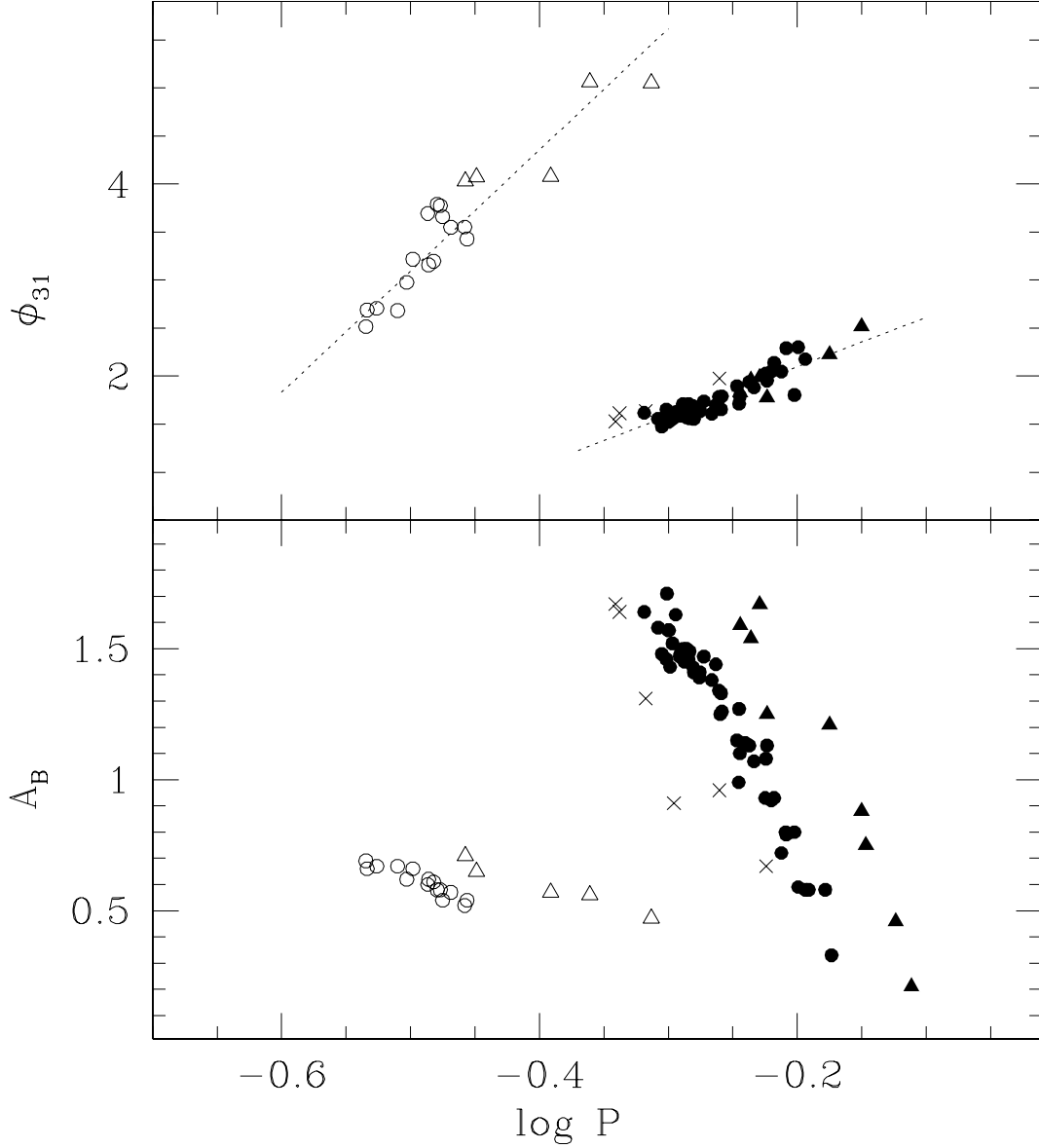


Fig. 15.— Lower panel: blue light curve amplitude A_B vs. $\log P$ for the RRc (open symbols) and RRab (filled symbols and crosses), as in Fig. 2. Here the Blazhko stars are not shown, for the sake of clarity. Upper panel: the ϕ_{31} parameter from the Fourier series representation of the V light curves ($Dm \leq 5$ only for the RRab stars). The two dotted lines show the linear relations representing in first approximation ϕ_{31} vs. $\log P$ for the RRc stars ($\phi_{31} = 9.403 + 12.619 \log P$) and the RRab stars ($\phi_{31} = 3.124 + 5.128 \log P$).

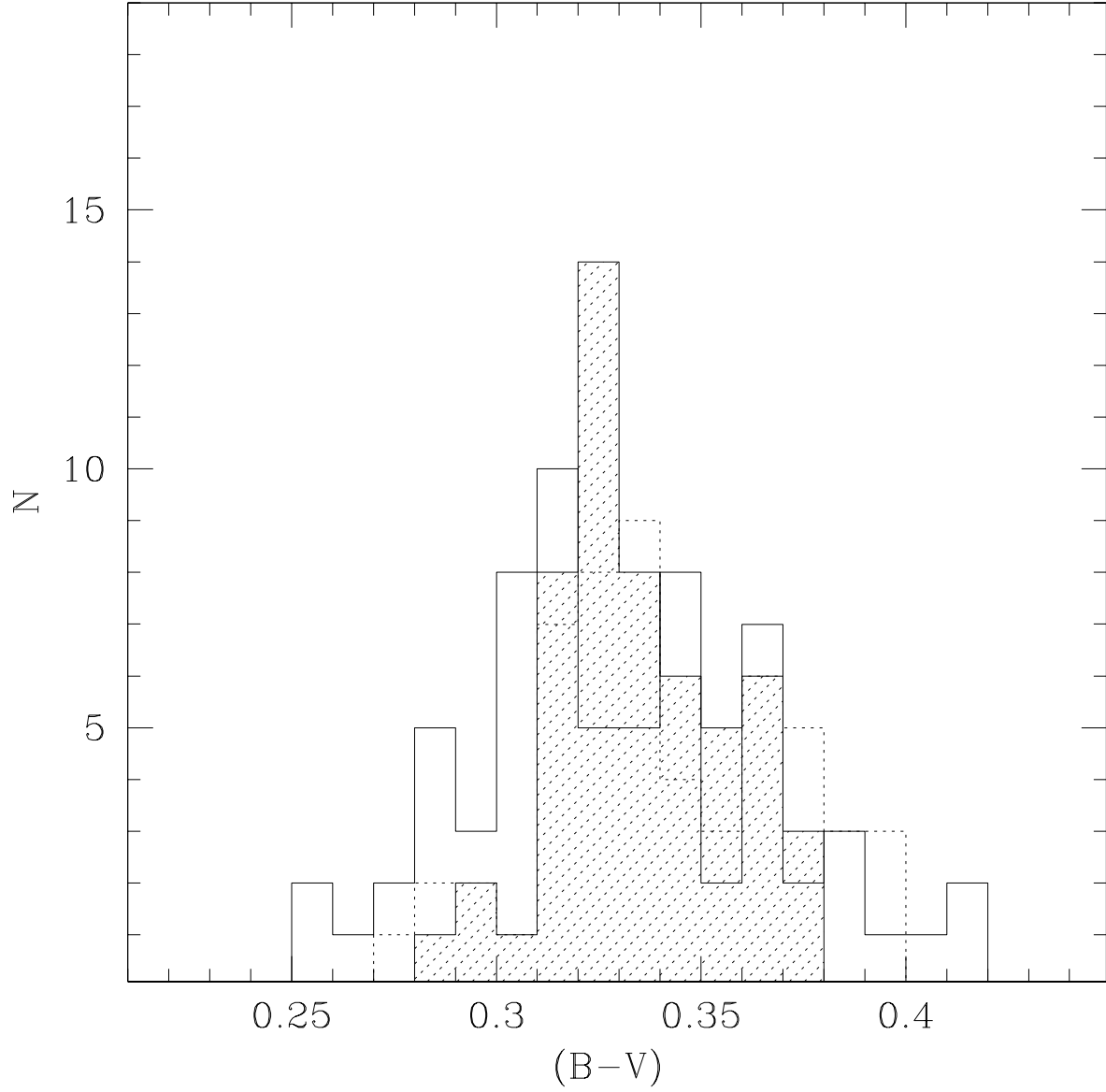


Fig. 16.— Histograms of the observed $(B-V)_{mag}$ (dotted line) and adopted $(B-V)_S$ (solid line) colors from column 9 and 10 in Table 2, and intrinsic $(B-V)_0$ colors estimated from eq. (11) and listed in column 5 in Table 12 (shaded area).

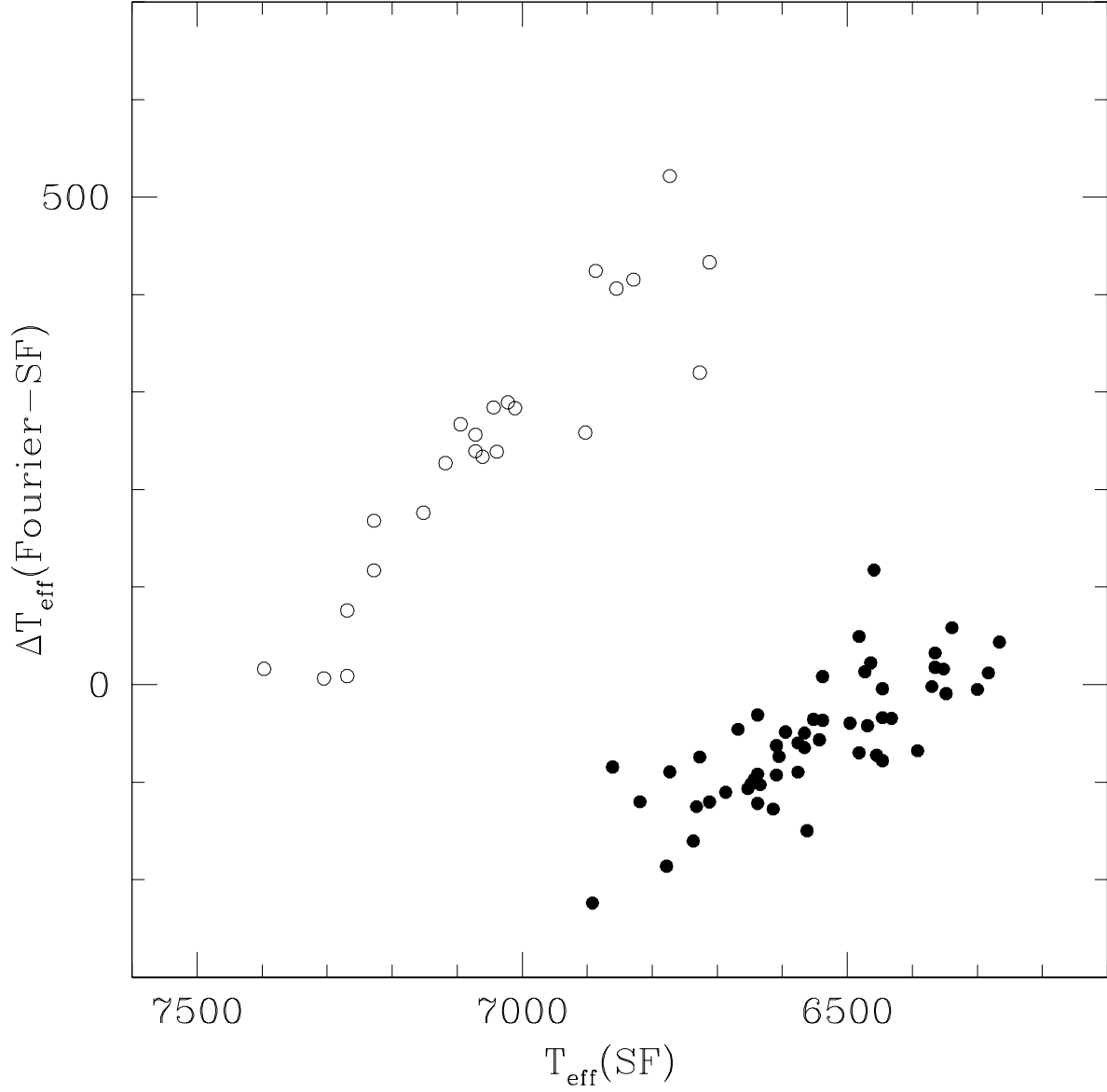


Fig. 17.— Comparison of temperatures derived from the Fourier coefficients using eq. (13) for RRab stars (filled circles) and eq. (15) for RRC stars (open circles), and from the $(B-V)_S$ colors and the SF color-temperature calibration. The Y axis shows the differences $\Delta T_{\text{eff}}(\text{Fourier} - \text{SF})$.

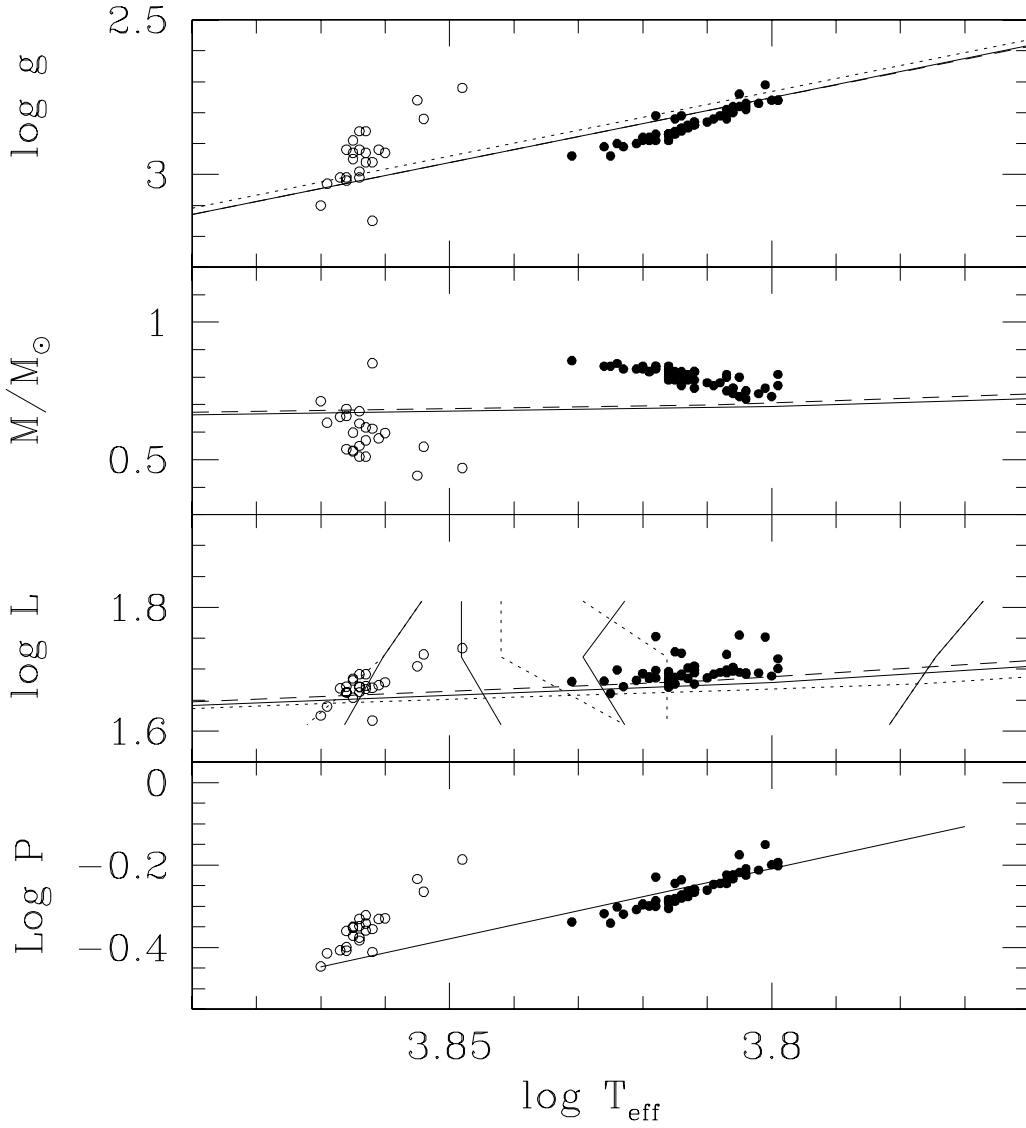


Fig. 18.— Same as Fig. 9, with the physical parameters derived from the coefficients of the Fourier series decomposition of the V light curves (cf. Sect. 6).

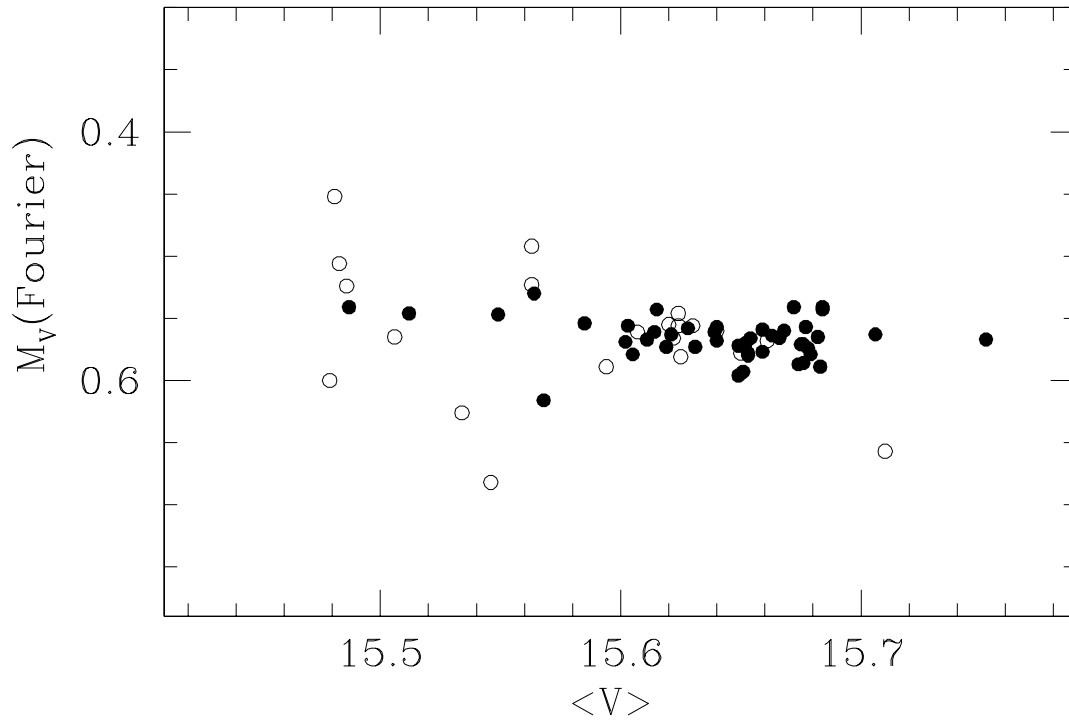


Fig. 19.— M_V vs. $\langle V \rangle$, for the RRc stars (open circles) and the regular RRab stars with $Dm < 5$ (filled circles). The values of M_V have been derived from the Fourier parameters and eq.s (17) and (18), respectively.